AUDITORY INFORMATION PROCESSING IN THE MIDBRAIN OF THE GRASSFROG

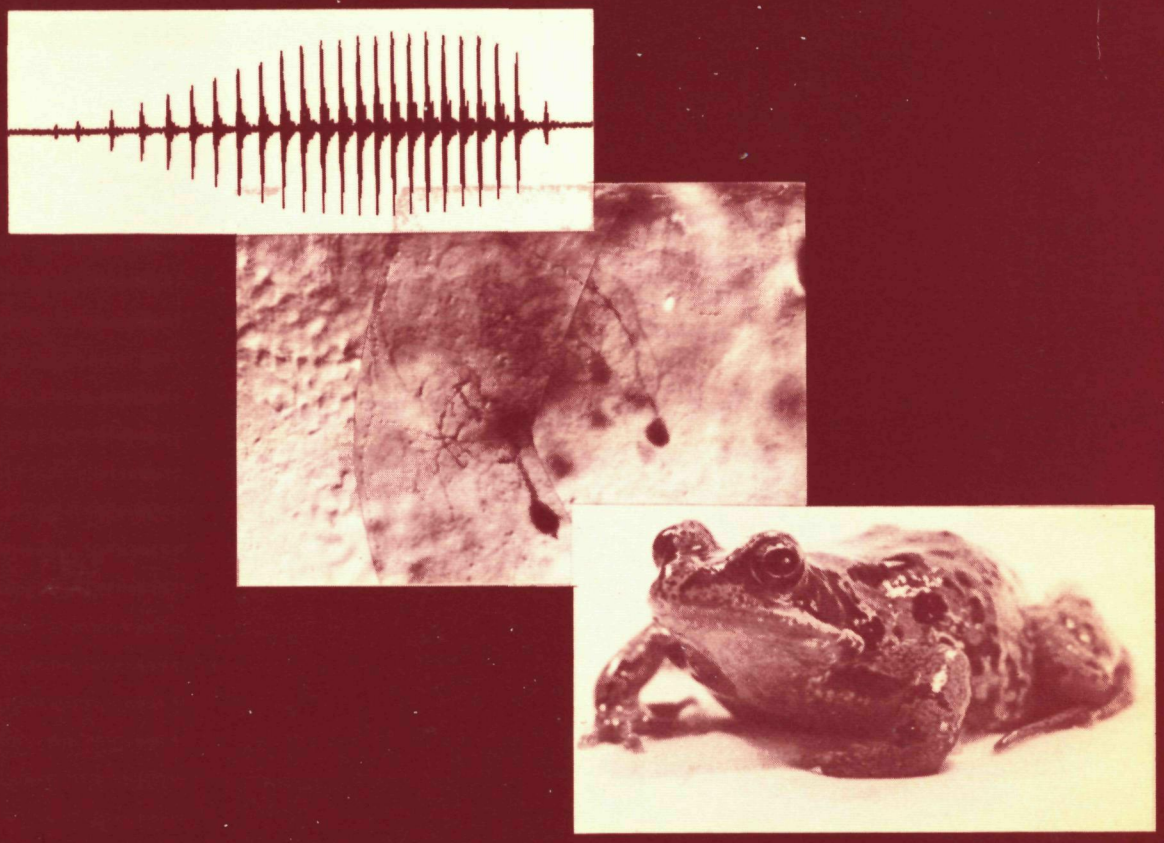

Willem Epping

Front Cover. Triptych representing the three basic elements of this thesis: auditory information, neural processing and the experimental object. In the upper left part of the figure the oscillogram of the most important vocalization, the mating call, is shown. The centre picture is a differential interference contrast (Nomarski) micrograph of a cell cluster located caudo-ventrally in the auditory midbrain. At least six cells were labeled with horseradish peroxidase. Two large (~ 15 m) unipolar cells with an extensive dendritic arborization are clearly visible, the others appear as dark shadows. To the left many unlabeled cells may be discerned as round to ovoidal structures. In the lower right corner a beautiful example of a grass-frog (*Rana temporaria* L.) is displayed. Note the large eardrum in rear of the eye.

The various stages of staining, preparation and photographing leading to the centre picture were carried out with much enthusiasm and expertise by Peter van Mier of the Department of Anatomy and Embryology.

AUDITORY INFORMATION PROCESSING IN THE MIDBRAIN OF THE GRASSFROG

Promotor: Prof. Dr. J. J. Eggermont
Co-referent: Dr. P. I. M. Johannesma

AUDITORY INFORMATION PROCESSING IN THE MIDBRAIN OF THE GRASSFROG

PROEFSCHRIFT

ter verkrijging van de graad van
doctor in de Wiskunde en Natuurwetenschappen
aan de Katholieke Universiteit te Nijmegen,
op gezag van de Rector Magnificus
Prof. Dr. J. H. G. I. Giesbers
volgens besluit van het College van Dekanen
in het openbaar te verdedigen op
vrijdag 20 september 1985
des namiddags te 2.00 uur precies

door

Wilhelmus Johannes Maria Epping

geboren te Silvolde

krips repro meppel

Graag wil ik iedereen bedanken, die ofwel in materiele dan wel in morele zin heeft bijgedragen aan de totstandkoming van dit proefschrift. Het gepresenteerde onderzoek werd financieel ondersteund door de Nederlandse Organisatie voor Zuiver Wetenschappelijk Onderzoek (Z.W.O.).

CONTENTS

General Introduction

Acoustic communication is of vital importance in the reproductive behavior of anuran amphibians (frogs and toads). During the mating season males produce a repertoire of species-specific calls which serve to attract females of their own species, to maintain breeding aggregations and to demarcate territories. In the grassfrog (*Rana temporaria* L.), as in most other anurans, the male mating call is the most prominent vocalization. It is characterized by both temporal and spectral features (Fig. 1), which are used to identify and localize a sound source correctly.

The auditory system (Fig. 2) has evolved to discriminate complex acoustic signals, be it conspecific or not, in a background of other sounds. Thereby the peripheral acoustic receiver has to sense and transmit information of sufficient spectral range and resolution. In the central auditory nervous system the spectrally segregated information transmitted by both auditory nerves is integrated resulting in a coherent spatio-temporal pattern of neural activity, which represents the

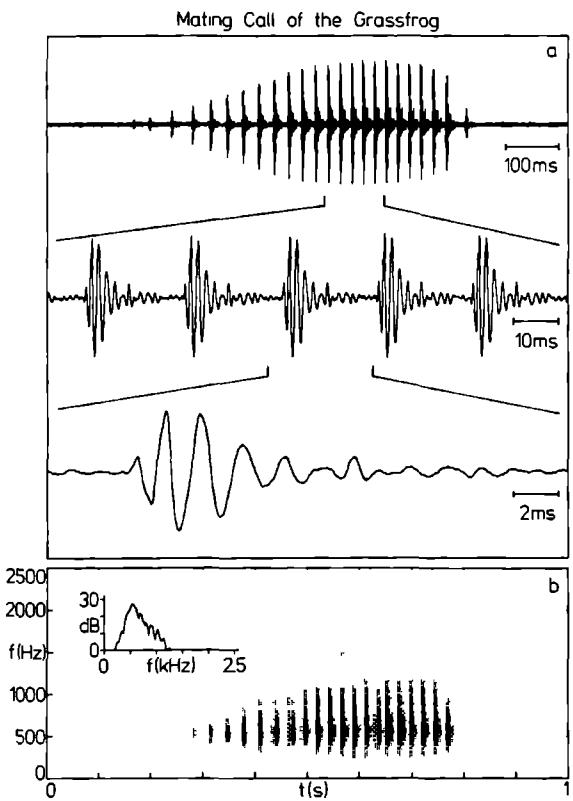

Fig. 1. The most important natural vocalization, the mating call of the male grassfrog. (a) Oscillogram displaying the distinct temporally structured call on various timescales. (b) Sonogram representing a spectro-temporal image of the mating call on the same timescale as the upper oscillogram. The inset shows the spectral content of the call averaged over time.

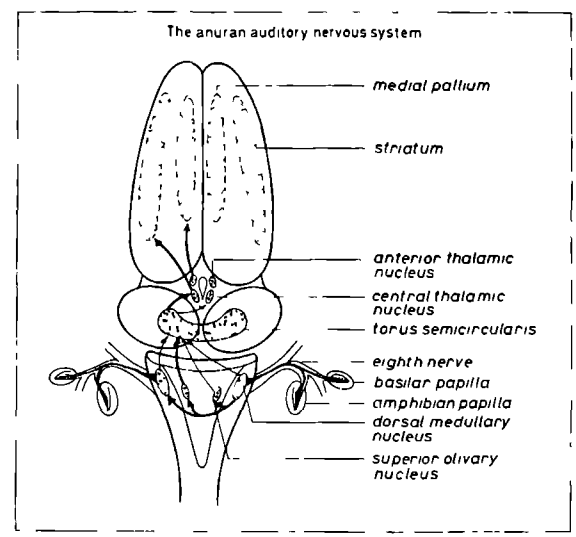

Fig. 2. Schematic overview of the organization of the anuran auditory nervous system. For convenience only ascending neural pathways entering and leaving the left torus semicircularis are indicated. Neurons sensitive to auditory stimulation have been recorded up to the level of the thalamus. In two forebrain regions, medial pallium and striatum, auditory evoked potentials have been obtained.

identity ('who') and location ('where') of the sound emitter. The central auditory nervous system is characterized by extensive ascending, commissural and descending connections between the auditory nuclei. Each nucleus contains 1000-10000 neurons, each of which makes contacts with thousands of other neurons. Because of this highly interconnected structure it has to be expected that at least part of the central auditory information processing takes place by populations of neurons, called 'ensemble coding'. Only by the simultaneous recording of spatio-temporal activity patterns of neural populations the role of ensemble coding may be assessed.

The torus semicircularis, the anuran large auditory midbrain nucleus, is the third central station in the ascending auditory pathway and receives direct information from the two brainstem nuclei of both hemispheres. The torus which presumably is the homologue of the inferior colliculus in higher vertebrates is supposed to play a major role in both aspects of auditory information processing: identification and localization.

For this thesis electrical activity was recorded from single neurons and small ($2 \leq n \leq 7$) neural populations in the auditory midbrain of the immobilized grassfrog by way of a dual micro-electrode configuration. Each electrode was able to sense the superimposed activity, which afterwards was separated into the component single-neuron spiketrains, of up to four proximate neurons. A large variety of stimulus ensembles has been applied, ranging from simple artificial ones such as tonepips and wideband noise via clicks and continuously amplitude modulated sound to stimuli mimicking the mating call. By this approach both single-neuron stimulus-response relations as well as functional connectivities between neurons and possible stimulus influences thereupon were determined.

Traditionally two basic complementary, and often separately applied, procedures to study stimulus-response relations of auditory neurons have been used. The forward correlation approach, which may be viewed as 'experimenter centered', relies on controllable stimuli of short duration, e.g. tonepips, sinusoidally amplitude modulated soundbursts, periodic click trains, and represents the stimulus response relation in peri-stimulus time histograms, dotdisplays and iso-intensity histograms. The reverse correlation or 'subject centered' approach chooses the neural activity as point of departure, thereby reflecting the brain's point of view. Stimulus-response relations are represented as (orthogonal) expansions of various functionals, e.g. envelope or spectro-temporal intensity, of the stimulus. Formally this leads to expressions known from nonlinear system theory, from which also the stimuli are borrowed: Gaussian wideband noise and Poisson distributed impulse ensembles. In this thesis spectral (chapter 2), temporal (chapters 4 and 5) and to a lesser extent spatial (chapter 3) sensitivities of single-neurons have been investigated using and confronting both (forward and reverse correlation) procedures. Thereby a possible bias due to the one or the other method was avoided. It may not be assumed apriori that the sensitivities to the afore mentioned aspects of sound are mutually independent. Therefore neural sensitivities were represented as combined (spatio-) spectro-temporal entities of which possible separability into the components was determined afterwards.

Functional connectivities between neurons were established by correlating simultaneously recorded activity from individual neurons with each other in a large variety of stimulus conditions (chapter 6). The main question posed was is the functional association of neurons a static one or instead dynamic depending on external influences as stimulus (or context), possibly explaining the observed stimulus dependency of single-neuron spectro-temporal sensitivities. Furthermore information about functional organization of the auditory midbrain was obtained with respect to mapping of stimulus features as well as divergence of neural connections. Finally a first attempt was made to combine single-unit stimulus response and interneuronal correlation analysis in a multi-unit spectro-temporal sensitivity approach (chapter 7).

The results presented in this thesis are based on data of 497 neurons, 181 obtained in single neuron recordings and 316 in separable population recordings, of 50 frogs.

SINGLE-UNIT CHARACTERISTICS IN THE AUDITORY MIDBRAIN OF THE IMMOBILIZED GRASSFROG

Willem J.M. Epping and Jos J. Eggermont

Department of Medical Physics and Biophysics, University of Nijmegen, Geert Grooteplein Noord 21
NL-6525 EZ Nijmegen, The Netherlands

The anuran auditory midbrain of the grassfrog (*Rana temporaria* L.) was studied by a combined spectro-temporal analysis of sound preceding neural events. From the spectro-temporal sensitivities (STS) estimates of best frequencies (BF) and latencies (LT) were derived. Several types of STSs were observed: monomodal excitatory STSs comprised about half of the cases. Bimodal excitatory STSs, i.e. STSs with two discrete excitation regions were observed in about 25%. Trimodal and broadly tuned STSs comprised about 5%. The remaining 20% of the STSs were characterized by inhibitory phenomena such as pure inhibition, sideband inhibition and post-activation inhibition. The distribution of best frequencies matches the frequency spectrum of the animal's vocalizations. A relative absence of monomodal units was noted in the mid frequency range. The distribution of latencies was bimodal over the range 7-108 ms. For each unit 6 functional parameters were determined, besides BF and LT these were: form of the STS (i.e. monomodality versus multimodality), spontaneous activity, binaural interaction, and firing mode (i.e. sustained versus transient) upon continuous noise stimulation. In addition 2 structural parameters were considered: location in the torus and action potential waveform. Large correlations appeared between LT and action potential waveform, and between BF and binaural interaction type. Tonotopy was not found. A comparison was made between results from this study with a previous study on lightly anesthetized grassfrogs, using the same stimulus paradigms [31,32]. Spontaneous activity, inhibitory phenomena and complex STSs were common using immobilization, whereas these have hardly been observed using anesthesia. Furthermore, interdependencies between the neural characteristics are substantially weaker for the immobilized preparation.

anesthesia, anurans, auditory midbrain, immobilization, spectro-temporal sensitivity

1. Introduction

Acoustic communication plays a crucial role in the reproductive behavior of anuran amphibians. During the mating season males produce species specific calls which serve to attract females of their own species and to maintain breeding aggregations. In the investigation of the anuran auditory system various methodologies and preparations have been applied. This has resulted in an amount of sometimes hardly comparable information. Stimulus ensembles and stimulus-event analysis have been inspired on both ethological (e.g. [26,37,48]) as well as on system-theoretical considerations [31,32]. The combination of both is often hampering because of conflicting demands. Whereas the ethological point of view leads to the use of a rich non-stationary and well structured stimulus ensemble derived from the acoustic biotope [4,47], system theory usually asks for a stationary nonstructured stimulus such as gaussian wide-band noise [46]. The presence of a strong acoustical coupling of both tympanic membranes by way of the Eustachian tubes and oral cavity (e.g. [43]) emphasizes the relevance of binaural interaction experiment conditions. Are these experiments performed with open or closed sound delivering systems and is the mouth shut or not? In addition it has been shown that anesthesia can severely alter properties of auditory neurons: spontaneous activity is reduced, excitatory thresholds are elevated and inhibitory

---

Abbreviations: BF best frequency; BEF best excitatory frequency; BIF best inhibitory frequency; CoSTID coherent spectro-temporal intensity density; IFT intensity frequency time; LT latency; PESE pre event stimulus ensemble; RT response time; SE stimulus ensemble; SPL sound pressure level; STS spectro-temporal sensitivity.

effects almost disappear [18,20].

The torus semicircularis, the anuran large auditory midbrain nucleus, which presumably is the homologue of the inferior colliculus in higher vertebrates, is supposed to play a major role in identification and localization of sound (e.g [10]). Focussing on the aspect of identification coding of temporal and spectral cues has been studied, mostly separately, on the single-unit level. Generally this resulted in post stimulus time and side (e.g. [42]). For lower stations in the auditory pathway, e.g. the auditory nerve, this approach leads to a sufficient characterization, i.e. on the basis of timing and tuning properties neural responses can be predicted to a variety of stimuli ranging from simple tones to complex sounds [19]. Considering that ethological important sounds have intricately-coupled temporal and spectral features (e.g. [8,27-29]), separate study of these features may result in an incomplete understanding of stimulus coding in higher auditory nuclei such as the torus semicircularis.

In an attempt to incorporate the ethological point of view within a system-theoretical approach, the latter being quantitative and having predictive capacity [14,15], combined spectro-temporal single unit characteristics have been determined by second-order correlation analysis of stimulus and neural events ([31,32]; see also Materials and Methods). For a substantial portion of neurons in the torus semicircularis it could indeed be shown that these do not encode temporal and spectral aspects independently [12]. First-order stimulus event crosscorrelation, estimating the average sound stimulus preceding an actionpotential, is of limited value when applied to cold-blooded animals studied at low temperatures. At 15°C, the ambient temperature in the biotope of the grassfrog, only neurons with a frequency tuning below 350 Hz exhibit phase-lock to the stimulus, which is a necessary prerequisite for a significant first-order crosscorrelation result.

Some of the results of Hermes et al. [32], using lightly anesthetized grassfrogs are at odds with outcomes of investigations working with immobilized preparations [5,48]. For example in the case of lightly anesthetized grassfrogs Hermes et al. [32] found that the fractions of torus neurons receiving input from the amphibian and basilar papilla are roughly equal. Walkowiak [48] to the contrary reported for the immobilized grassfrog a four times larger fraction that receives amphibian papilla information.

In order to facilitate comparison with other investigations we applied the system-theoretical approach of Hermes et al. [31,32] to immobilized grassfrogs. As an additional advantage inhibitory effects could be studied more extensively, because of a higher level of spontaneous activity. As stimuli continuous gaussian wide-band noise, commonly applied in system-theoretical approaches, and tone-pip ensembles are used. The latter in order to investigate those neurons, which are unresponsive to continuous noise. Besides the spectro-temporal dependency and properties derived from it such as best frequency and latency, also interrelationships of these and other neural characteristics such as action potential waveform, spontaneous firing rate, mono- or multimodality of spectro-temporal sensitivity, sustained firing to a continuous noise stimulus, binaural interaction type and location in the torus have been investigated. Most of these correlations have also been studied in the lightly anesthetized grassfrog [13,32,34], leading to the proposal of a two-stage information processing scheme for the auditory midbrain. The first simple stage is characterized by units with, as opposed to the second more complex stage, a predominantly short latency, type I (axonal) waveform, sustained firing to continuous noise, simple spectro-temporal sensitivity and a location in ventro-anterior parts. Comparison with results from the immobilized frog enables conclusions about influences of anesthesia on functional organization in the anuran auditory midbrain.

2. Materials and Methods

2.1. Animal Preparation

Adult grassfrogs (Rana temporaria L.) from

Ireland were anesthetized by a 0.05% solution of MS-222. An incision was made and the skin overlying the upper part of the skull was folded away. A screw for fixing the head was glued upside down to the frontal bones with dental resin (Palacav). A hole was drilled into the parietal bones above the tectum mesencephali, the dura was kept intact and the skin flap refolded. The animals were allowed to recover for two days.

Before the experimental session local anesthetic (Xylocaine 4%) was applied to the wound margins and the animal was immobilized with an intralymphatic injection of Buscopan (0.16 mg per gram bodyweight). The animal was placed onto a damped vibration isolated frame in a sound attenuated room (IAC type 1202A). Temperature was kept constant ($\pm$ 1°C) around 16° C and the skin was kept moist by a thin layer of cotton gauze to ensure skin respiration to be sufficient for metabolic demands. During recordings the oral cavity was shut. The ECG was monitored using a right fore leg - left hind leg recording and served as a measure for pain or arousal of the animal during the experiments. The heart rate was very constant and slightly dependent on temperature and state of the paralysis. For the collection of frogs studied the rate at 16° C usually was between 25 and 35 per min. Any pain deliberately induced or presentation of intense wide-band noise caused the ECG to increase in rate by up to 10%. We interpreted constancy of the ECG therefore as an indication that neither pain nor arousal were present.

2.2. Acoustic Stimulus Presentation

Acoustic stimuli were generated by a dual channel programmable stimulus generator build around a PDP 11/10. It comprises a.o. two programmable frequency synthesizers (Rockland 5100), two pseudorandom binary-sequence noise generators (Hewlett Packard HOI 3722A), several serial 12-bits multiplying DA-converters (Hybrid Systems DAC 316-12) for amplitude modulation, dual adders and selectors. The generated waveform was low-pass filtered (two cascaded -24 dB/oct Bessel filters, each -3 dB at 5 kHz) before it was amplified and presented to the animal by two electrodynamic microphones (Sennheiser MD 211N) coupled to the tympanic membranes with a closed sound system. Care was taken to minimize mechanical crosstalk of stimulus apparatus to the ears. The sound pressure level was measured in situ with a half-inch condensor microphone (Bruel and Kjaer 4143) connected to the coupler (for details see [31]). The frequency response of the sound system was flat within 5 dB for frequencies between 100 and 3000 Hz, a sufficient range for studying the auditory system in the grassfrog (e.g. [7]). The amplitude characteristics of left and right couplers were equal within 2 dB for the range of interest. Usually stimuli were presented at two intensity levels: 70 and 90 dB SPL and in three situations: binaural, ipsi- or contralateral with respect to recording side.

Tonal stimuli consisted of sequences of tonepips, so called γ-tones (Fig. 1a). A γ-tone is an approximative formal description of a single sound element from the male grassfrog's vocalization [2] and is defined by:

$$e(t) = a(t)\cos(\omega t+\phi)$$

The amplitude modulator a(t) is described by:

$$a(t) = A(t/\beta)^{\gamma-1}\exp(-t/\beta) \quad ; t > 0$$

$$= 0 \quad ; t < 0$$

The amplitude factor A, form parameter $\gamma = 3$ and phase angle $\phi = -\pi/2$ were kept constant. The frequency range was 4 octaves, either from 125-2000 or 250-4000 Hz depending on the frequency characteristics of the neuron. Two γ-tone ensembles with different durations of tones and intervals have been used.

The short interval ensemble consisted of tonepips with duration parameter $\beta = 1.45$ ms. These tonepips were truncated after 16 ms when the envelope had decreased to 0.36% (-49 dB) of its maximum. Onset intervals were 128 ms. Frequencies were selected pseudorandomly from 255 logarithmically equidistant values. One sequence of 255 tones was repeated 9 times, resulting in a total stimulus duration of 4 min 54 s.

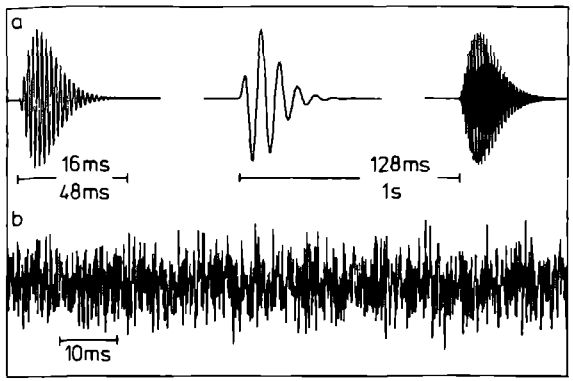

Fig. 1. Acoustic stimuli presented to the frog. a Segment from a γ-tone ensemble. The short interval ensemble consists of tonepips with duration of 16 ms and onset of 128 ms. The long interval ensemble has tonepip duration of 48 ms and onset intervals of 1s. Carrier frequency was varied pseudorandomly. b Segment from continuous pseudorandom gaussian wide-band noise. Further explanation in the text.

The long interval ensemble consisted of tonepips with β = 4.35 ms, which were truncated after 48 ms. The onset intervals were 1 s, and 127 frequency values were selected pseudorandomly. This sequence of tones was repeated 4 times. So this ensemble lasts 8 min 28 s.

Noise stimuli consisted of pseudorandom gaussian wide-band noise obtained by low-pass filtering (> 25 dB/octave) a binary signal with a sequence length of 1,048,575 steps (Fig. 1b). In order to improve the second order statistical properties of the noise, two feedback loops were added. For units with best frequencies above 900 Hz a cut off frequency (-3 dB) of 5 kHz was used resulting in a sequence duration of about 10.5 s. The complete noise stimulus consisted of 32 sequences presented immediately after each other resulting in a total duration of 5 min 36 s. Units with best frequencies below 900 Hz were generally stimulated with noise low-pass filtered at 1.5 kHz (-3 dB) producing a sequence duration of about 35 s. In this case 16 sequences were presented resulting in a total stimulus duration of 9 min 20 s.

2.3. Recording Procedure

Ultra-fine or tapered tungsten microelectrodes coated with parylene-c, having a 10-15 µm exposed tip with a 1 kHz impedance of 1.5-2.5 MΩ (Bak Electronics Inc.) were used for extracellular recordings. The electrodes were advanced through the intact dura and lowered into the auditory midbrain using a motorized hydraulic microdrive (Trent-Wells 3-0661), stepping precision was 1 µm. The electrode signal was amplified using a Dagan 2400Z extracellular preamplifier bandpassed between 100 Hz and 10 kHz.

In this configuration simultaneous activity of small neural populations (up to four neurons) regularly is recorded at one electrode. In order to separate the superimposed few-unit activity into the component single-unit spiketrains use is made of features of the action potential waveform (Fig. 9). Feature extraction, based on a generalized matched filter principle, occurs on-line by way of a hardware spikeanalyzer (for details the reader is referred to [16]). Waveform features and spike epochs are handled and stored by a data-acquisition system build around a PDP 11/34 for off-line classification and further analysis. Temporal resolution of the system is 60 µs.

2.4. Stimulus-Event Relation

A systematic analysis of the stimulus-event relation comprises two different stages [1]:

1. Existence: to what extent does a relation exist between the acoustic stimulus and simultaneously occurring action potentials?
2. Nature: if such a relation exists, which stimulus properties determine the occurrence of action potentials?

The existence of a stimulus-event relation can be studied by considering the reproducibility of the neural events upon presentation of at least two identical stimulus sequences. The neural activity is then regarded as a particular realization of a stochastic point process. A measure of reproducibility is obtained by crosscorrelating the neural activity in response to the identical stimulus sequences. A sharp peak around the origin in the resulting existence histogram points to a strong time-lock to the stimulus. Generally units in peri-

pheral stations of the auditory pathway tend to have a narrower peak than units in more central regions [1].

The nature of the stimulus-event relation for single auditory neurons is reflected in the properties of the Pre-Event Stimulus Ensemble (PESE): the ensemble of stimuli preceding the occurrence of action potentials. The characteristics of the PESE as compared to the total stimulus ensemble (SE) indicate which stimulus properties determine the occurrence of action potentials [3]. Because of the inherent stochastic nature of the neural activity averaged measures of the PESE have to be determined. Formally this is equivalent to the calculation of crosscorrelation functions of neural activity and various functionals of the stimulus.

First-order stimulus-event crosscorrelation is equivalent to the determination of the average sound preceding a neural event. This is called the oscillogram or 'revcor' function as introduced by de Boer and Kuyper [6]. Lack of phase-lock, however, causes the oscillogram to be not significantly different from the result obtained by averaging arbitrary parts of the SE. The degree of phase-lock is reduced by time-jitter of events and by spatio temporal integration e.g. in dendrites. When many synapses are involved, as is the case in more central regions of the nervous system, time-jitter can be considerable and phase-lock diminishes [44]. Temperature also plays a crucial role. In mammals, at temperatures of 37°C, phase-lock in the auditory nerve is manifest for frequencies below 5000 Hz (e.g. [45]). In the caiman at 27°C phase-lock is lacking above 1700 Hz [36]. For Eleutherodactylus coqui Narins and Hillery [39] found phase-lock up to 900 Hz at 23-24°C. At 15°C phase-lock in the grassfrog is present only up to 350 Hz and therefore first-order crosscorrelation is not very informative.

Second-order stimulus-event crosscorrelation results in the average spectro-temporal intensity preceding an event. This entity is not sensitive to absolute phase and therefore less degraded by time jitter than the oscillogram is. A well known example of a second-order representation is the dynamic spectrum or sonogram, often used to characterize vocalizations or speech. The dynamic spectrum of a signal can be obtained by passing it through a battery of band-pass filters and measuring the intensities of the filter outputs as a function of time. This procedure, however, has several disadvantages. First the result is not unique, because it depends on the filter specifications, and second phase relations between filter outputs are lost.

In the case of an ensemble of narrow-band signals, a relatively simple spectro-temporal representation is obtained by parametrizing the stimulus in terms of instantaneous frequency $f(t)$ and temporal envelope $a(t)$. A graphical representation of this type of analysis is the Intensity Frequency Time (IFT) representation [3]. Intensity $a^2(t)$ is depicted as a function of both time τ before an event and carrier frequency $f(\tau) = \omega(\tau)/2\pi$. The average IFT representation for the PESE should be compared with the average IFT representation of arbitrary parts of the SE. The latter, however, results in a two-dimensional image of constant value in the case of our γ-tone ensemble.

In the case of more complex signals such as wide-band noise and vocalizations a parametric description is not feasible. A generalized Coherent Spectro-Temporal Intensity Density (CoSTID) of signals has to be introduced. From the CoSTID description both the parametric IFT as well as the sonogram representation can be deduced, however, not the inverse. A complete description of the CoSTID formalism requires a series of mathematical manipulations which is beyond the scope of this paper. For an elaborate mathematical treatment of the CoSTID-type of analysis, its properties and some examples the reader is referred to [33]. We only give the necessary definitions. The CoSTID for a signal $x(t)$ is defined by means of the analytic signal $\xi(t)$ of $x(t)$ which equals:

$$\xi(t) = x(t) + i\tilde{x}(t) \qquad ; \quad i = \sqrt{-1}$$

Where $\tilde{x}(t)$ is the Hilbert transform or quadrature signal of $x(t)$, defined by:

$$\tilde{x}(t) = \frac{1}{\pi} \int_{-\infty}^{\infty} \frac{x(s)ds}{t-s}$$

The integral has to be interpreted in the Cauchy principal value sense. For example if $x(t)=\cos(\omega t)$, then $\tilde{x}(t)=\sin(\omega t)$ and $\xi(t)=\exp(i\omega t)$. The CoSTID $\Xi(\omega,t)$ of $x(t)$ is defined by:

$$\Xi(\omega,t) = \hat{\xi}^*(\omega)\exp(-i\omega t)\xi(t)$$

Where $\hat{\xi}^*(\omega)$ is the complex conjugate of the Fourier transform of $\xi(t)$. In general $\Xi(\omega,t)$ is complex valued. The temporal and spectral intensity of $x(t)$ can be obtained by integrating the CoSTID over ω and t respectively. The average CoSTID of the PESE has to be compared with the average CoSTID of the SE. In the case of stationary low-pass noise the latter is flat along the temporal dimension. Along the frequency-axis intensity is decreasing above the cut-off frequency of the noise, below it the intensity is constant. In order to correct for this stimulus artefact a normalization procedure is applied based on both intuitive as well as system theoretical arguments [4]. The normalized PESE CoSTID is obtained by first subtracting the SF CoSTID from the PESE-CoSTID and subsequently dividing the result by the SE-CoSTID. The same normalization procedure has been used by Hermes et al. [31].

Both the IFT and the normalized CoSTID representation of the PESE are estimates of the Spectro Temporal Sensitivity (STS) of a unit upon tonal respectively noise stimulation. The STS is depicted as a two-dimensional image (the CoSTID representation results in two images describing the realand imaginary parts) of frequency and time. Because of properties of the applied stimuli, the frequency axis of the IFT has a logarithmic scale, whereas the frequency-axis of the CoSTID is linear. Intensity is represented by means of a gray-scale. Darker than average regions indicate excitation, light regions point at inhibitive or suppressive effects. It is an empirical finding that, in addition to the real part, the imaginary part of the CoSTID when applied to the PFSE of midbrain units of the frog is not very informative. Often the imaginary part appears to be noisier than the corresponding real part [31]. Estimates of latency (LT) and best frequency (BF) are derived from the location of the extrema of the integrals of an activation or suppression region along the spectral and temporal dimension respectively [31]. Theoretically it can be shown that only the real part contributes to these integrals [33]. Because of these reasons we will mostly display the real part only. In other applications, such as prediction of responses, the imaginary part contains essential information. An elegant and compact representation may then be obtained by displaying both real and imaginary parts integrated into one picture using color [33]. The IFTs were computed on a PDP 11/45 and the CoSTIDs, because of larger computer power demands, on a VAX 11/780. (The computation of a 512 × 205 points CoSTID costs about 10 s CPU-time per spike on a VAX 11/780 and about 60 s on a PDP 11/45).

2.5. Location of Recording Site

Electrode tracks were made approximately orthogonal to the surface of the midbrain in both hemispheres. No histological techniques were used to determine the location of units in the torus. However, because we proceeded in the same way as Hermes et al. [32], who verified by histological techniques that almost all auditory units were localized within the torus, we believe that a large majority of our units is originating from the torus also. Position in the rostrocaudal-mediolateral plane was determined by localizing the entrance of a track on a photograph made of the surface of the midbrain. In the dorsoventral direction position was determined by the distance the electrode had advanced. The occurrence and disappearing of auditory background activity was considered to be the beginning, respectively the end of the torus. Because this is a rather crude method to localize units ($\pm$ 200 µm in each direction), we did not try to adjudge units to the five anatomical subdivisions of the torus [41]. Instead the torus was subdivided into eight rectangular compartments, two in each direction. The orthogonal intersection planes of the compartments were chosen on statistical grounds such that a roughly equal portion of units in each compartment was obtained. This resulted in an intersectionplane between medial and lateral

compartments, which was 900 µm lateral to the midline between the two hemispheres. The intersection plane separating caudal and rostral parts was 650 µm rostral to the boundary between midbrain and cerebellum. The plane between dorsal and ventral compartments was positioned 1350 µm beneath the surface of the optic lobes. Correlations between neural characteristics of neighbouring (< 50 µm) units could be studied by recording from two or more units simultaneously at one electrode [16].

3. Results

Experiments were performed during the entire year, except for the summer season, on a total of 20 male and female grassfrogs. Stable and reliable single-unit activity could be recorded from 151 midbrain units, 48 of which were obtained simultaneously in two- or more-unit recordings. In addition to auditory responsiveness often a vibrational sensitivity was observed, especially of units from lateral recording sites. Spontaneous activity, the presence of which was defined as at least 1 spike per 10 s during zero-stimulus conditions, was exhibited by 44% of the units. Its distribution was decreasing as function of discharge rate and ranged from 0.1-9 spikes/s.

3.1. Existence of a Stimulus-Event Relation

The existence of a stimulus-event relation, characterizing a unit as auditory, was established by means of the existence histogram (see Materials and Methods). In the case of 142 units, for at least one stimulus condition, a histogram resulted which was, by visual inspection, clearly different from the one expected for activity uncorrelated with the stimulus. The width of the peak of the existence histogram, a measure for degree of time lock to the stimulus, appears to be strongly correlated with latency. Long latency units tend to have low degrees of time-lock. Two examples representing the extrema of the histograms encountered are depicted in fig. 2. Unit 237-3-1 (Fig. 2a) is an example exhibiting a very strong time-lock, within

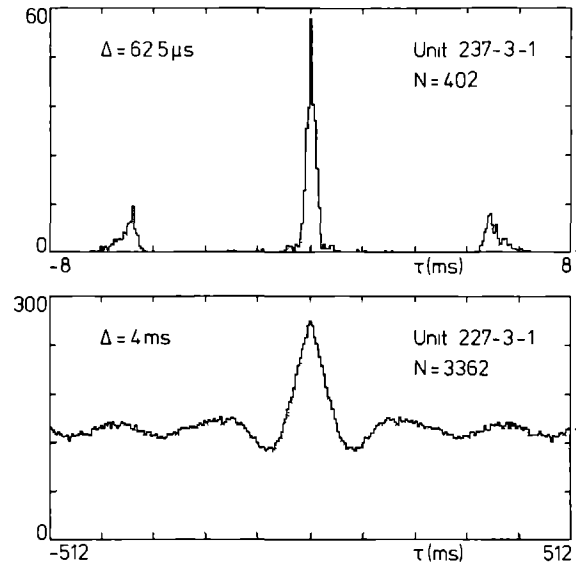

Fig. 2. Existence histograms of two midbrain units estimating the degree of reproducibility of neural activity upon auditory stimulation. a Unit 237-3-1 has a very narrow peak with a halfwidth of about 300 µs. The smaller peaks at ± 5.5 ms are due to repetitive firing. The stimulus was the long interval γ-tone ensemble presented binaurally at 90 dB SPL. b Unit 227-3-1 shows a broad peak with a halfwidth of about 60 ms, note the different time scale. Also some secondary peaks and valleys are present. The stimulus was continuous noise (5 kHz cut-off) presented at 90 dB SPL binaurally.

300 µs, to the stimulus. Unit 227-3-1 (Fig. 2b) is only loosely bound to the stimulus, its time-lock is about 60 ms. On the average units have narrower existence peaks for the long interval γ-tone ensemble than for the short interval ensemble ($p < 1\%$, sign test). Noise stimulation elicits the broadest existence peaks mostly ($p < 1\%$, sign test).

Henceforth only the collection of the 142 (out of 151) units, exhibiting an existence of a stimulus event relation, will be considered further. Of the remaining 9 units 3 were located at the end of a track with auditory activity, the other 6 units were recorded simultaneously at the same electrode with units showing a stimulus-event relation.

3.2. Nature of the Stimulus-Event Relation for Tonal Stimuli

The long interval γ-tone ensemble was presen-

ted to 128 units. All units, except one, responded in a sustained way with respect to overall firing behavior to this stimulus ensemble. The short interval ensemble was presented to 89 units, 10 (11%) ceased firing after a few seconds. In the case of the remaining 79 units it frequently was observed that a constant average discharge rate was reached only after one or more stimulus sequences. The initial, mostly higher, activity band was discarded from further analysis. The spectro-temporal sensitivities (STS) of the units upon these tonal ensembles were investigated by means of the IFT representation. Several types of IFTs were observed.

frequency 400-900 Hz and high frequency above 900 Hz. An example is depicted in Fig. 3a. The STS of this unit is characterized by a clear dark region, which points at excitation. This excitation region extends in the frequency range of 1100-2400 Hz. Its maximum value was obtained at 1550 Hz and will be called the best excitatory frequency (BEF), because it implies that the unit fired best to tones of this frequency. At BEF the excitation region extends from 35 ms to 11 ms before a spike. Only the first half of the γ-tone envelope is visible with the gray-scale used, causing a temporal extension to the right of 24 ms for the long interval ensem-

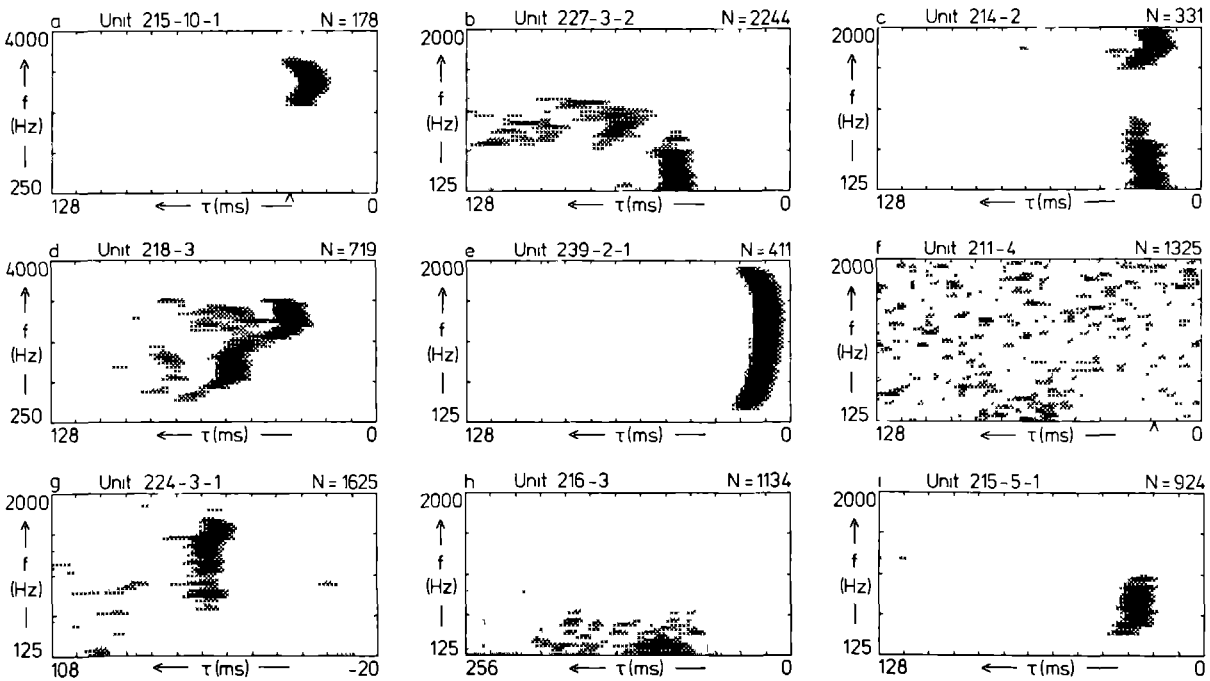

Fig. 3. IFT types estimating spectro-temporal sensitivities to tonal stimuli. The horizontal axis represents time before an event. The vertical axis, representing frequency, has a logarithmic scale. Intensity is coded in gray. Activation is represented by a darker than background gray level, inhibition by a lighter than background gray level. a Monomodal IFT. b-d Bimodal IFTs. e Broadly tuned IFT. f Inhibitory IFT. g Inhibitory IFT with a post-inhibitory activation. h Example with inhibitory sidebands. i Example of post activation inhibition. All examples, except f, were stimulated with the long interval ensemble. The arrowheads in a and f mark the position of latency for excitatory and inhibitory regions respectively. Note the different time scale in g and h. A detailed description of the IFTs is given in the text.

The monomodal purely excitatory IFT is the most common type encountered (52%). It represents a relatively simple excitatory STS in one of the three frequency ranges: low frequency 0-400 Hz, mid

ble and 8 ms for the short interval ensemble. Therefore the latency (LT) is defined as that time before a spike corresponding to the right edge of the activation region plus 24 ms resp. 8 ms. In the

case of units firing transiently to a tonepip LT is also equal to the time corresponding to the left edge. In the case of a tonic response, however, the activation region is enlarged to the left, then the time corresponding to the left edge would overestimate LT. For the transiently firing unit 215-10-1 LT is estimated at 35 ms before a spike, indicated by the arrowhead in Fig. 3a. It is observed that latencies are slightly frequency dependent, becoming longer for frequencies differing from BEF. This is a rather general phenomenon especially for short latency units.

Bimodal excitatory IFTs, with excitation in two of the three frequency regions, were observed in 27% of the cases. In Fig. 3b a low-mid frequency combination (25% of the bimodal IFTs) is depicted. The low frequency region has a BEF of 140 Hz and a LT of 50 ms. The mid frequency range shows a considerable time-jitter, not uncommon in long latency regions, its BEF is 400 Hz and LT is 72 ms. A low high combination (35% of the bimodal IFTs) is unit 214-2 (Fig. 3c). BEFs are 180 Hz and 1350 Hz LTs are 27 and 23 ms respectively. Sometimes this unit responded with two or three spikes to high frequency tones. Unit 218-3 is an example of a mid-high frequency bimodal IFT (40% of the cases), Fig. 3d. BEFs are 650 Hz and 1300 Hz, LTs are 42 ms and 66 ms respectively. Also a clear repetitive firing is present.

Trimodal or broadly tuned excitatory IFTs represent 7% of the STSs. The excitation region extends into all three frequency regions. An example is unit 239-2-1 (Fig. 3e). The latency of this unit is 18 ms. No clear BEF can be designated.

In a minority (10%) of the IFTs inhibitory regions dominated. An example of a purely inhibitory IFT is that of unit 211-4, Fig. 3f. As a consequence of a total lack of activity in such inhibitory regions, it is not straightforward to define the best inhibitory frequency (BIF) and LT, because no precise minimum can be appointed. Therefore we estimated the BIF as that frequency at which the inhibitory region was most conspicuous, or when more appropriate as the median of the inhibitory region. The LT was defined as the time corresponding to the right edge of the inhibitory effect, marked by the arrowhead. This estimate for LT corresponds well with the one obtained from post stimulus time histograms. For unit 211-4 these definitions resulted in BIF is 140 Hz and LT is 18 ms. In about half of these IFTs the inhibitory region was at the left preceded by an excitation within the same frequency range. (The word preceded is used because of the definition of τ as time before an event). This might be interpreted by saying that tonepips in a certain frequency region first decrease and thereafter increase firing probability. This phenomenon is called post-inhibitory activation. An example is unit 224-3-1, Fig. 3g. The inhibitory region is broadly tuned and has a latency of 8 ms. The activation region has a latency of 53 ms and a BEF of about 800 Hz and is in the low frequency region flanked by an offshoot of the initial inhibitory band. Most inhibitory regions are in the low and mid frequency range. Sometimes the inhibitory regions are very broad extending also into the high frequency range. The latencies often are short: 60% has LTs less than 20 ms.

A combination of pronounced excitatory and inhibitory effects occupying more or less different frequency bands, called sideband inhibition, was observed in 4% of the IFTs. This type of IFT cannot be due to lateral suppression, because only one stimulus frequency was presented at a time. Unit 216-3 is an example of a mid-high frequency inhibition with LT is 12 ms flanking a low frequency excitation with BEF is 150 Hz and LT is 42 ms (Fig. 3h). Other combinations, however, are also observed, high frequency side inhibition about equally often as low frequency side inhibition. Sometimes in predominantly excitatory IFTs also minor inhibitory aspects were present, e.g. in Fig. 3b inhibition flankes, at the right and on the high frequency side, the excitatory areas.

Post-activation inhibition, i.e. a period of decreased activity following excitation is present in 7% of the units. An example is unit 215-5-1, Fig. 3i. A low frequency excitatory area at 31 ms is immediately preceded at the left by a region of no activity; also an inhibitory sideband is present. Post-activation inhibition was observed in IFTs with BEFs in all frequency regions.

A further subdivision of the STSs might be made considering the temporal response patterns of the units, which is sometimes more pronounced in post stimulus time histograms than in IFTs. We will not proceed along this line in much detail but describe only some general observations. Of the units 67% responded only at the beginning of a tone, a phasic response. A tonic response, i.e. sustained firing during a large portion of the tone presentation, was observed in 33% of the units. In a large majority, about 40%, of the tonic responders and 10% of the phasic responders a chopper-like response pattern, i.e. structured repetitive firing, could be discerned too. In Figs. 3c and 3d some chopper-like activity is existent in the high frequency region. Often also two or three equally pronounced excitation areas spaced at regular intervals have been observed. Temporal response patterns often are dependent on stimulus presentation conditions such as intensity and side of stimulation (contra- or ipsilateral).

parison of the IFTs for both stimulus ensembles shows that on the average LT is longer for the short interval ensemble ($p < 1\%$, sign test). In 73% of the cases the same IFT type resulted, with BEFs and BIFs corresponding within a tolerance region of 10%. In 22% the IFT on the long interval ensemble was more broadly tuned, whereas in the remaining 5% the contrary was the case. Mostly this was due to a change from a bimodal to a monomodal IFT, sometimes also from a broadly tuned to a monomodal one.

In 30% of the frogs it was observed that the BEFs in the high frequency range were not equal within the same animals. This phenomenon was already noticed by Hermes et al. ([32], their Fig. 12i). Sometimes this may have been due to a tuning mismatch of the left and right papilla as in the example of Hermes et al. [32]. In most cases in the present study, however, a double or multiple tuning on one side could be ascertained, by stimulating units separately contra- and ipsilaterally. The multiple tuning mostly was not different for both

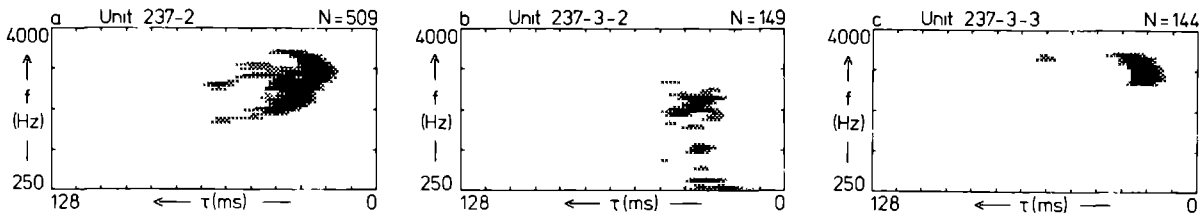

Fig. 4. IFTs of three units recorded at nearby positions in one and the same frog, indicating multiple tuning in the high frequency range. The stimulus was the long interval γ-tone ensemble presented binaurally at 90 dB SPL. Explanation in the text.

The relative frequencies of IFT-types were based on those stimulus conditions which elicited the most pronounced effects. Generally this was a binaural stimulus presentation at 90 dB SPL. Only in cases where ipsilateral input had a strong inhibitory influence, resulting in too little activity for analysis, the IFT upon contralateral stimulation was considered. In Fig. 3 all examples, except Fig. 3f, were obtained from stimulation with the long interval ensemble. Stimulation with both γ-tone ensembles was used in 80 units, for 70 units this resulted in an IFT for both ensembles. A comstimulus presentation sides. This points to a corresponding multiple tuning in left and right papilla. An example is frog 237, Fig. 4. The three units shown were recorded at nearby positions in the same hemisphere. Unit 237-2 (Fig. 4a) exhibits a somewhat vague double tuning with BEFs of 1100 and 1900 Hz and LTs of 36 and 26 ms respectively. Unit 237-3-2 (Fig. 4b) has a BFF of 1200 Hz, its LT is 38 ms. Unit 237-3-3 (Fig. 4c) has a BEF of 1900 Hz, its LT is 26 ms. The stimulus conditions were equal for the three IFTs shown, the long interval γ-tone ensemble was presented at 90 dB SPL binaurally.

Similar IFTs resulted in the case of ipsi- or contralateral stimulation. The same conclusions can be drawn on the basis of the short interval tonal ensemble or continuous noise. The differences between high frequency BEFs in frogs exhibiting this phenomenon were in the range 400-800 Hz. Possible smaller differences in the remaining frogs might not be noticed because of limitations in resolution.

3.3. Nature of the Stimulus-Event Relation for Noise Stimuli

Stationary gaussian wide-band noise was presented to 102 units. In 65 units noise stimulation resulted in an activation pattern clearly discernable from spontaneous activity. In 60 noise-responsive units an existence of a stimulus-event relation to this type of stimulus could be established. The 5 remaining noise-responsive units were strongly inhibited. In only 4 units having an existence a first-order crosscorrelogram, the 'revcor' function, resulted. These 4 units had low BEFs, the most pronounced example is unit 214-3 (Fig. 5). It

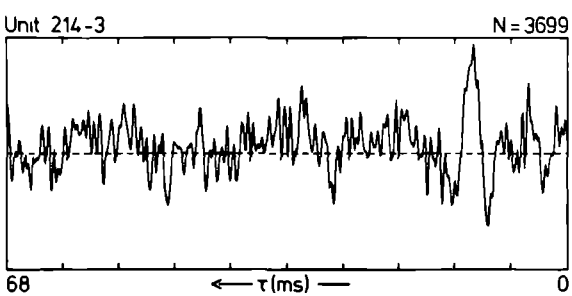

Fig. 5. First-order crosscorrelogram, the 'revcor' function, of noise stimulus and neural activity.

shows a deviation from background values at about 9 ms before an event, the power spectrum of this revcor function attains its maximum at about 250 Hz. These values agree very well with LT and BEF of the corresponding second-order STS. In 45 units showing an existence an STS resulted, i.e. an average PESE CoSTID different from the average SE-CoSTID (see Materials and Methods). Various types of STSs were encountered.

The monomodal excitatory type is observed in 58% of the units with a noise STS. An example is shown in Fig. 6a. A darker than average region, which is interpreted as excitation, is present at 750 Hz. A measure for latency is the response time (RT) which is defined as the time before a spike when the activation is maximal. For unit 236-2-1 this results in an estimate of 19 ms.

Bimodal excitatory STSs, having two distinct activation regions, were observed in 21%. Unit 215-2 (Fig. 6b) is an example. BEFs are 200 and 800 Hz, RTs are 13 and 15 ms respectively. All combinations of frequency ranges were noticed. One example of a STS with even three discrete excitatory regions was observed, Fig. 6c. The strength of the excitation is diminishing towards higher frequencies. The BEFs are 230, 750 and 1450 Hz and the respective RTs are 20, 15 and 13 ms.

An inhibitory STS was found in 2% of the cases. Unit 211-4 (Fig. 6d) shows a lighter than average region with a BIF of 80 Hz and a RT of 42 ms. In addition this unit exhibits post-inhibitory activation within the same frequency range and with a RT of 65 ms.

Sideband inhibition was observed in 19% of the units with a noise STS. An example is shown in Fig. 6e. Unit 220-7 has an excitatory region with a BEF of 125 Hz and a RT of 35 ms. On the high frequency side of the excitation an inhibitory region is present with a BIF of about 320 Hz and a RT of about 38 ms. In the noise ensemble a broad range of frequencies is present at any time. Therefore it is possible that some of the sideband inhibition STSs reflect lateral suppression. Inhibition both on the low as well as on the high frequency side of the excitation region was observed. All inhibitory sidebands, however, were contained in the low or mid frequency range suggesting amphibian papilla origin.

Post-activation inhibition, i.e. an excitation region followed by inhibition within the same frequency range, is present in 14% of the noise STSs. Unit 211-2 (Fig. 6f) has BEFs of 85 and 550 Hz with RTs of 24 and 11 ms respectively. The mid frequency range excitation is preceded at the left side by an inhibitory region with a RT of about 14 ms. Post

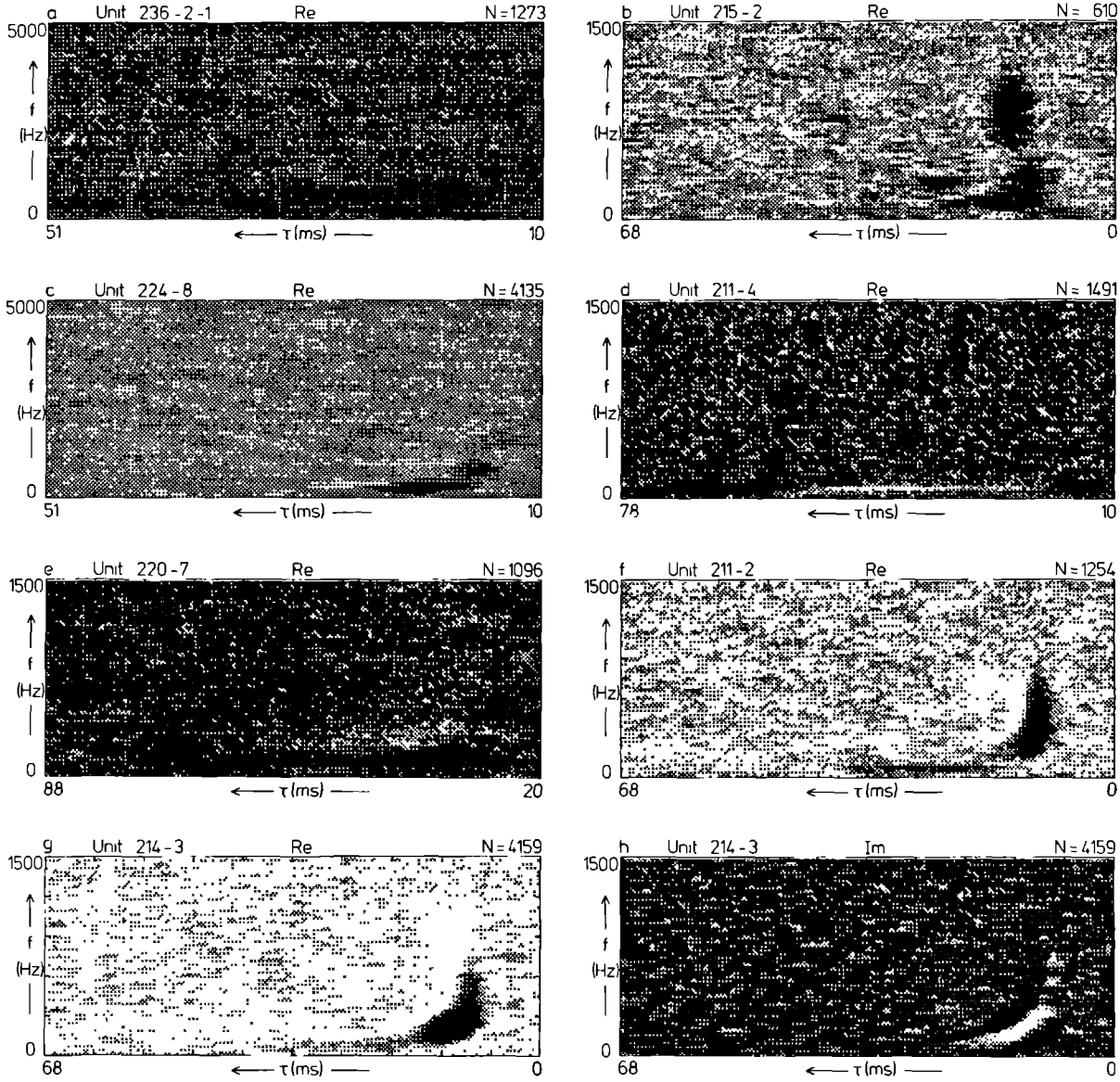

Fig. 6. STS types upon continuous noise stimulation. The horizontal axis represents time before an event. The vertical axis represents frequency on a linear scale. Intensity representing activation or inhibition is coded in gray. Only the real (Re) parts of the STSs are shown except for unit 214-3. a Monomodal excitatory STS. b Bimodal excitatory STS. c Trimodal excitatory STS. d Inhibitory STS. e STS with sideband inhibition. f STS with post-activation inhibition. g STS indicating a preference for upward sweeping frequencies. h Imaginary (Im) part of STS of which the corresponding real part is shown in g. The figures are scaled to their own extrema for better visualization. A drawback of this choice is that gray levels represent different values in different images. The extrema are: -1.6,1.8 (a); -1.8,3.1 (b); -1.1,1.8 (c); -0.9,0.9 (d); -1.3,1.2 (e); -1.1,2.4 (f); -0.7,1.9 (g); -1.1,1.1 (h). Note different time scales.

activation inhibition is also present in the low and mid frequency range in Fig. 6c. All units with post-activation inhibition upon noise stimulation, had BEFs in the low or mid frequency range.

A rather remarkable STS is that of unit 214-3, Fig. 6g. The excitatory region starts at 34 ms before a spike with a frequency of 120 Hz. At 20 ms it sweeps upward to reach 500 Hz at 9 ms before a spike. On the high frequency side an inhibitory sideband is present, that sweeps accordingly from 240 to 1000 Hz in the same time span. This unit had a very pronounced imaginary part in its STS (Fig. 6h), that corroborates the upsweeping character of the frequency sensitivity. This STS might point to a preference of this unit for upsweeping frequency, which however was not tested with frequency modulated tones. Notwithstanding a possible preference for frequency modulated tones, this unit was also excited by constant frequency tones. The unit did not show any frequency dependent latency to these tones, so it is unlikely that frequency dependent latency can account for the noise STS.

3.4. Comparison of STSs to Tonal and Noise Stimuli

To 107 units both tonal and noise stimuli were presented at the same overall stimulus intensity. Per frequency band, however, intensity for noise is less than for tonal stimuli. For only 44 units a STS was obtained for both types of stimuli, due to the absence of mostly a noise STS for the remaining units. Of these 44 units 28 had the same type of STS for both noise and tonal stimulus ensembles, apart from some shift in latency. Often latency for noise was longer than for tones. The remaining 16 units had different STSs for the two types of stimuli. These 16 units all had multimodal STSs upon tonal stimulation. Upon noise stimulation 12 of these units had a monomodal STS, caused by a disappearing of a mid or a high frequency excitation region that was present together with a low frequency excitation region for tonal stimuli. In 3 units an inhibitory region, present for tonal stimuli, was absent in the case of noise. In 3 other units the opposite occurred. In 1 unit a mid frequency excitatory region present for tonal stimuli was replaced by a high frequency excitatory region upon noise stimulation.

3.5. Intensity Effects on Spectro-Temporal Sensitivities.

It is known that intensity of a stimulus influences firing rate, latency and quality of tuning (e.g. [37,48]). In general, firing rate is an increasing function of intensity, whereas latency and quality of tuning are mostly decreasing. However, units were observed with other than monotonically varying relationships. From our sample of units 29 were stimulated at intensities of both 70 and 90 dB SPL. Two of these units responded only at 90 dB SPL, whereas one unit reacted only at onset at 90 dB SPL but fired in a sustained way at 70 dB SPL.

Of the remaining 26 units 21 had larger firing rates at 90 dB SPL (17%-79%), 3 units had about the same firing rate at both intensities and 2 units had a smaller firing rate at 90 dB SPL. In 16 units the latency at 90 dB SPL was smaller (2-24 ms), the other 10 units had comparable latencies at both intensities. In 20 units tuning was broader at 90 dB SPL, whereas in 2 units the opposite was observed. Sometimes this was due to a change from a multimodal to a monomodal STS, indicating different thresholds for the different frequency bands. In 5 units, all with BEFs in the mid or high frequency range, an increase of the BEF at 90 dB SPL with respect to that at 70 dB SPL was observed ranging from 100-400 Hz.

3.6. Distribution of Best Frequency and Latency

For 65 monomodal and 46 multimodal units unequivocal estimates of respectively single and multiple BEFs and BIFs could be determined to tonal stimuli at 90 dB SPL. Their distribution is shown in Fig. 7, the maximum BF encountered was 2200 Hz. A separation can be observed around 400 Hz. This probably reflects the division between units receiving input from the two parts of the amphibian papilla, which exhibit two-tone suppression or not [48]. No clear separation is present between the mid and high frequency regions, that discriminates

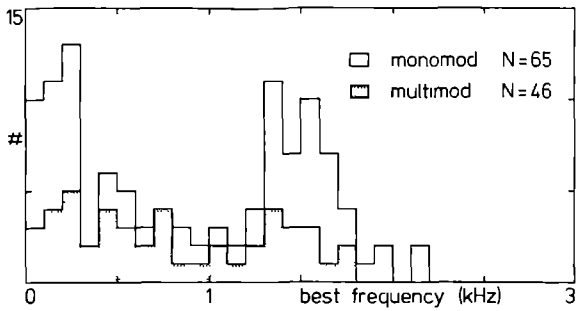

Fig. 7. Distribution of best frequencies (excitatory and inhibitory) upon tonal stimulation at 90 dB SPL. A distinction is made between units with monomodal and multimodal spectro-temporal sensitivities. In order to get equal contributions of mono- and multimodal units, the contributions of the latter were spread evenly over their respective best frequency bins.

units receiving input from the amphibian or basilar papilla. Walkowiak [48] reports a separation at about 900 Hz on the basis of characteristic frequencies measured at threshold. Relatively few monomodal units are present in the 400-1200 Hz range. The BIFs were almost all contained in the low and mid frequency region.

Reliable estimates of single or multiple latencies could be obtained for 75 monomodal and 63 multimodal units to tonal stimuli at 90 dB SPL. Their distribution is depicted in Fig. 8, it ranges from 7-108 ms. A large peak around 28 ms and a smaller one around 55 ms are observed. The distributions for monomodal and multimodal units are not very different, although there is a slight overrepresentation of multimodal units in the short latency range (< 20 ms). This is partly due to the short latencies of inhibitory regions, that often accompany excitatory regions.

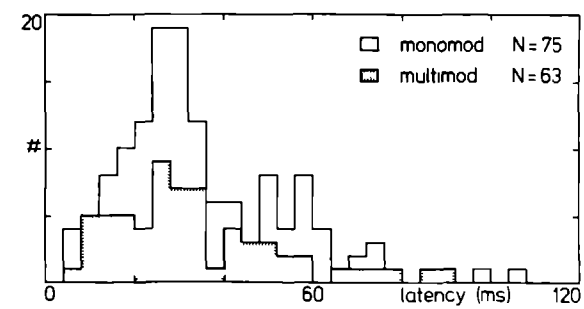

Fig. 8. Distribution of response latencies upon tonal stimulation at 90 dB SPL. A distinction is made between units with monomodal and multimodal spectro-temporal sensitivities. In order to get equal contributions of mono- and multimodal units, the contributions of the latter were spread evenly over their respective latency bins.

3.7. Binaural Interaction Pattern

Under closed mouth conditions binaural interaction was determined for 46 monomodal and 37 multimodal units. Of the 37 multimodal units 21 showed a complex binaural interaction pattern: different types of binaural interaction occurred for different frequency bands in one and the same unit. This complex behavior was already noted by Feng and Capranica [21] in a small fraction of superior olivary units in Hyla cinerea. Binaural interaction type was classified into three categories according to the response on ipsi-, contra- and bilateral stimulation. In 33% an EO response was obtained, i.e. the unit was excited by stimulation of one ear, whereas stimulation of the other ear had no influence both in monaural and binaural stimulus presentations. In 36% an EE response was determined, i.e. the unit was excited by stimulation of both ears separately or simultaneously. An EI response was observed in 31%: the unit is excited by stimulation of one ear and inhibited by the other ear. In the case of multimodal units each excitation or inhibition region was considered separately. No significant difference was observed in distribution of binaural interaction type for mono- and multimodal units, although an LL response seemed to occur more often in monomodal units. The relation of binaural interaction type and spectro temporal sensitivity will be considered more extensively in a forthcoming paper [17].

3.8. Action Potential Waveforms

On the basis of single-unit or separated few unit recordings five distinct types of action potential waveforms could be distinguished (Fig. 9). Type I waveforms, comprising 18%, are mono- or bi-

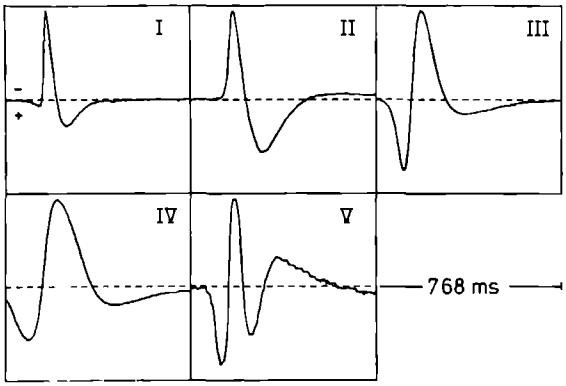

Fig. 9. Action potential waveform types from the frog's auditory midbrain. Generally type I and II action potentials are of small amplitude, whereas type III, IV and V have larger amplitudes. Negative polarity is upwards.

phasic initially negative spikes with a short duration of about 2 ms. Sometimes also a small positive going phase preceding the larger negative one is present. Type II waveforms (45%) are biphasic negative starting spikes, the second positive phase is more pronounced than for type I. The duration is about 3 ms. Also action potential waveforms, which have an intermediate form between type I and II, were noticed. Both types I and II have small amplitude (< 200 μV). Type III (34%) starts with a large positive deflection and is mostly triphasic, its duration is about 5 ms. Type IV (2%) is an elongated version of type III with a duration sometimes exceeding 7 ms. Occasionally type V polyphasic action potentials (1%) were recorded. The amplitudes of type III, IV and V are of larger voltage (> 300 μV), and sometimes exceed 1 mV. This multitude of waveform types has also been observed in the olfactory epithelium [30] as well as in the optic tectum [50] of the frog; duration and amplitude were in the same range. With present-day knowledge, however, it is difficult to relate action potential type to discrete classes of neurons or parts thereof. Presumably type I actionpotentials, because of there small and fast waveforms, are recorded near axonal processes.

3.9. Correlations among Neural Characteristics

A single unit can be described by many functional and structural parameters. Functional properties as the average STS, from which BF, LT and aspects of multimodality can be derived, binaural interaction type, mode of firing upon continuous noise and spontaneous activity provide information about the units role in identification and localization of sound. Structural properties as action potential waveform and location inform about aspects of morphology and anatomy. Studying correlations among these properties might provide evidence whether or not various aspects of auditory information processing are handled by different neural populations. Furthermore it might answer whether or not certain aspects are processed independently from others. These correlations are basically complex and multivariate. In a first approximation only bivariate correlations were established based on χ^2-tests (Fig. 10).

Best frequency was correlated with latency, multimodality of STS, spontaneous activity and binaural interaction type. Units with long latencies (LT > 40 ms) were somewhat overrepresented in the population of mid and especially low frequency units ($p < 5\%$). Only 15% of the high frequency units had long latencies. Monomodal units are slightly overrepresented in the population of high frequency units and relatively absent in the mid frequency range ($p < 0.5\%$). Spontaneous activity was more common in low frequency units than in high frequency units ($p < 0.5\%$), mid frequency units showed intermediate spontaneous activity. High frequency units were overrepresented in the population of EE units, whereas low frequency units were abundant in the EI population ($p < 0.5\%$). Mid frequency units and EO units were more or less evenly distributed over the categories. No significant correlation of BF with location in the torus was found.

Latency was correlated, besides with BF, with waveform, multimodality, sustained firing to noise and location in the torus. Units with type I waveforms had predominantly, although not exclusively, short latencies: more than half of the type I units had LTs < 20 ms, but also some type I units were

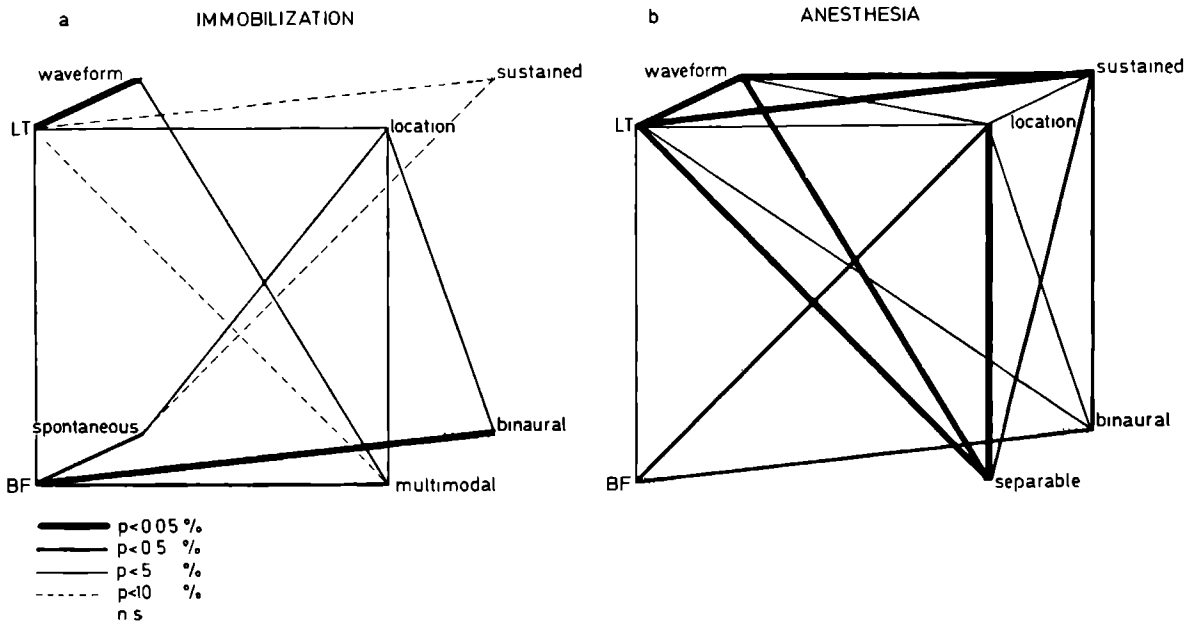

Fig. 10. Diagram showing the relations of functional characteristics of auditory neurons in the midbrain of the immobilized (a) and lightly anesthetized (b) grassfrog. The diagram for the anesthetized frog was adopted from [34]. Strength of the pairwise correlations are based on χ^2-tests. The thin dotted lines along the edges are drawn just for a better visualization of the correlation cube, they do not indicate significant correlation.

found with LT > 60 ms. Type II units were relatively absent in the short latency region, whereas type III units had latencies more or less evenly distributed over the categories. Multimodal units were slightly overrepresented in the short latency range ($p < 10\%$). Although there is considerable overlap of latency distributions of units with sustained or transient activity to noise, sustained units tend to have somewhat shorter latencies ($p < 10\%$). Units in caudal parts of the torus had on the average shorter latencies than units in rostral parts ($p < 5\%$).

Location in the torus was, besides with LT, correlated with multimodality, spontaneous activity and binaural interaction. Multimodal units are overrepresented in lateral parts of the torus ($p < 5\%$) Moreover simultaneously recorded units had, more often than expected by mere chance, all monomodal or all multimodal STSs ($p < 1\%$). Spontaneously active units were more common in caudal parts of the torus than in rostral parts ($p < 5\%$). Simultaneously recorded units shared, more than expected by mere chance, the same type of binaural interaction type ($p < 5\%$).

Relatively many type I units (63%) had multimodal spectro-temporal sensitivities. Type II waveforms were equally distribruted over the populations of monomodal and multimodal units. Of the units with a type III waveform only 30% had a multimodal STS.

Spontaneous active units tended to fire more often sustained to noise than non spontaneous units ($p < 10\%$).

The correlations among the various properties are summarized in a correlation diagram (Fig. 10a). For comparison also the diagram for the lightly anesthetized grassfrog is shown (Fig. 10b), which was adopted from [34] and based on the methods and data of Hermes et al. [31,32]. In the latter diagram spontaneous activity is not considered because of its lack in anesthetized frogs. Torus units in the lightly anesthetized frog had almost

all monomodal or sometimes broad STSs [32], therefore multimodality was considered less appropriate. Instead separability of STS was determined. A STS is separable if it can be factorized into its respective temporal and spectral components without loss of information. Units with non separable STS mostly had frequency dependent latencies [12]. These units were regarded as being elements of the second complex stage of information processing in the torus semicircularis of the lightly anesthetized grassfrog [32]. There appeared to be a very strong positive correlation between multimodality and lack of separability of STSs ($p < 0.01\%$) for units in the immobilized frog. Therefore separability was not considered separately for the immobilized frog.

A comparison of the diagram for immobilized and lightly anesthetized frogs shows that correlations in the immobilized frog are distinctly weaker. This points to a more complex and less predictable mode of behavior of torus units in the immobilized frog. On the basis of latency it often was possible to predict well other characteristics in the anesthetized frog, in the immobilized frog this task is hardly feasible. Apart from a different strength of correlation, most relations between the various neural characteristics are qualitatively about the same for the two animal preparations, e.g. short latency units tend to show a sustained firing upon noise stimulation in both preparations. An exception is the relation between form (i.e. multimodality or separability) of the STS and latency. In anesthetized frogs long latency units strongly tend to have non separable STSs, whereas in the immobilized frog there is a slight tendency for short latency units to have multimodal STSs.

4. Discussion

4.1. Neural Responsiveness

The responsiveness of the units investigated in this study agrees well with the results of Walkowiak [48]. About the same fraction of units showed a sustained overall discharge behavior to a tonal stimulus ensemble. The spontaneous activity is somewhat less in our study, presumably due to recording in different seasons. Walkowiak [48] reports an enhanced spontaneous activity during the summer, a season in which we did not experiment. About the same numbers were obtained for immobilized toads, Alytes obstetricans and Bufo viridis [37]. Striking differences, however, are observed comparing these results with those of the lightly anesthetized grassfrog [31,32]. In these papers hardly any spontaneous activity was reported, also the responsiveness to tonal and noise stimuli was distinctly less compared with the present study.

The large fraction of units responding to the γ-tone ensembles could be due to a sampling bias in our study (and also that of Hermes et al. [31, 32]). Mostly the long interval γ-tone ensemble was presented during search for units. Therefore units only responsive to a combination of different frequency bands or to natural sounds might have been unnoticed. Evidence for the latter was obtained by Walkowiak [48] and in recent investigations in our laboratory. Fuzessery and Feng [24] reported some units located in rostral parts of the torus in Rana pipiens, that responded only to certain frequency combinations.

4.2. Distribution of Best Frequencies

The distribution of best frequencies matches well with the frequency spectrum of the grassfrog's vocalizations. Also a large portion of very low frequency (< 300 Hz) sensitive units is present, perhaps for detection of substrate vibrations or water surface waves during the mating season. The relative abundance of mid frequency BFs in multimodal units maybe reflects the important role of this frequency range in complex stages of frequency discrimination. The BF distribution as obtained in this study is not very different from the distribution for anesthetized grassfrogs [32]. This indicates that anesthesia does not affect the amphibian and basilar papilla differently. A difference, however, remains between the ratios of units receiving amphibian or basilar papilla input in our study and those conducted by others. Bibikov [5] reports, al-

so for the grassfrog, a distribution of 62%-38% receiving amphibian respectively basilar papilla input. This is not very different from our results. Walkowiak [48], on the contrary, arrives at 80%-20% for the same species. In other species 3:1 or 4:1 ratios were noticed: Fuzessery and Feng [24] found 84%-16% for Rana pipiens, Mohneke [37] reports 75%-25% for Alytes obstetricans and Bufo viridis. These studies used closed stimulation systems. In a study using an open stimulation system Feng [22] estimates 56%-44% for Rana pipiens.

Our results (and those of Hermes et al. [32]) do not correspond well either with results from more peripheral parts of the auditory pathway. For the auditory nerve in Rana catesbeiana Feng et al. [20] found a 3:1 ratio, this was corroborated by Dunn [11] in an anatomical study. In the dorsal nucleus of Rana pipiens Fuzessery and Feng [25] report a 87%-13% distribution. In the same study a 55%-45% distribution for the superior olivary nucleus was observed, whereas Feng and Capranica [21] observed 76%-24% in the same nucleus in Hyla cinerea. Several factors might explain these different findings. 1) There may be a difference between species, reflecting innate mechanisms serving frequency selection matched to different mating calls. 2) Experiments conducted with open or closed stimulation systems and open or closed mouth conditions may result in different ratios, because of the important role of the ear-mouth system in shaping resonances [43]. 3) Most studies were conducted at threshold intensities. This study (and that of Hermes et al. [32]) used relatively high intensities, probably corresponding to more natural levels. Fuzessery and Feng [24] report a decrease of BF for units with CF < 500 Hz and an increase of BF for units with CF > 500 Hz as sound level increases. This finding is corroborated in this study for high frequency units. Therefore the division at 900 Hz for the grassfrog between units receiving amphibian or basilar papilla input [48], probably shifts upwards at higher stimulus intensities. 4) There may also be a seasonal influence especially on mid frequency units, which seem to be more abundant in the mating season than in other seasons [37].

The double tuning found for high frequency units in the same animals might indicate a double tuning of the basilar papilla. This, however, would disagree with almost all other studies. These state that the basilar papilla is a simple organ tuned to one narrow band of frequencies, the variation seen in the high frequency part of the BF distribution being due to inter-individual variations. We are not certain whether the double tuning in the same animal is originating from the basilar papilla itself. The lower frequency portion (1100-1200 Hz) of the double tuning might as well originate from the amphibian papilla, due to an upward shift of BFs at higher intensities. Further study is necessary to settle this issue.

4.3. Distribution of Latencies

The bimodal distribution of latencies found in this study agrees well with the distribution for the anesthetized grassfrog [32], apart from some shift towards smaller latencies for the immobilized preparation. Advancing along the auditory pathway latencies on average are increasing. In the auditory nerve latencies vary from 3-10 ms [8]. In the dorsal nucleus latencies range from 6-12 ms [25]. In the superior olivary nucleus the latency range is 10-50 ms [25]. In the torus semicircularis latencies for intense sounds are contained in the range 7-108 ms (this study). In the thalamic auditory center latencies between 26 and 75 ms were reported [26]. The trend of increasing latencies towards higher centers, besides conduction and synaptic delays, presumably reflects an increasing level of complexity of auditory processing. A considerable amount of overlap, however, remains between the latency distributions at the various stations. This might indicate that a substantial part of the auditory processing does not take place sequentially but acts in parallel or even is distributed [10]. The relatively short latencies of many inhibitory effects suggest a partly inhibitory influence of lower auditory stations on the auditory midbrain. Possible inhibitory modulations originating from higher stations might be more subtle and more difficult to notice.

4.4. Types of Spectro-Temporal Sensitivities

A rich collection of STS types for both tonal and noise stimuli was obtained. Only about 50% of the STSs in this study were of the monomodal excitatory type. This type comprises about 90% in the lightly anesthetized grassfrog, in which also fewer inhibitory phenomena were manifest [31,32]. Comparison with other studies is hindered because of different stimulus intensities applied and different entities determined, i.e. STSs versus tuning curves. Walkowiak [48] reports that 97% of the tuning curves are V-shaped excitatory. At higher intensities, however, the tuning may broaden to comprise more frequency regions. Fuzessery and Feng [24] observed in 95% V-shaped excitatory and in 5% W-shaped excitatory tuning curves. The latter indicates double tuning already at threshold intensities. In addition they present iso-activity contour plots, which are more comparable to the STS concept. From these contour plots double and multiple tuning at supra-threshold intensities can be observed. A somewhat richer collection of tuning curves was reported by Mohneke [37], who described also inhibitory phenomena upon stimulation with pure tones.

In the auditory nerve and dorsal nucleus all units have excitatory V-shaped tuning curves for pure tones. This indicates a sensitivity to a restricted continuous band of frequencies at least for low intensities [8,25]. The first auditory nucleus in which bimodal W-shaped tuning curves appear is the superior olivary nucleus, Fuzessery and Feng [25] reported this type of tuning curve in 6% of the units. In the thalamic auditory center convergence is already so complex that only 10% of the units have V-shaped tuning curves. A lot of these thalamic units seem to operate as AND-gates for the different frequency regions [26].

The same conclusions apply to temporal response patterns upon tonal stimulation. In the auditory nerve all units fire tonically [8]. For higher stations the number of tonically firing units steadily decreases to reach zero level in the thalamic auditory center [26]. The numbers found in our study, taking an intermediate position, fit well into this scheme.

4.5. Interdependencies among Neural Characteristics

The relations between the various neural characteristics were qualitatively the same for both the immobilized and anesthetized preparations. The strength of the correlations, however, was distinctly less in the immobilized frog. In the auditory midbrain properties seem to vary gradually from simple to complex. Short latency units may even reflect properties of lower auditory stations. Multimodal STSs in short latency units point at the presence of multiple tuning in lower auditory stations agreeing with the study of Fuzessery and Feng [25]. In the lightly anesthetized frog a discrete separation between simple and complex units could be made already on the basis of the bimodal latency distribution. This discrete two-stage information processing scheme is not appropriate to the auditory midbrain of the immobilized frog.

4.6. Tonotopic Organization of the Auditory Midbrain

On the basis of evoked potential studies [40] a tonotopic organization is claimed for the anuran auditory midbrain. On the basis of multi-unit recordings conflicting results were reported. Mohneke [38] established a tonotopic organization in Alytes obstetricans, whereas Walkowiak et al. [49] found no indications for it in Bufo viridis. Single-unit studies (e.g [32]) did not succeed in establishing a clear tonotopic structure. This may be due to inaccurate location of units, to lumping data from different individuals and different types of units. On the other hand, we found a mixture of frequency ranges in units recorded at close positions with the same electrode as well as in multimodal units. In the light of these findings it is unlikely that a clear and simple tonotopic organization is present in the entire auditory midbrain. This, however, does not exclude that a certain presumably complex shaped tonotopic structure may be present in restricted regions of the auditory midbrain. A candidate would be the nucleus princi-

palis, which is shown to have a circular lamellar anatomical organization [23].

4.7. Influence of Anesthesia

From a comparison of the present results obtained in immobilized grassfrogs and those obtained by Hermes et al. [31,32] in lightly anesthetized grassfrogs, which have been obtained in the same seasonal range using identical stimulus-analysis paradigms and electrode characteristics, it may be concluded that anesthesia makes the auditory midbrain appear like a more simple structure. This is evident on the single-unit level where less complex behavior is found, as well as on the organizational level where the discrete two-stage division comes forth.

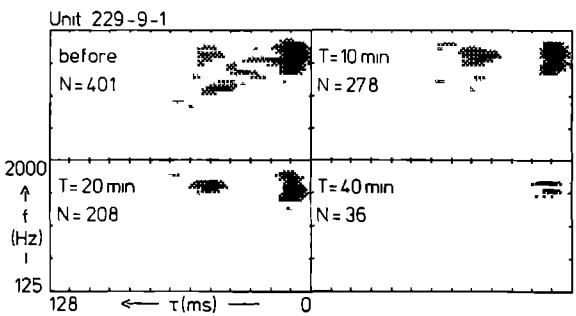

Fig. 11. IFTs of a unit before and at 10, 20 and 40 min after administration of MS-222 anesthesia.

Direct evidence for the influence of anesthesia on the STS is shown in Fig. 11. During the stable recording of this unit an anesthetic (MS-222) was added to the bathing solution of the immobilized grassfrog. Spike count decreased to about 10% of its original level and the STS area became much smaller. The initially rather broad STS separated into two discrete activation regions, the second of which is marked by an increasing latency. Furthermore, this initially noise responsive unit did not respond to continuous noise 45 minutes after the administration of the anesthetic.

The influence of anesthesia can be summarized in the following points: 1. spontaneous activity disappears, 2. the number of units that respond in a sustained way to stationary noise decreases, 3. the responsiveness of the units to stimulation decreases, 4. the STSs become smaller and simpler, 5. nearly all short latency units become simpler, and 6. inhibitory effects disappear. On the basis of this study it is hard to decide whether anesthesia alters the properties of all units, or that it selectively silences certain classes of units, while others remain unaffected.

In mammals hardly any effect of anesthesia upon activity from the auditory nerve and ventral cochlear nucleus is noted, but the effect is marked in the dorsal cochlear nucleus [19]. However, Capranica and Moffat [9] remarked that "the only difference in result obtained between the two types of preparation (anesthesia vs. immobilization) for this species (Bufo americanus) was that the level of spontaneous activity recorded (in the auditory nerve) from anesthetized animals was appreciably lower - many of the units were not spontaneously active. However, thresholds, BEF distribution, sensitivity to two-tone suppression, etc., were comparable".

Thus no single mechanism can be responsible for the observed facts, yet most of the phenomena can be accounted for by a threshold increase. This could account for items 3, 4 and 5 and probably also for 6, while the combination of decreasing spontaneous activity and threshold increase could account for item 2. The threshold increase is probably a central phenomenon and could be the result of an effect of anesthetic on modulatory pathways involved with complex information processing. These pathways could be residing in the auditory midbrain or be descending from nuclei in the thalamus and forebrain. The effect is probably also present on a lower level than the torus semicircularis, because of the pronounced effect of anesthesia on the short latency units in our population.

Acknowledgements

This investigation forms part of the research program "Brain and Behaviour" at the Department of Medical Physics and Biophysics of the University of Nijmegen and was supported by the Netherlands Orga-

nization for the Advancement of Pure Research (ZWO). The authors wish to thank Jan Bruijns and Wim van Deelen for software development, Koos Braks for the animal preparations and technical assistance, Hans Krijt and his group for electronic support and Marianne Nieuwenhuizen for typing the manuscript. Ad Aertsen, Henk van den Boogaard, Jan van Gisbergen and Peter Johannesma are gratefully acknowledged for critically reading the manuscript.

References

1 Aertsen, A.M.H.J., Smolders, J.W.T. and Johannesma, P.I.M. (1979): Neural representation of the acoustic biotope: on the existence of stimulus-event relations for sensory neurons. Biol. Cybern. 32, 175-185.

2 Aertsen, A.M.H.J. and Johannesma, P.I.M. (1980): Spectro-temporal receptive fields of auditory neurons in the grassfrog. I. Characterization of tonal and natural stimuli. Biol. Cybern. 38, 223-234.

3 Aertsen, A.M.H.J., Johannesma, P.I.M. and Hermes, D.J. (1980): Spectro-temporal receptive fields of auditory neurons in the grassfrog. II. Analysis of the stimulus-event relations for tonal stimuli. Biol. Cybern. 38, 235-248.

4 Aertsen, A.M.H.J. and Johannesma, P.I.M. (1981): A comparison of the spectro-temporal sensitivity of auditory neurons to tonal and natural stimuli. Biol. Cybern. 42, 145-156.

5 Bibikov, N.G. (1974): The impulse activity of torus semicircularis neurons of the frog *Rana temporaria*. Zh. Evol. Biokhim. Fiziol. 10, 40-47.

6 Boer, E. de and Kuyper, P. (1968): Triggered correlation. IEEE Trans. Biomed. Eng. 15, 169-179.

7 Brzoska, J., Walkowiak, W. and Schneider, H. (1977): Acoustic communication in the grass frog (*Rana t. temporaria* L.): calls, auditory threshold and behavioral responses. J. Comp. Physiol. A 118, 173-186.

8 Capranica, R.R. (1976): Morphology and physiology of the auditory system. In: Frog Neurobiology, pp. 551-575. Editors: R. Llinas, W. Precht. Springer, Berlin.

9 Capranica, R.R. and Moffat, A.J.M. (1980): Nonlinear properties of the peripheral auditory system of anurans. In: Comparative studies of hearing in vertebrates, pp. 139-165. Editors: A.N. Popper and R.R. Fay. Springer, New York, Heidelberg, Berlin.

10 Capranica, R.R. and Rose, G. (1983): Frequency and temporal processing in the auditory system of anurans. In: Neuroethology and behavioral physiology, pp. 136-152. Editors: F. Huber and H. Markl. Springer, Berlin, Heidelberg.

11 Dunn, R.F. (1978): Nerve fibers of the eighth nerve and their distribution to the sensory nerves of the inner ear in the bullfrog. J. Comp. Neurol. 182, 621-636.

12 Eggermont, J.J., Aertsen, A.M.H.J., Hermes, D.J. and Johannesma, P.I.M. (1981): Spectro temporal characterization of auditory neurons: redundant or necessary? Hearing Res. 5, 109-121.

13 Eggermont, J.J., Hermes, D.J., Aertsen, A.M.H.J. and Johannesma, P.I.M. (1981): Response properties and spike waveforms of single units in the torus semicircularis of the grassfrog *(Rana temporaria)* as related to recording site.- In: Neuronal Mechanisms of Hearing, pp. 341-345. Editors: J. Syka and L. Aitkin. Plenum Press, New York London.

14 Eggermont, J.J., Aertsen, A.M.H.J. and Johannesma, P.I.M. (1983): Quantitative characterisation procedure for auditory neurons based on the spectro-temporal receptive field. Hearing Res. 10, 167-190.

15 Eggermont, J.J., Aertsen, A.M.H.J. and Johannesma, P.I.M. (1983): Prediction of the responses of auditory neurons in the midbrain of the grassfrog based on the spectro-temporal receptive field. Hearing Res. 10, 191-202.

16 Eggermont, J.J., Epping, W.J.M. and Aertsen, A.M.H.J. (1983): Stimulus dependent neural correlations in the auditory midbrain of the grassfrog (*Rana temporaria* L.). Biol. Cybern. 47, 103-117.

17 Epping, W.J.M. and Eggermont, J.J. (1985): Relation of binaural interaction and spectro-temporal characteristics in the auditory midbrain of the grassfrog. Hearing Res. (in press).

18 Evans, E.F. and Nelson, P.G. (1973): The responses of single neurones in the cochlear nucleus of the cat as a function of their location and anaesthetic state. Exp. Brain Res. 17, 402-427.

19 Evans, E.F. (1974): Neural processes for the detection of acousticpatterns and for sound localization. In: The Neurosciences, third study program, pp. 131-145. Editors: F.O. Schmitt and F.G. Galambos. MIT Press, Cambridge Mass.

20 Feng, A.S., Narins, P.M. and Capranica, R.R. (1975): Three populations of primary auditory fibers in the bullfrog *(Rana catesbeiana)* their peripheral origins and frequency sensitivities. J. Comp. Physiol. A 100, 221-229.

21 Feng, A.S. and Capranica, R.R. (1978): Sound localization in anurans. II. Binaural interaction in superior olivary nucleus of the green tree frog *(Hyla cinerea)*. J. Neurophysiol. 41, 43-54.

22 Feng, A.S. (1981): Directional response characteristics of single neurons in the torus semicircularis of the leopard frog *(Rana pipiens)*. J. Comp. Physiol. A 144, 419-428.

23 Feng, A.S. (1983): Morphology of neurons in the torus semicircularis of the northern leopard frog, *Rana pipiens pipiens*. J. Morphol. 175, 253-269.

24 Fuzessery, Z.M. and Feng, A.S. (1982): Frequency selectivity in the anuran auditory midbrain: single unit responses to single and multiple tone stimulation. J. Comp. Physiol. A 146, 471-484.

25 Fuzessery, Z.M. and Feng, A.S. (1983): Frequency selectivity in the anuran medulla: excitatory and inhibitory tuning properties of single neurons in the dorsal medullary and superior olivary nuclei. J. Comp. Physiol. A 150, 107-119.

26 Fuzessery, Z.M. and Feng, A.S. (1983): Mating call selectivity in the thalamus and midbrain of the leopard frog *(Rana p. pipiens)* : single and multiunit analysis. J. Comp. Physiol. A 150,

333-344.
27 Gelder, J.J. van, Evers, P.M.G. and Maagnus, G.J.M. (1978): Calling and associated behaviour of the common frog, *Rana temporaria* , during breeding activity. J. Anim. Ecol. 47, 667-676.
28 Gerhardt, H.C. (1974): The significance of some spectral features in mating call recognition in the green treefrog *(Hyla cinerea)*. J. Exp. Biol. 61, 229-241.
29 Gerhardt, H.C. (1978): Mating call recognition in the green treefrog *(Hyla cinerea)* : the significance of some fine-temporal properties. J. Exp. Biol. 74, 59-73.
30 Getchell, Th.V. (1973): Analysis of unitary spikes recorded extracellularly from frog olfactory receptor cells and axons. J. Physiol. 234, 533-545.
31 Hermes, D.J., Aertsen, A.M.H.J., Johannesma, P.I.M. and Eggermont, J.J. (1981): Spectro-temporal characteristics of single units in the auditory midbrain of the lightly anaesthetised grass frog (*Rana temporaria* L.) investigated with noise stimuli. Hearing Res. 5, 147-178.
32 Hermes, D.J., Eggermont, J.J., Aertsen, A.M.H.J. and Johannesma, P.I.M. (1982): Spectro temporal characteristics of single units in the auditory midbrain of the lightly anaesthetised grass frog (*Rana temporaria* L.) investigated with tonal stimuli. Hearing Res. 6, 103-126.
33 Johannesma, P., Aertsen, A., Cranen, L. and Erning, L. van (1980): The phonochrome: a coherent spectro-temporal representation of sound. Hearing Res. 5, 123-145.
34 Johannesma, P.I.M. and Eggermont, J.J. (1983): Receptive fields of auditory neurons in the frog's midbrain as functional elements for acoustic communication. In: Advances in vertebrate neuroethology, pp. 901-910. Editors: J.P. Ewert, R.R. Capranica and D.J. Ingle. Plenum Press, New York, London.
35 Kaulen, R., Lifschitz, W., Palazzi, C. and Adrian, H. (1972): Binaural interaction in the inferior colliculus of the frog. Exp. Neurol. 37, 469-480.
36 Klinke, R. and Pause, M. (1977): The performance of a primary hearing organ of the cochlear type: primary fiber studies in the caiman. In: Psychophysics and physiology of hearing, pp. 101-111. Editors: E.F. Evans and J.P. Wilson. Academic Press, London.
37 Mohneke, R. (1982): Coding of simple acoustic stimuli and conspecific calls in anuran auditory midbrain nuclei (*Alytes o. obstetricans* and *Bufo v.viridis*). Zool. Jb. Physiol. 86, 90-140.
38 Mohneke, R. (1983): Tonotopic organisation of the auditory midbrain nuclei of the midwife toad (*Alytes obstetricans*). Hearing Res. 9, 91-102.
39 Narins, P.M. and Hillery, C.M. (1983): Frequency coding in the inner ear of anuran amphibians. In: Hearing - Physiological basis and psychophysics, pp. 70-76. Editors: R. Klinke and R. Hartmann. Springer, Berlin, Heidelberg, New York, Tokyo.
40 Pettigrew, A., Chung, S.-H. and Anson, M. (1978): Neurophysiological basis of directional hearing in amphibia. Nature 272, 138-142.
41 Potter, H.D. (1965): Mesencephalic auditory region of the bullfrog. J. Neurophysiol. 28, 1132-1154.
42 Potter, H.D. (1965): Patterns of acoustically evoked discharges of neurons in the mesencephalon of the bullfrog. J. Neurophysiol. 28, 1155-1184.
43 Rheinlaender, J., Walkowiak, W. and Gerhardt, H.C. (1981): Directional hearing in the green treefrog: a variable mechanism? Naturwissenschaften 67: S. 430.
44 Ribaupierre, F. de, Rouiller, E., Toros, A. and Ribaupierre, Y. de (1980): Transmission delay of phase-locked cells in the medial geniculate body. Hearing Res. 3, 65-77.
45 Rose, J.E., Brugge, J.F., Anderson, D.J. and Hind, J.E. (1967): Phase locked responses to low-frequency tones in single auditory nerve fibers of the squirrel monkey. J. Neurophysiol. 30, 769-793.
46 Schetzen, M. (1980): The Volterra and Wiener theories of nonlinear systems. Wiley, New York.
47 Smolders, J.W.T., Aertsen, A.M.H.J. and Johannesma, P.I.M. (1979): Neural representation of the acoustic biotope, a comparison of the response of auditory neurons to tonal and natural stimuli in the cat. Biol. Cybern. 35, 11-20.
48 Walkowiak, W. (1980): The coding of auditory signals in the torus semicircularis of the fire bellied toad and the grassfrog: responses to simple stimuli and to conspecific calls. J. Comp. Physiol. A 138, 131-148.
49 Walkowiak, W., Capranica, R.R. and Schneider, H. (1981): A comparative study of auditory sensitivity in the genus *Bufo* (Amphibia). Behav. Processes 6: 223-237.
50 Witpaard, J. and Keurs, H.E.D.J. ter (1975): A reclassification of retinal ganglion cells in the frog, based upon tectal endings and response properties. Vision Res. 15, 1333-1338.

RELATION OF BINAURAL INTERACTION AND SPECTRO-TEMPORAL CHARACTERISTICS IN THE AUDITORY MIDBRAIN OF THE GRASSFROG

Willem J.M. Epping and Jos J. Eggermont

Department of Medical Physics and Biophysics University of Nijmegen, Geert Grooteplein Noord 21, NL-6525 EZ Nijmegen, The Netherlands

The relation between binaural interaction type and spectro-temporal characteristics was studied for single-units in the auditory midbrain of the grassfrog. Tonal and continuous wideband noise ensembles have been used as stimuli. Spectro-temporal sensitivities were determined for ipsi-, contra- and bilateral stimulus presentation by a closed sound system. Binaural interaction was classified in monaural EO (one ear excitatory), binaural EE (both ears excitatory) and EI (one ear excitatory, the other inhibitory) and purely inhibitory categories. Binaural interaction appeared to be rather invariant to alterations in stimulus intensity and type. A very clear correlation was observed between best frequency and binaural interaction type: EE-units are predominantly of high best frequency, whereas EI-units are predominantly of low best frequency. The correlation with latency was less significant: EE units tended to have somewhat shorter latencies than EI units. EO units take an intermediate position. Comparisons of ipsi-, contra- and bilateral spectro-temporal sensitivities, revealed differences in best frequency, latency and temporal discharge pattern. In some units a complex interplay of excitatory and inhibitory monaural influences was demonstrated. A number of units was recorded, which were characterized by multiple activation or suppression areas. The majority of these units exhibited frequency dependent binaural interaction types. In some units it was noticed that binaural interaction type can be dependent on state of adaptation. A comparison of binaural interaction types of neighbouring units provided only weak evidence for a binaural organization in the anuran auditory midbrain, since simultaneously recorded pairs shared the same binaural interaction type only slightly more than expected by mere chance (χ^2-test, $p < 0.10$).

anurans, auditory midbrain, binaural interaction, spectro-temporal sensitivity

1. Introduction

Behavioral studies have shown that anurans are able to localize sound sources, emitting conspecific mating calls, with an accuracy of 10^{o}-15^{o}. In order to do this both ears have to be intact and unobstructed [6,22,34]. The directional properties of the coupled middle ear system are such that the minute interaural intensity, time and phase differences are converted into the range that central nervous system neurons can realistically measure [4,21,33,37].

The anuran central auditory nervous system is characterized by extensive ascending bilateral and commissural projections already at the level of the dorsal medullary nucleus [40]. Units receiving binaural inputs have been reported in the dorsal medullary nucleus [19], superior olivary nucleus [20] and torus semicircularis [27,29,30,31]. The sensitivity for interaural intensity and time difference is enhanced towards more central nuclei [20], indicating additional spatial processing in the central auditory system. The existence of central spatial processing was corroborated by Feng [18] who showed that directional response curves of torus units could not be explained on basis of the properties of the peripheral acoustic receiver.

Almost all of the above mentioned studies on binaural processing in central auditory nuclei, were conducted at or near threshold stimulus inten-

---

Abbreviations: BF best frequency; CL contralateral; CoSTID coherent spectro-temporal intensity density; IFT intensity frequency time; IL ipsilateral; LT latency; PSTH post-stimulus time histogram; SPL sound pressure level; STS spectro-temporal sensitivity.

sities. At these intensities units generally can be characterized by one best excitatory or inhibitory frequency, although a small fraction of torus units has more complex tuning curves [23,38]. Binaural interaction type and temporal response patterns are then derived at these best frequencies. However, in a recent study using stimuli at higher and more natural intensities, a large population of torus units exhibited complex spectro-temporal properties: multiple excitatory or inhibitory frequency bands occurred, spectral and temporal properties often were interdependent [14]. The aim of the present study is to determine the relation between binaural interaction and spectro-temporal characteristics at natural and thus relatively high stimulus intensities. Furthermore the distribution of binaural interaction type of neighbouring units was investigated in order to obtain information about a possible binaural organization in the torus. Pettigrew et al. [30,31] claimed a spatial organization on the basis of evoked potential studies.

2. Materials and Methods

Details of animal preparation, acoustic stimulus presentation, recording procedure and stimulus response analysis have been described extensively in a previous paper [14]. Of these subjects only a brief description will be given here.

2.1. Animal Preparation

Under MS-222 anesthesia the dura above the tectum mesencephali of adult grassfrogs (Rana temporaria L.) was exposed. After two days of recovery the animals were immobilized with an intralymphatic injection of Buscopan (0.16 mg per gram bodyweight). The animal was placed dorsal side up onto a damped vibration isolated frame in a sound attenuated room (IAC type 1202A). During recordings the oral cavity was kept shut. Temperature was maintained constant around 16°C and the skin kept moist. The animal's condition was monitored by recording the ECG. Usually the preparation was kept intact, without any signs of deterioration, for at least two consecutive days.

2.2. Acoustic Stimulus Presentation

Acoustic stimuli were generated by a dual channel programmable stimulus generator build around a PDP 11/10. The generated stimuli were presented to the animals by two electrodynamic microphones (Sennheiser MD 211N) coupled to the tympanic membranes with a closed sound system. Care was taken to minimize mechanical crosstalk of stimulus apparatus to the ears. The sound pressure level was measured in situ with a half-inch condensor microphone (Brüel and Kjaer 4143) connected to the coupler. The frequency response of the sound system was flat within 5 dB for frequencies between 100 and 3000 Hz. The amplitude characteristics of left and right couplers were equal within 2 dB for the range of interest.

Tonal stimuli consisted of sequences of tonepips with a γ-envelope [1]. The duration of the tonepips was either 16 ms with onset intervals of 128 ms, or 48 ms with onset intervals of 1 s. The carrier frequencies were pseudorandomly varied and selected from 255 or 127 logarithmically equidistant values in a range comprising 4 or 5 octaves (125-2000 Hz, 250-4000 Hz, 100-3200 Hz). Noise stimuli, that consisted of pseudorandom gaussian wideband noise with satisfactory statistical properties, were presented continuously for at least 5 min. All stimuli consisted of at least 4 identical sequences.

2.3. Recording Procedure

Ultra-fine or tapered tungsten microelectrodes coated with parylene-c, having a 10-15 µm exposed tip with a 1 kHz impedance of 1.5-2.5 MΩ (Micro Probe Inc.) were used for extracellular recordings. The electrode (in later stages two simultaneously) was advanced through the intact dura and lowered into the auditory midbrain using a motorized hydraulic microdrive (Trent-Wells 3-0661 or Frederick Haer & Co), stepping precision was 1 µm. Electrode signals were amplified using Dagan 2400 Z extracellular preamplifiers bandpassed be-

tween 100 Hz and 10 kHz.

In this configuration simultaneous activity of small neural populations (up to four neurons, located within a sphere with a radius of about 25 μm) regularly is recorded on one electrode. In order to separate the superimposed few-unit activity into the component single-unit spike-trains a pattern recognition technique using the action potential waveform is applied (for details the reader is referred to [11]). Waveform features and spike-epochs are stored by a data-acquisition system build around a PDP 11/34 for off-line analysis. Temporal resolution is 60 μs.

2.4. Stimulus-Event Relation

Combined spectro-temporal characteristics for single-units were studied by determining spectro temporal sensitivities (STSs). The STS is defined as the average spectro-temporal stimulus intensity preceding a neural event, and is normalized to correct for overall stimulus properties. For the tonal stimulus ensemble the procedure is equivalent to a sonogram-type of analysis and is called IFT (intensity frequency time) analysis. In case of continuous noise ensembles complex-valued (in a mathematical sense) STSs result, called CoSTID (coherent spectro-temporal intensity density). This procedure is formally equivalent to determining the second order Wiener-Volterra kernel in nonlinear system theory. For both types of stimuli the procedures have been discussed and illustrated extensively in literature [1,13,14,26,27,28].

2.5. Location of Recording Site

Electrode tracks were made approximately orthogonal to the surface of the midbrain in both hemispheres. Position in the rostrocaudal-mediolateral plane was determined by marking the entrance of a track on a photograph made of the surface of the midbrain. All entrances were made within a region extending from 300-1100 μm rostral to the boundary between midbrain and cerebellum and from 600-1100 μm lateral to the midline between the two hemispheres. Dorsal-ventral position was read from the stepping motor devices. All units were recorded on a depth between 800 μm and 1800 μm beneath the surface of the optic lobes. No lesions were made, but because the location of the recording sites as determined above was well within the classical boundaries of the torus semicircularis, as verified by Hermes et al. [26] in an analogous study with histological techniques, we are certain that almost all our auditory units were indeed located inside the torus.

3. Results

Experiments were performed during the entire year, except for the summer season, on a total of 22 male and female grassfrogs. Tonal and noise stimulus ensembles were presented monaurally at ipsi- and contralateral positions with respect to recording side, as well as binaurally. In the case of binaural stimulus presentation there were no differences in intensity, phase and time of arrival of the sounds at both ears. Usually the stimulus was presented at 70 or 90 dB SPL (relative to 20 $\mu N/m^2$). Spectro-temporal sensitivities (STSs) at the two monaural and the binaural stimulus conditions could be determined for 122 units. Of these 122 units, 65 units were obtained in single-unit recordings, 38 in double-unit, 15 in triple-unit and 4 in a quadruple-unit recording on one electrode. Spontaneous activity, the presence of which was defined as at least 1 spike per 10 sec during zero-stimulus conditions, was exhibited by 54 (44%) units. In 77 (63%) units only one activation or suppression region was present in the STS, these units will be called monomodal [14]. The remaining 45 (37%) units had multiple activation and/or suppression regions in their STSs, these units will be called multimodal [14].

3.1. Binaural Interaction Type

3.1.1. Classification of Binaural Interaction Type

Classification of binaural interaction type was based on comparison of the STSs obtained upon

ipsilateral, contralateral and bilateral stimulus presentations. In the case of multimodal units each activation or suppression region was treated separately, resulting in a multiple characterization per unit. A total of 167 separate regions was present in the STSs of the 122 units. At first a purely phenomenological classification scheme was adopted, considering activation and/or suppression regions in the STSs.

(i) Binaural activation (AA, Aa, aA) regions. If in a certain frequency band activation was present on both ipsi- and contralateral stimulus presentations a unit was considered binaurally activated in this frequency band. If the amount of activation, defined as the spike activity integrated over the STS region, was equal within 20% for both stimulation sides, the region was classified as AA. If the amount of activation was more than 20% apart for both sides the classification was Aa (contralateral stronger) or aA (ipsilateral stronger). A criterion of 20% was chosen in order to neglect small differences due to statistical variability and slight nonstationarities. A further subdivision was made considering binaural facilitation or occlusion. If the amount of activation under bilateral stimulus presentation was at least 20% stronger than the strongest of the ipsi- or contralateral stimulation, binaural facilitation was present. This was indicated by the subscript "+", e.g. Aa_+. If the amount of activation in the bilateral STS was at least 20% weaker than the strongest of the ipsi- or contralateral activation, binaural occlusion was considered to occur, indicated by the subscript "-". When no signs of binaural facilitation or occlusion could be discerned, this was indicated by the subscript "o". It was never observed that the bilateral activation was more than 20% weaker than the weakest of the ipsi- or contralateral activation.

(ii) Monaural activation (AO, OA) regions. If in a certain frequency band activation was present upon contralateral stimulation and no effects were observed upon ipsilateral stimulation, the region was classified as AO. If the activation was present only ipsilaterally the classification was OA. Binaural facilitation and occlusion are defined analogously to the case of binaurally activated regions. Sometimes the binaural occlusion was so strong, that activation was completely absent under bilateral stimulation.

(iii) Binaural activation-suppression (AS, SA) regions. Regions characterized by activation upon stimulation on one side and suppression of spontaneous activity on the other were classified as AS (contralateral activation) or SA (ipsilateral activation). Upon tonal stimulation this can be observed only in case of spontaneous units, because only then suppression becomes apparent. Upon noise stimulation suppression can also be observed when activity due to other frequency bands or arousal is suppressed. The relative strengths of the excitatory and inhibitory influences can be compared by considering whether the region is activated (indicated by "+") or suppressed (indicated by "-") under bilateral stimulation. A complete balance between excitatory and inhibitory influences under bilateral stimulation did not occur.

(iv) Suppression (SO, OS, SS) regions. Frequency bands in which only suppression occurred where characterized as SO or OS, when the suppression was monaural and as SS in case it was binaural. Because of the low level of spontaneous activity in the anuran auditory midbrain suppression regions could not be quantified as accurately as activation regions. Therefore suppression regions were not studied in further detail.

We will illustrate some of the various types defined above and have selected a binaural activation type aA_o with one activation region, a case with two activation regions (Aa_-,AO_-) in both of which binaural occlusion occurred, and a case with activation for contralateral and suppression for ipsilateral (AS) stimulation. In these

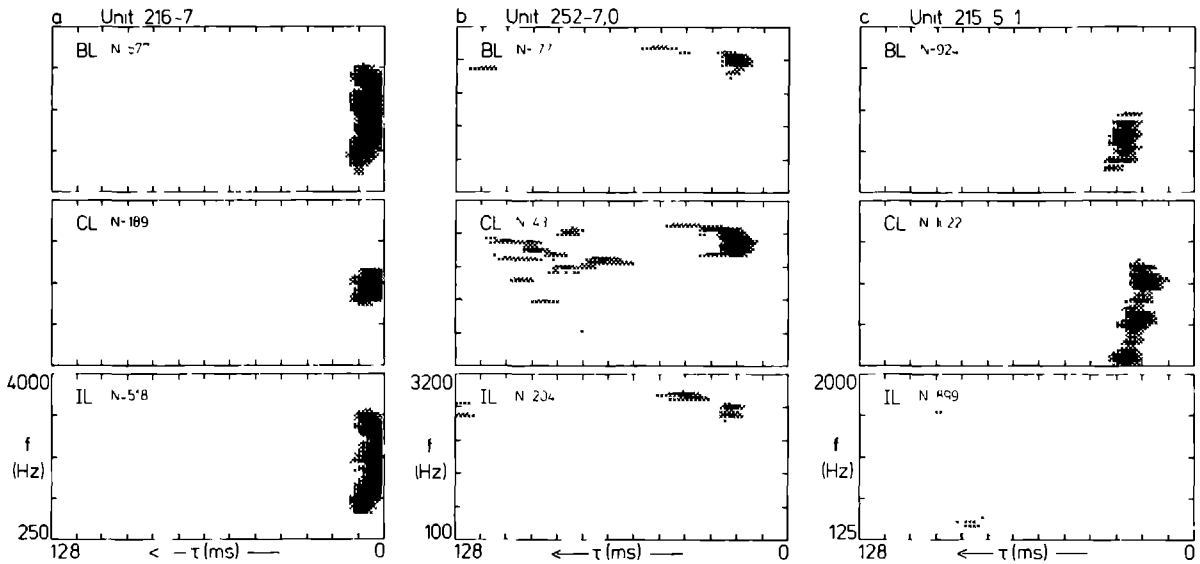

Fig. 1. Spectro-temporal sensitivities to tonal stimulation presented bi- (BL), contra- (CL) and ipsilaterally (IL) at 90 dB SPL, displayed in the first, second and third row respectively. Duration of tonepips was 48 ms and onset interval between tonepips 1 s. The horizontal axis represents time before a neural event. The vertical axis, representing frequency, has a logarithmic scale at which each tick mark indicates an octave. Intensity is coded in gray. Activation is represented by a darker than background gray level, suppression by a lighter than background gray level. a aA_O unit. b bimodal unit that is Aa_- at high frequencies and AO_- at low frequencies. c AS_+ unit. A detailed description of these STSs is given in the text.

three examples toneburst stimulation was used. In addition two examples with continuous broadband noise as stimulus will serve to illustrate some quite diverse binaural interactions.

In Fig. 1 STSs upon tonal stimulation, so called IFTs, for three units are displayed. The first row contains IFTs upon bilateral (BL) stimulation, the second row contains IFTs upon contralateral (CL) stimulation and in the third row IFTs for ipsilateral (IL) stimulation are presented. The amount of activation is coded in gray: the more activation, the more gray.

In Fig. 1a, an example of an aA_O unit is presented. This unit is activated both contra- and ipsilaterally, the latter side being more effective. Upon ipsilateral stimulation the unit is activated by a rather broad band of frequencies from 300 Hz to 3000 Hz. Its best frequency is 1000 Hz and latency is 9 ms. Upon contralateral stimulation frequency selectivity is much more restricted around a BF of 900 Hz and latency of 11 ms. Bilateral stimulation had the same effect as ipsilateral stimulation.

In Fig. 1b a bimodal unit is shown, for which contralateral stimulation was most effective. Upon contralateral stimulation two activation regions resulted. One at a BF of 1300 Hz and latency 27 ms, the other at 250 Hz and latency of 73 ms. Upon ipsi- and bilateral stimulation only the high frequency region is present, although less pronounced than at contralateral stimulation. Note that in this high frequency region the initial burst of activity is followed by a second one at about 60 ms in the contralateral STS and at about 100 ms in the ipsi- and bilateral STSs. The high frequency region was classified as Aa_-, the low frequency region as AO_-.

An AS unit is shown in Fig. 1c. Stimulated contralaterally this unit was activated by frequencies between 125 and 700 Hz at a frequency dependent latency between 25 and 30 ms. In the ipsilateral STS a very clear suppression of spontaneous ac-

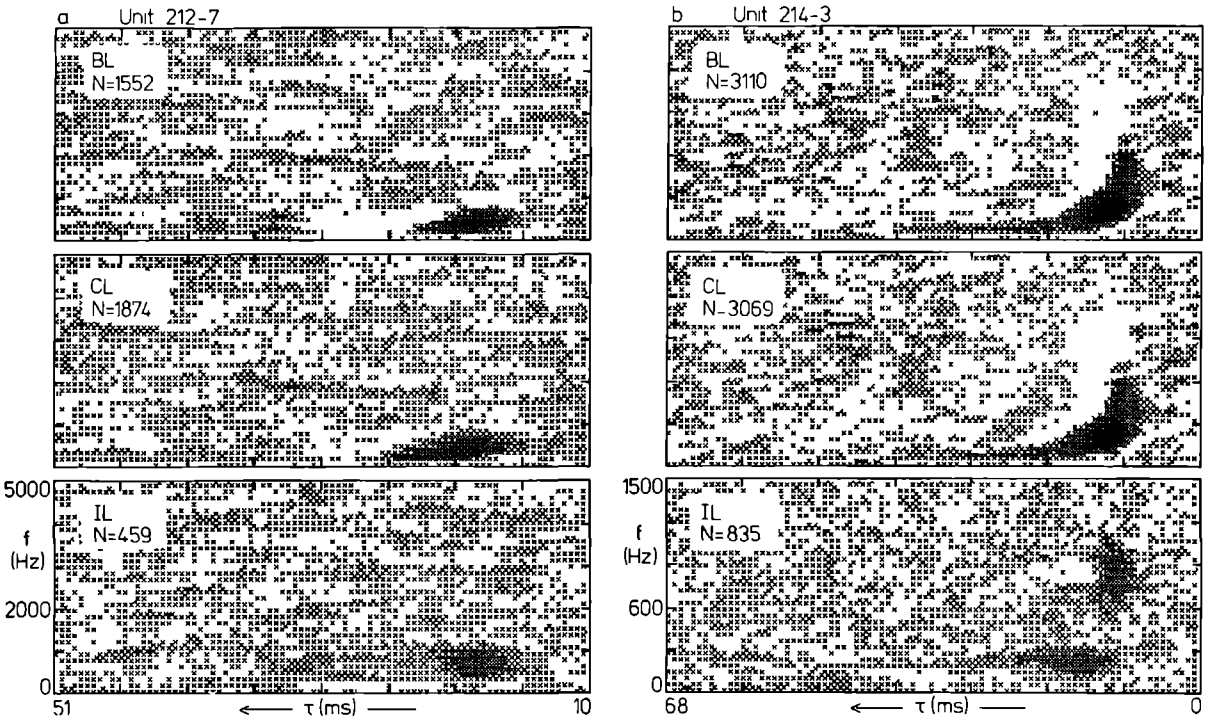

Fig. 2. Spectro-temporal sensitivities to continuous wideband noise stimulation presented bi- (BL), contra- (CL) and ipsilaterally (IL) at 90 dB SPL, displayed in the first, second and third row respectively. The horizontal axis represents time before a neural event. The vertical axis represents frequency on a linear scale. Intensity representing activation or suppression is coded in gray. Only the real parts of the complex-valued STSs are shown. a Aa_0 unit. b bimodal unit that is Aa_0 at low frequencies and SA_- at higher frequencies. A detailed description is given in the text.

tivity, which extends over the whole frequency range, can be noticed. In the bilateral STS both activation and suppression effects are present. Activation is caused by frequencies around a BF of 350 Hz and at a latency of 31 ms. Other frequencies suppress spontaneous activity. This unit was classified as an AS_+ unit.

In Fig. 2 STSs upon noise stimulation, so called CoSTIDs, for two units are presented. In fact CoSTIDs are complex valued entities, but because in case of anuran auditory midbrain units the real part of it often contains already all relevant information [26], the imaginary part has been omitted.

In Fig. 2a an Aa_0 unit is displayed. Upon contralateral stimulation this unit had an activation region around 350 Hz and 20 ms. Upon ipsilateral stimulation a less pronounced activation region is present around 750 Hz and 19 ms. Best frequencies obviously are not equal for both sides. Bilateral stimulation resulted in a STS with an activation region comparable to the one in the contralateral STS. In the bilateral STS post-activation suppression, which is not present in the other STSs can also be discerned clearly. After onset of the continuous noise stimulus units often exhibited adaptation. In those cases the first minute of the activity had to be discarded in determining noise STSs, because STSs essentially are estimates of stationary processes. Sometimes, however, upon ipsilateral stimulation a reverse phenomenon was observed: at stimulus onset activity was suppressed and increased to a stationary level within one minute, whereas upon contra- and bilateral stimulation these units exhibited common adaptation. The unit in Fig. 2a is an example of this phenomenon:

AS behavior during initial activity, AA behavior in the stationary situation, the latter being expressed in SISs. Different binaural interaction types during initial and steady-state activity were observed in a total of 3 units.

An example of a bimodal unit is shown in Fig. 2b. Upon contra- and bilateral stimulation this unit exhibited activation around 250 Hz at a latency of 11 ms, a suppression region can be noted around 1000 Hz and 11 ms. Ipsilateral stimulation resulted in less pronounced activation regions at 250 Hz and 16 ms and also at 1000 Hz and 11 ms. Thus this unit exhibited Aa_0 behavior at low frequencies and SA_ behavior at higher frequencies.

Table I. Distribution of activation (A,a) and suppression (S) regions upon ipsi-, contra- and bilateral tonal stimulus presentation.

activation or suppression	+	o	-	?	totals
AA	0	5	0	1	6
Aa	4	25	10	4	43
aA	1	6	0	1	8
AO	7	30	23	4	64
OA	0	5	4	1	10
AS	11	0	9	1	21
SA	0	0	0	0	0
SS					8
SO					5
OS					2

Contralateral characterization is indicated first. In case of binaural activation regions (AA, Aa, aA), or monaural activation regions (AO, OA) binaural facilitation or occlusion is indicated by "+" or "-" respectively and "o" otherwise. In case of binaural activation suppression regions (AS, SA) a "+" indicates a stronger excitatory, "-" a stronger inhibitory influence. A "?" means that binaural facilitation/occlusion or balance between excitatory and inhibitory influences could not be determined. Total n = 167.

The results of the classification upon tonal stimulation (mostly at 90 dB SPL) are summarized in Table I. From Table I it can be concluded that stimulation at the contralateral side provided the dominant source of activation (76%). The ipsilateral side of stimulation was more dominant with respect to activation in 11% of the regions. Equal effectiveness was present in 4%. The remaining 9% were purely suppressive regions. Binaural facilitation appeared in 9% of the binaural and monaural activation regions. Binaural occlusion occurred in 28%, no signs of facilication or occlusion was found in 55%, while it could not be determined reliably in 8% of the cases due to a large variability. In the binaural activation-suppression regions activation was stronger than suppression about as often as the opposite.

From the phenomenological classification of regions as summarized in Table I a mechanistic classification scheme corresponding to the conventional binaural interaction type was established. EE-regions receive excitatory inputs from both ears, following Table I these are the AA, Aa, aA, AO_+ and OA_+ regions. In the latter two categories the weaker excitatory input was subthreshold when activated on its own, its influence became apparent only in combination with the stronger excitatory input from the other ear. EO-regions receive an excitatory input from only one ear and no input from the other: these are the AO_0 and OA_0-categories of Table I. EI-regions receive an excitatory input from one ear and an inhibitory one from the other, these are the AO_, OA_, AS and SA categories. In the case of spontaneous units AO_ and OA_ regions indicated subthreshold inhibitory input from the non-excitatory ear. In the case of non spontaneous units supra-threshold inhibitory input

Table II. Distribution of binaural interaction type.

binaural interaction	number	percentage
EE	64	38
EO	35	21
EI	48	29
I	15	9
n.d.	5	3

EE: binaural excitatory region. EO: monaural excitatory. EI: binaural excitatory-inhibitory. I: purely inhibitory. Total n = 167; (n.d.: not unambiguously determined).

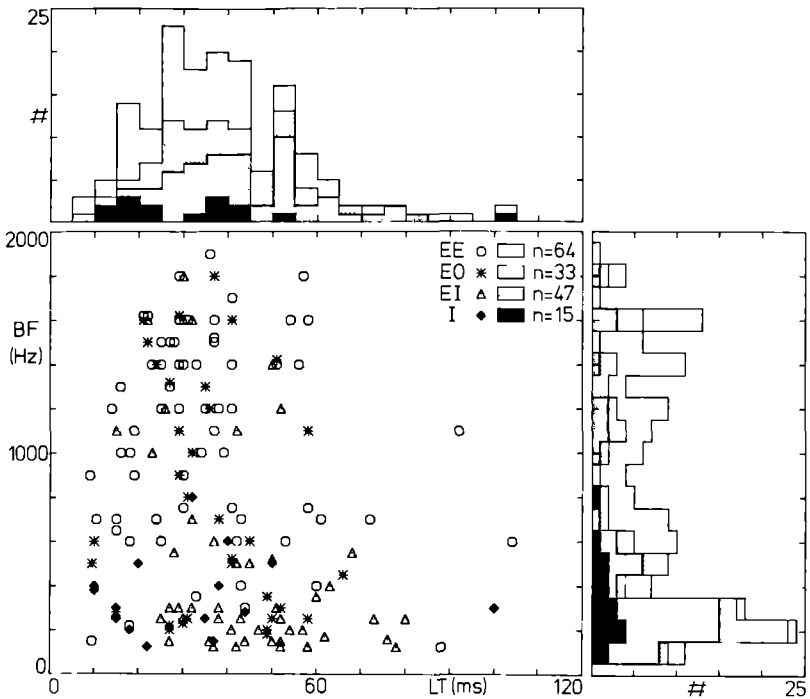

Fig. 3. Binaural interaction type as function of latency (LT) and best frequency (BF). Marginal distributions of LT and BF are drawn along the axes.

is obscured when only the non-excitatory ear is stimulated. The distribution of binaural interaction type is summarized in Table II. All purely suppressive regions are lumped into the category inhibition (I).

3.1.2. Best Frequency and Latency Distributions for Binaural Interaction Type

To study the relation between binaural interaction type, latency (LT) and best frequency (BF), binaural interaction type was plotted as a function of both LT and BF (Fig. 3). A strict separation between the different categories is not apparent. However, some trends are noticeable. The EE category is hardly present at low frequencies (< 400 Hz), but abundant in the high frequency domain (> 900 Hz). The EO category is evenly distributed over all frequencies. The EI and I categories are overrepresented at low frequencies. Tested statistically this trend is significant at the 0.05% level (χ^2 test). Another less pronounced trend is that the EE and I categories tend to have shorter latencies than the EI category, the EO-category takes an intermediate position. This trend appeared to be significant only at the 10% level (χ^2-test).

3.2. Comparison of Temporal and Spectral Properties of STSs obtained by Ipsi-, Contra- and Bilateral Stimulation.

In the previous section STSs obtained for ipsi-, contra- and bilateral stimulation were compared. BFs and LTs were found mostly in the same range for ipsi- and contralateral stimulation. In order to study temporal and spectral aspects in more detail, BFs and LTs were compared quantitatively for the different stimulation sides. Because a sufficient degree of accuracy is obtained only for activation regions, this comparison was restricted to the AA, Aa and aA regions, which belong to the EE category. In addition temporal discharge pattern upon stimulation with tonepips was investigated qualitatively.

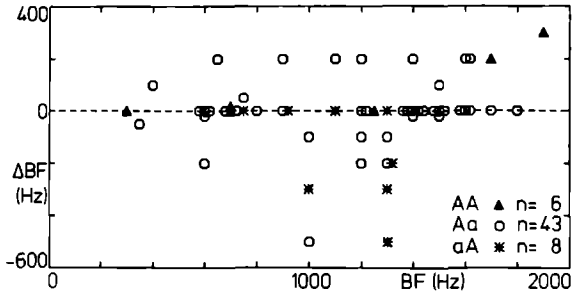

Fig. 4. Differences in best frequency ΔBF, as obtained under ipsi- (IL) and contralateral (CL) stimulation, as a function of BF for EE-regions. In case of AA and Aa regions BF = BF_{CL} and for aA regions BF = BF_{IL}; $\Delta BF = BF_{CL} - BF_{IL}$.

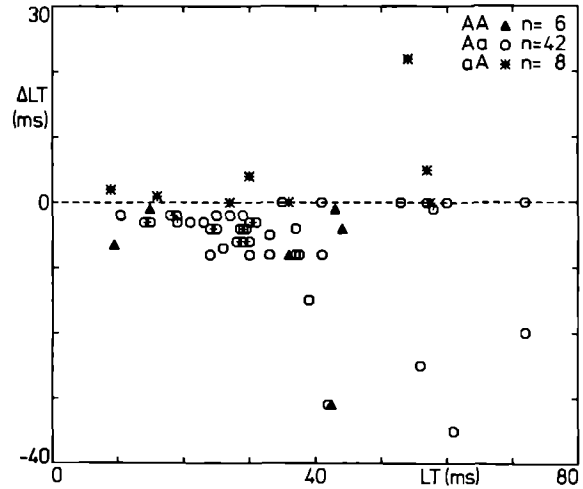

Fig. 5. Differences in latency ΔLT, as obtained under ipsi- (IL) and contralateral (CL) stimulation, as a function of LT for EE-regions. In case of AA and Aa regions LT = LT_{CL} and for aA regions LT = LT_{IL}; $\Delta LT = LT_{CL} - LT_{IL}$.

3.2.1. Differences in Best Frequency

Differences in BF: ΔBF ($=BF_{CL}-BF_{IL}$) were plotted as a function of BF in Fig. 4. The accuracy in the determination of ΔBF is $\pm$ 50 Hz for BF < 800 Hz and $\pm$ 100 Hz for BF > 800 Hz. In most regions (68%) ΔBF is not clearly different from zero. In the region below BF = 800 Hz we observe 3 out of 14 cases, all of the Aa type, that have BF differences up to 200 Hz. In the region above 800 Hz clear BF differences are observed in 15 out of 43 cases, about half thereof showed a higher BF for contralateral stimulation, the other half for ipsilateral stimulation. Overall no clear correlation is obvious between ΔBF and BF. The BF for bilateral stimulation was always very close to the BF of the stronger unilateral activation side.

3.2.2. Differences in Latency

Latency differences ΔLT ($=LT_{CL}-LT_{IL}$) are plotted against LT in Fig. 5. The accuracy in determining ΔLT is 1 ms. Latency differences are zero or negative for AA and Aa regions and zero or positive for aA regions: the dominant side is characterized by the shortest latency. Furthermore $|\Delta LT|$ is positively correlated with LT ($r^2 = 0.118$, $p < 1\%$). At short latencies (LT < 25 ms) $|\Delta LT|$ is smaller than 4 ms, probably corresponding with one synaptic delay. At intermediate latencies (25 ms < LT < 40 ms) $|\Delta LT|$ is smaller than 8 ms, probably corresponding with two synaptic delays. In the long latency domain (LT > 40 ms) large differences occur, suggesting in addition large integration times. The latency for bilateral stimulation resembled very well the one belonging to the stronger unilateral activation side.

3.2.3. General Temporal Discharge Properties

In order to study the temporal discharge pattern in detail neural activity was plotted as a function of both time after the onset of a tonepip and frequency of a tonepip. Temporal discharge pattern was judged with respect to time-lock to the stimulus, presence of chopper activity [32], interval between repetitive firings in case of chopper activity and phasic-tonic character. Comparisons were made between temporal discharge patterns upon ipsi-, contra- and bilateral stimulation for 96 EE, EO and EI regions. In the case of EE regions temporal discharge pattern upon bilateral stimulation was always very similar to the one belonging to the stronger activation side. It appeared that the phasic-tonic character was not dependent on side of stimulation, except in case of chopper activity. An example is unit 216-6, an EF unit, with LT = 23 ms,

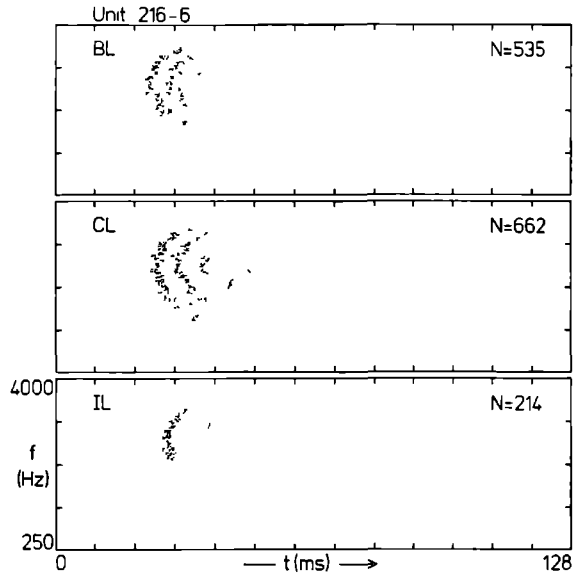

Fig. 6. Dotdisplay of neural activity as a function of time after onset of a tonepip and frequency of a tonepip upon bi-, contra- and ipsilateral stimulation. The horizontal axis represents time after tonepip onset, the vertical axis represents frequency on a logarithmic scale. Duration of tonepips was 48 ms, onset intervals between tonepips 1 s, and stimulus intensity 90 dB SPL.

ΔLT = -3 ms, BF = 1400 Hz and ΔBF = 0 Hz (Fig. 6). Upon bilateral and contralateral stimulation chopper activity exists during a large portion of the tonepip duration (48 ms). Upon ipsilateral stimulation only onset activity is present. Of the 96 regions 79 (82%) did not exhibit clear differences in discharge pattern. The other 17 (18%) had discharge patterns differing in time-lock or presence and character of chopper activity, sometimes discharge patterns differed in all these aspects.

3.3. Stimulus Ensemble and Level Dependency of Binaural Interaction Type

The activity of almost all units was recorded upon stimulation with at least the γ-tone ensemble, with duration of tonepips of 48 ms and onset interval between tonepips of 1 s, at 90 dB SPL. A considerable portion of units was also stimulated with the other γ-tone ensemble, tonepip duration 16 ms and onset interval 128 ms, and/or continuous wideband noise at 70 and 90 dB SPL. Previous studies [2,12,14] have shown that in general STSs are not invariant to alterations of stimulus ensemble and intensity indicating a rather complex level of spectro-temporal coding mechanisms. Studying the stimulus ensemble and level dependency of binaural interaction type might indicate which properties are important for spatial coding.

The binaural interaction type of 29 regions was compared at the same intensity for stimulation with both γ-tone ensembles. Of these 29 regions, 28 showed the same binaural interaction type, whereas 1 region changed from an EE into an EI type. Within the group of 28 units sharing the same binaural interaction type 12 regions, however, showed changes in binaural facilitation and occlusion in the case of EE regions and changes in strength of excitatory and inhibitory influences in the case of EI regions.

Wideband noise and γ-tone ensembles at the same peak intensity level were presented to 25 units, exhibiting 30 spectro-temporal regions. Equal binaural interaction types to both kinds of stimuli were shown by 21 regions, of which 2 showed some variation in binaural facilitation/occlusion. A change from EE (tonal) into EO (noise) was observed in 6 regions. A change from EI (tonal) into EO (noise) in 2 regions. In 1 region the FE type to tones changed into IO upon noise stimulation.

Identical stimulus ensembles at two different intensity levels were presented to 19 units, containing 23 regions. Of these, 16 regions shared the same binaural interaction type at the two intensity levels. In 5 regions an EE type at 90 dB SPL changed into an EO type at 70 dB SPL. In 1 region an EI type at 90 dB SPL changed into an OI at 70 dB SPL, and a change from EE into EI was noticed in another region. Sometimes it was observed that EE units, which had activation regions in bi-, contra- and ipsilateral STSs at 90 dB SPL, displayed an activation region at 70 dB SPL only in the bilateral STS.

Summarizing we may conclude that for the two γ-tone ensembles studied in 28 out of 29 regions the binaural interaction type remained basically the same. In 30 regions for which both noise and γ-tone stimulation were compared 21 had the same

binaural interaction type. Finally comparing STSs obtained at stimulus intensities of 70 and 90 dB SPL resulted in invariance of binaural interaction type in 16 out of 23 regions. Thus in a large majority of cases the binaural interaction type remained rather invariant for the stimuli used. The variations that occurred probably are due to different levels of adaptation (γ-tones versus noise) and threshold effects (70 dB versus 90 dB SPL). An additional cause of differences between results obtained by γ-tone and continuous noise ensembles probably is the inherently larger statistical variability in the noise STS estimates. Because of this subtle effects observable in γ-tone STSs might have been overlooked in the corresponding noise STSs.

3.4. Binaural Interaction Type for Different Frequency Regions of Multi-Modal Units

So far each activation or suppression region has been studied separately. The issue remains whether binaural interaction type is a characteristic of a unit or whether it depends on stimulus frequency. Of the 45 multimodal units 34 units had two regions, that were of the EE, EO or EI type. Of these 34 units, 14 units appeared to have the same binaural interaction type irrespective of stimulus frequency, while the other 20 units were characterized by different binaural interaction types at different frequencies. The remaining 11 units had one purely suppressive region accompanying an activation region, therefore also having different binaural interaction types. Thus of the 45 multimodal units only 14 (31%) can be characterized by one binaural interaction type for the whole sensitivity range.

3.5. Binaural Interaction Type of Units Recorded Simultaneously with One Electrode.

To investigate whether a topographical organization with respect to binaural coding exists in the anuran auditory midbrain, binaural interaction categories of neighbouring units have been compared. A distinction was made between EE, EO, OE, EI, IE (contralateral ear leading) and purely inhibitory categories. In the case of multimodal units both regions were taken into account.

A total of 40 simultaneously recorded pairs can be formed out of the 57 units that were obtained in our 19 double-, 5 triple- and 1 quadruple units recordings. By a χ^2-test it was investigated whether simultaneously recorded unit pairs shared the same binaural interaction category more often than expected by mere chance. This was found to be significant only at the 10% level. We did not apply a statistical test to triplets and the one quadruplet, because of their low number. In these triplets and quadruplet also different binaural interaction types were observed together. Thus it can be concluded that if a binaural interaction type organization on the single-unit level would exist, it is only vague.

4. Discussion

4.1. Open Mouth versus Closed Mouth Conditions

In this investigation, and those of Hermes et al. [26,27] experiments were performed under closed mouth conditions. Because of the acoustical coupling of both tympanic membranes, which is tight at frequencies around 900 Hz with a closed mouth [4, 21,33,37] binaural interaction has to be interpreted with caution. Binaural interaction is apart from neural connections shaped by the properties of the peripheral acoustic receiver. In comparison with other studies conducted on anuran auditory midbrain units [15,29] we found an overrepresentation of EE units in this study and that of Hermes et al. [27]. Apart from a possible bias due to different recording procedures this difference presumably is due to closed mouth versus open mouth conditions. Because crosstalk under closed mouth conditions might result in a neuron's response on stimulating either ear, uncoupling the ears by opening the mouth may result in excitation for stimulating one ear only. This effect should be most prominent around 1 kHz [4,21,33,37], a region in fact in which most of our EE-units were encountered. EI

units were encountered about as often as in the studies of Kaulen [29] and Hermes et al. [27]. Feng [15], however, reports that the majority of his units are of the EI type. This discrepancy cannot solely be accounted for by peripheral crosstalk, because this is below -30 dB at those frequencies where most EI regions have their BFs.

The potential effect of closed-mouth conditions on the study of binaural interaction type therefore is an overrepresentation of EE-units in a broad frequency region around 1 kHz.

4.2. Multimodality and Binaural Interaction

In some EE units (n = 10, Table I) binaural occlusion occurred. Stimulated monaurally these units receive excitatory input from both ears. Upon binaural stimulation, however, one ear suppresses the response from the other. This phenomenon indicates that, even in a single frequency band, some units do not receive pure excitatory or inhibitory monaural information. A combination of properties of the peripheral acoustic receiver and the extensive ascending bilateral and commissural neural projections, from the dorsal medullary nucleus up to the torus semicircularis, cause a complex interplay of excitatory and inhibitory effects, especially at suprathreshold intensities. A similar interplay has been reported by Goldberg and Brown [24] in the superior olivary complex of the dog and by Aitkin et al. [5] in the inferior colliculus of the rabbit. Due to these effects a large population of units cannot be characterized by one single binaural interaction type at high intensities. Instead these units have to be characterized per frequency time region and thereby might explain the apparent discrepancy regarding the number of EI units between our and Feng's [15] results.

In most theories on binaural hearing coding of absolute intensity levels: identification, irrespective of position of the sound source, is ascribed to EE units. Coding of spatial position: localization, independent of sound intensity, should be performed by EI units. In the present study a highly significant relation was found between binaural interaction type and BF. Hermes et al. [27] arrived at the same result for the lightly anesthetized grassfrog. This suggests a different role of separate frequency bands in binaural hearing. Low frequency components of sound presumably are involved in localization aspects, while high frequency components serve in identification. In this context it is remarkable that Feng [18] did not observe a relation between BF and directional response type for torus units under free-field conditions. The evoked potential studies of Pettigrew et al. [30,31] are not in conflict with our hypothesis.

Besides the strong correlation between binaural interaction type and BF, which is already apparent in monomodal units, another relation between these two characteristics is obvious in multimodal units exhibiting frequency dependent binaural interaction types. A few of these multimodal units have also been observed by Feng and Capranica [20] in the anuran superior olivary complex. In view of the coupling of directionality and frequency properties of the peripheral receiver, these findings are not surprising. What is the role of these multimodal units in spatial processing? Perhaps these units, especially those with one EI or I region, have an important function in detection and recognition of certain sounds against a background of other sounds or environmental noise by enhancing the signal to noise ratio when these sounds emanate from different directions (a kind of 'contrast enhancement'). For example a unit with an EE characteristic in the mid-frequency region would more reliably recognize a mid-frequency sound in a noisy environment when it has an EI characteristic at other frequency bands in addition. This possibility was already pointed at by Schlegel and Singh [36] in the case of auditory midbrain units of the bat.

4.3. BF-Mismatch and Latency Differences

Best frequencies, latency and temporal discharge pattern for ipsi- and contralateral stimulus presentation differed for a number of units. A mismatch in BF is remarkable, since others [19,20,41] report a very close resemblance of excitatory and inhibitory tuning curves, apart from a threshold shift, and therefore also for the threshold charac-

teristic frequency for both ears in almost all anuran auditory units. In the cat's superior olivary complex different tuning curves for both ears have been found [25]. A possible explanation for this discrepancy is that characteristic frequency is measured at threshold and thus may differ from the best frequency, i.e. the frequency eliciting maximal response, which is a suprathreshold estimate [13]. For a number of units BF is dependent on stimulus intensity due to asymmetrical tuning curves [8,14,23] and therefore might not be equal for the two ears if these have different thresholds. Latency is also a measure strongly dependent on intensity [38] and therefore part of the latency differences of Fig. 5 might be accounted for by differences in threshold. However, a clear correlation remains between $|\Delta LT|$ and LT, indicating complex spatial processing at long latencies, in which many synapses and long integration times are involved. Different temporal discharge patterns for both ears have also been reported by Schlegel [35] for binaural brainstem units of the bat. Temporal discharge patterns, however, are strongly dependent on intensity, frequency and type of stimulus [9,14, 25]. Therefore its role, like that of ΔBF, in spatial coding remains to be affirmed.

4.4. Multivariate versus Univariate Neural Characterization

A previous study [10] showed that for at least one third of the investigated anuran auditory midbrain units a combined spectro-temporal description is more adequate than separate determination of spectral and temporal characteristics. In this study spectro-temporal sensitivities were determined for ipsi-, contra- and bilateral stimulation. In a number of cases evidence was obtained that binaural and spectro-temporal coding cannot be treated separately without loosing information, because they are intricately coupled; e.g. frequency dependent binaural interactions in multimodal units. In some units, using the noise stimulus, it appeared that binaural interaction type changed with different levels of adaptation. A possible explanation might be that these units receive excitatory inputs from both ears and a stronger inhibitory input, which adapts faster, from one ear. A similar phenomenon was reported by Goldberg and Brown [24] who observed that upon tonal stimulation the initial response of units in the superior olivary complex of the dog was of a different binaural interaction type than the steady-state response. Therefore not only steady-state responses, expressed in (spatio-) spectro-temporal sensitivities, but also the dynamic behavior as expressed e.g. in initial transient responses deserve attention. In this context also the use of sound derived from the acoustic biotope [1] particularly the species specific mating call, has to be considered especially because of the pronounced amplitude-modulated structure. Phase-locking to an amplitude-modulated envelope, as reported up to the level of the torus [7,39] could provide additional information useful in spatial coding. Thus the effect of the stimulus parameters - frequency, intensity, location, adaptation and temporal structure - should preferably be investigated simultaneously, because they influence neural responsiveness in an intricately coupled way.

Summarizing: 1) Single units in the torus semicircularis cannot be assigned a single binaural interaction type, this can differ from one frequency region to another. 2) Single units do not depend in an univariate way on stimulus parameters, but must if possible be characterized in a multivariate way.

Acknowledgements

This investigation forms part of the research program "Brain and Behaviour" at the Department of Medical Physics and Biophysics of the University of Nijmegen and was supported by the Netherlands Organization for the Advancement of Pure Research (ZWO). The authors wish to thank Jan Bruijns and Wim van Deelen for software development, Koos Braks for the animal preparations and technical assistance, Hans Krijt and his group for electronic support. Ad Aertsen, Henk van den Boogaard and Peter Johannesma provided valuable comments on the manuscript, which was typed carefully by Marianne Nieuwenhuizen.

References

1 Aertsen, A.M.H.J. and Johannesma, P.I.M. (1980): Spectro-temporal receptive fields of auditory

neurons in the grassfrog. I. Characterization of tonal and natural stimuli. Biol. Cybern. 38, 223-234.

2 Aertsen, A.M.H.J. and Johannesma, P.I.M. (1981): A comparison of the spectro-temporal sensitivity of auditory neurons to tonal and natural stimuli. Biol. Cybern. 42, 145-156.

3 Aertsen, A.M.H.J., Johannesma, P.I.M. and Hermes, D.J. (1980): Spectro-temporal receptive fields of auditory neurons in the grassfrog. Biol. Cybern. 38, 235-248.

4 Aertsen, A.M.H.J., Vlaming, M.S.M.G., Eggermont, J.J. and Johannesma, P.I.M. (1985): Directional hearing in the grassfrog (*Rana temporaria* L.) II. Acoustics and modelling of the auditory periphery. (submitted)

5 Aitkin, L.M., Blake, D.W., Fryman, S. and Bock, G.R. (1972): Responses of neurones in the rabbit inferior colliculus. II. Influences of binaural tonal stimulation. Brain Res. 47, 91-101.

6 Arak, A. (1983): Sexual selection by male-male competition in natterjack toad choruses. Nature 306, 261-262.

7 Bibikov, N. and Gorodetscaya, O. (1983): Coding of amplitude modulated tones in the midbrain auditory region of the frog. In: Neuronal Mechanisms of Hearing. p. 347-352. Editors: J. Syka and L. Aitkin. Plenum Press, New York.

8 Capranica, R.R. (1976): Morphology and physiology of the auditory system. In: Frog Neurobiology. p. 551-575. Editors: R. Llinas and W. Precht. Springer, Berlin.

9 Coles, R.B. and Aitkin, L.M. (1979): The response properties of auditory neurones in the midbrain of the domestic fowl *(Gallus gallus)* to monaural and binaural stimuli. J. Comp. Physiol. A 134, 241-251.

10 Eggermont, J.J., Aertsen, A.M.H.J., Hermes, D.J. and Johannesma, P.I.M. (1981): Spectro temporal characterization of auditory neurons: redundant or necessary? Hearing Res. 5, 109-121.

11 Eggermont, J.J., Epping, W.J.M. and Aertsen, A.M.H.J. (1983): Stimulus dependent neural correlations in the auditory midbrain of the grassfrog (*Rana temporaria* L.). Biol. Cybern. 47, 103-117.

12 Eggermont, J.J., Aertsen, A.M.H.J., and Johannesma, P.I.M. (1983): Quantitative (1983): Quantitative characterisation procedure in auditory neurons based on the spectro-temporal receptive field. Hearing Res. 10, 191-202.

13 Eggermont, J.J., Johannesma, P.I.M. and Aertsen, A.M.H.J. (1983):Reverse-correlation methods in auditory research. Quart. Rev. Biophysics 16, 341-414.

14 Epping, W.J.M. and Eggermont, J.J. (1985): Single-unit characteristics in the auditory midbrain of the immobilized grassfrog. Hearing Res. (in press).

15 Feng, A.S. (1975): Sound localization in anurans: an electrophysiological and behavior study. Ph.D. Thesis, Cornell University.

16 Feng, A.S. (1980): Directional characteristics of the acoustic receiver of the leopard frog *(Rana pipiens)* : a study of eighth nerve auditory responses. J. Acoust. Soc. Am. 68, 1107-1113.

17 Feng, A.S. (1982): Quantitative analysis of intensity-rate and intensity-latency functions in peripheral auditory nerve fibers of northern leopard frogs *(Rana p. pipiens)*. Hearing Res. 6, 241-246.

18 Feng, A.S. (1981): Directional response characteristics of single neurons in the torus semicircularis of the leopard frog *(Rana pipiens)*. J. Comp. Physiol. A 144, 419-428.

19 Feng, A.S. and Capranica, R.R. (1976): Sound localization in anurans. I. Evidence of binaural interaction in dorsal medullary nucleus of bullfrogs *(Rana catesbeiana)*. J. Neurophysiol. 39, 871-881.

20 Feng, A.S. and Capranica, R.R. (1978): Sound localization in anurans. II. Binaural interaction in superior olivary nucleus of the green treefrog *(Hyla cinerea)*. J. Neurophysiol. 41, 43-54.

21 Feng, A.S. and Shofner, W.P. (1981): Peripheral basis of sound localization in anurans. Acoustic properties of the frog's ear. Hearing Res. 5, 201-216.

22 Feng, A.S., Gerhardt, H.C. and Capranica, R.R. (1976): Sound localization behavior of the green treefrog *(Hyla cinerea)* and the barking treefrog *(Hyla gratiosa)* . J. Comp. Physiol. A 107, 241-252.

23 Fuzessery, Z.M. and Feng, A.S. (1982): Frequency selectivity in the anuran auditory midbrain: single unit responses to single and multiple tone stimulation. J. Comp. Physiol. A 146, 471-484.

24 Goldberg, J.M. and Brown, P.B. (1968): Functional organization of the dog superior olivary complex: an anatomical and electrophysiological study. J. Neurophysiol. 31, 639-656.

25 Guinan, J.J., Guinan, S.S. and Norris, B.E. (1972): Single auditory units in the superior olivary complex I: responses to sounds and classifications based on physiological properties. Int. J. Neurosci. 4, 101-120.

26 Hermes, D.J., Aertsen, A.M.H.J., Johannesma, P.I.M. and Eggermont, J.J. (1981): Spectro-temporal characteristics of single units in the auditory midbrain of the lightly anaesthetised grass frog (*Rana temporaria* L.) investigated with noise stimuli. Hearing Res. 5, 147-178.

27 Hermes, D.J., Eggermont, J.J., Aertsen, A.M.H.J. and Johannesma, P.I.M. (1982): Spectro temporal characteristics of single units in the auditory midbrain of the lightly anaesthetised grass frog (*Rana temporaria* L.) investigated with tonal stimuli. Hearing Res. 6, 103-126.

28 Johannesma, P., Aertsen, A., Cranen, L. and Erning, L. van(1980): The phonochrome: a coherent spectro-temporal representation of sound. Hearing Res. 5, 123-145.

29 Kaulen, R., Lifschitz, W., Palazzi, C. and Adrian, H. (1972): Binaural interaction in the inferior colliculus of the frog. Exp. Neurol. 37, 469-480.

30 Pettigrew, A., Chung, S.-H. and Anson, M. (1978): Neurophysiological basis of directional hearing in amphibia. Nature 272, 138-142.

31 Pettigrew, A.G., Anson, M. and Chung, S.-H. (1981): Hearing in the frog: a neurophysiological study of the auditory response in the midbrain. Proc. R. Soc. Lond. B. 212, 433-457.

32 Pfeiffer, R.R. (1966): Classification of res-

ponse patterns of spike discharges for units in the cochlear nucleus: tone-burst stimulation. Exp. Brain Res. 1, 220-235.

33 Pinder, A.C. and Palmer, A.R. (1983): Mechanical properties of the frog ear: vibration measurements under free- and closed-field acoustic conditions. Proc. R. Soc. Lond. B. 219, 371-396.

34 Rheinlaender, J., Gerhardt, H.C., Yager, D.D. and Capranica, R.R. (1979): Accuracy of phonotaxis by the green treefrog *(Hyla cinerea)*. J. Comp. Physiol. A 133, 247-255.

35 Schlegel, P. (1977): Directional coding by binaural brainstem units of the CF-FM bat, *Rhinolophus ferrumequinum*. J. Comp. Physiol. A 118, 327-352.

36 Schlegel, P. and Singh, S. (1983): Unmasking in neurons of the inferior colliculus of *Eptesicus fuscus* with binaural stimulation. Hearing Res. 10, 331-343.

37 Vlaming, M.S.M.G., Aertsen, A.M.H.J. and Epping, W.J.M. (1984): Directional hearing in the grassfrog (*Rana temporaria* L.) I. Mechanical vibrations of tympanic membrane. Hearing Res. 14, 191-201.

38 Walkowiak, W. (1980): The coding of auditory signals in the torus semicircularis of the firebellied toad and the grassfrog: responses to simple stimuli and to conspecific calls. J. Comp. Physiol. A 138, 131-148.

39 Walkowiak, W. (1984): Neuronal correlates of the recognition of pulsed sound signals in the grass frog. J. Comp. Physiol. A 155, 57-66.

40 Wilczynski, W. and Capranica, R.R. (1984): The auditory system of anuran amphibians. Progr. Neurobiol. 22, 1-38.

41 Zakon, H.H. (1983): Reorganization of connectivity *in amphibian central auditory system* following VIIIth nerve regeneration: time course. J. Neurophysiol. 49, 1410-1427.

SENSITIVITY OF NEURONS IN THE AUDITORY MIDBRAIN OF THE GRASSFROG TO TEMPORAL CHARACTERISTICS OF SOUND

I. Stimulation with Acoustic Clicks

Willem J.M. Epping and Jos J. Eggermont

Department of Medical Physics and Biophysics, University of Nijmegen, Geert Grooteplein Noord 21
NL-6525 EZ Nijmegen, The Netherlands

The coding of fine-temporal structure of sound, especially pulse repetition rate, was investigated on the single-unit level in the auditory midbrain of the grassfrog. As stimuli periodic click trains and Poisson distributed click ensembles have been used. The response to periodic click trains was studied in two aspects, focussing on two types of possible codes: a rate code and a synchrony code. From the iso-intensity rate histogram five basic average response rate characteristics as function of pulse repetition rate have been established: low-pass, band-pass, high-pass, bimodal and non-selective unit types. The synchronization capability, expressed in a synchronization index, was for a small majority of units non-significant and a low-pass function of pulse repetition rate for most of the other units. The rate code showed the largest diversity of response types and an enhanced selectivity to pulse repetition rate. The stimulus-response relation to Poisson distributed click ensembles was investigated by a nonlinear system theoretical approach. On basis of first and second-order Poisson kernels possible neural mechanisms accounting for temporal selectivity were determined. A considerable fraction of units exhibited response characteristics that were invariant to changes in sound pressure level and average click rate. These units may function as feature detectors of fine-temporal structure of sound. The spectro-temporal sensitivity range of the auditory midbrain of the grassfrog appeared to be broad and not particularly tuned to the ensemble of conspecific calls.

anuran, auditory midbrain, click, Poisson distribution, temporal processing, Wiener-Volterra expansion

1. Introduction

In addition to spectral features, temporal characteristics of natural vocalizations are important in anuran auditory communication. In general anurans are sensitive to both gross-temporal features, such as call duration and call sequence, as well as to fine-temporal features, such as waveform, rate and depth of amplitude modulation (AM) [e.g. 10,13,31,33].The ensemble of natural vocalizations of the grassfrog (Rana temporaria L.) consists of sequences of calls with a distinct amplitude modulated structure. The calls are emitted in trains of brief repetitive pulses. The mating and territorial calls have a pulse repetition rate (PRR) of 25-35 pulses/s. The male and female release calls are emitted at a PRR of about 45 and 220 pulses/s respectively. The PRR is positively correlated with ambient temperature [5,12,31].

The auditory system might code the envelope of a sound in at least two ways. One possibility, the synchrony code is by synchronizing neural events to preferred phases of the envelope. Another possibility, the rate code, is by changing average firing rate at preferred frequencies of AM. In the anuran auditory system the synchrony code acts mainly in the lower stations up to the superior olivary nucleus, whereas the rate code dominates in the torus semicircularis.

Anuran auditory nerve fibers are able to synchronize their firings to pulse trains or sinusoidally amplitude modulated sounds with AM frequencies up to 200 Hz, without any preference to a particu-

---

Abbreviations: AM amplitude modulation; BF best frequency; BI bimodal; BP band-pass; BRR best repetition rate; HP high-pass; LP low -pass; LT latency; NS non-selective; PESE pre -event stimulus ensemble; PRR pulse repetition rate; SPL sound pressure level.

lar AM frequency [10,23]. The same type of low-pass response with a cut-off frequency of about 200 Hz, is present in the dorsal medullary nucleus and superior olivary nucleus [11]. Recently Schneider-Lowitz (cited in [30]) has reported a group of units at these medullary nuclei exhibiting a weak band-pass response. In the torus semicircularis a considerable portion of units still shows the same synchronization capability as observed in the lower stations. Another group is characterized by a reduced cut-off frequency at 15-50 Hz. A (small) third group of units synchronizes exclusively at intermediate AM frequencies [2]. However, a larger diversity of responses to AM sounds, including an enhanced selectivity, emerges in the torus semicircularis with respect to the rate code. Up to five basic response patterns have been reported: low pass, high-pass, band-pass, band suppression and bimodal response characteristics [23,24,29,30]. In general the most selective units have long latencies and rarely exhibit significant response synchronization at any AM frequency tested [24,30]. The most effective AM frequencies are species specific and correspond to the frequencies present in the natural vocalizations, especially the mating call [24,29]. In case of the grassfrog maximal responses are most frequently elicited by AM frequencies of 25-45 Hz [29].

The aim of this study was to investigate the coding of fine-temporal structure of sound, especially pulse repetition rate, in the auditory midbrain of the grassfrog. As stimuli have been used both periodic click trains as well as long duration click ensembles with a homogeneous Poisson interval distribution. The first type of stimulus is common in the investigation of neural sensitivity to fine temporal characteristics [e.g. 14,22,26,27]. The latter type is in use as test signal in the theory of non-linear systems with discrete inputs [20]. The Poisson distributed click stimulus already has been used for describing the linear part of the response of auditory units by determining the first order system kernel [2]. In addition to the first order kernel we also have determined the second order kernel, which gives an approximative description of the nonlinear neural response characteristics. The system-theoretical approach may reveal underlying neural mechanisms accounting for the temporal sensitivity as observed in periodic click train experiments. In a companion paper [9] an analogous study is described using continuous stimuli, such as sinusoidally and noise amplitude modulated sounds.

2. Materials and Methods

Details of animal preparation, acoustic stimulus presentation and recording procedure have been described extensively in previous papers [8,17, 18]. Of these subjects only a brief description will be presented here.

2.1. Animal Preparation

Under anesthesia (MS-222) the dura covering the tectum mesencephalic of adult grassfrogs (Rana temporaria L.) was exposed. After two days of recovery the animals were immobilized with an intralymphatic injection of Buscopan (0.16 mg per gram bodyweight). The animal was placed dorsal side up onto a damped vibration isolated frame in a sound attenuated room (IAC type 1202A). During recordings the oral cavity was kept shut. Temperature was maintained constant around 16°C and the skin kept moist. The animal's condition was monitored by recording the ECG. Usually the preparation was kept intact, without any signs of deterioration for two consecutive days.

2.2. Acoustic Stimulus Presentation

Acoustic stimuli were generated by a dual channel programmable stimulus generator build around a PDP 11/10. The generated stimuli were presented to the animals by two electrodynamic microphones (Sennheiser MD 211N) coupled to the tympanic membranes with a closed sound system. Care was taken to minimize mechanical crosstalk of stimulus apparatus to the ears. The sound pressure level (SPL) was measured in situ with a half-inch condensor microphone (Bruel and Kjaer 4143) connected to

the coupler. The frequency response of the sound system was flat within 5 dB for frequencies between 100 Hz and 3000 Hz. The amplitude characteristics of left and right couplers were equal within 2 dB for the range of interest. A stimulus ensemble consisting of natural vocalizations, artificial variations thereof, tone and noise bursts was used as search stimulus.

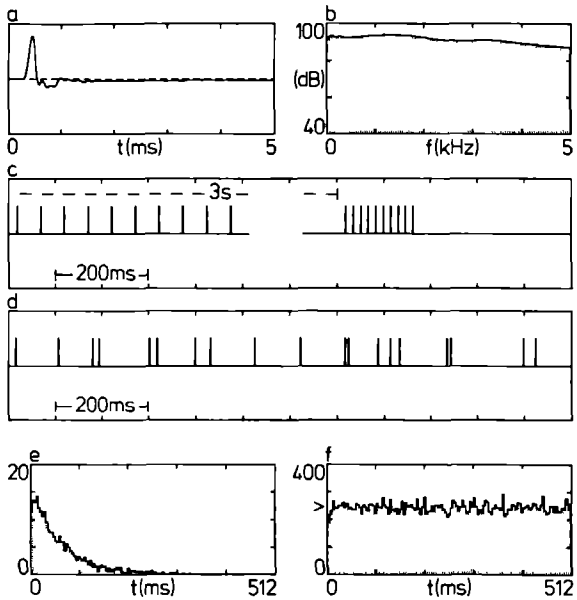

Fig. 1. Characteristics of click stimulus ensembles. (a) Waveform of an individual click as measured at the tympanic membrane. (b) Amplitude spectrum of a click. (c) Fragment of the periodic click train ensemble. (d) Fragment of the Poisson distributed click ensemble with $\lambda = 16$. (e) Interval distribution of the Poisson stimulus. (f) Autocorrelation density of the Poisson stimulus, the arrowhead indicates the expected value λ^2 for an ideal homogeneous Poisson process with intensity λ.

An ideal click should approximate an ideal impulse: the Dirac δ-function. The acoustic click waveform and amplitude spectrum, as measured at the tympanic membrane, are shown in Fig. 1a and 1b respectively. The duration of the click is less than 0.7 ms and its amplitude spectrum is flat within 5 dB for the range of interest. Periodic click trains were presented once per 3 s. Each train consisted of 10 equidistantly spaced clicks (Fig. 1c). Interclick intervals were selected from 16 logarithmically equidistant values in the 5 octave range 4-128 ms, corresponding to pulse repetition rates of 7.8-250/s. One stimulus sequence was composed of 16 pseudorandomly varied trains of different PRR. The total stimulus ensemble consisted of 10 identical sequences, with a total duration of 480 s.

Long duration click ensembles with a homogeneous Poisson interval distribution (Fig. 1d) had intensities (i.e. mean PRR) λ = 4, 8 or 16 clicks/s. The intervals of an ideal homogeneous Poisson process are independent of each other and have a negative exponential distribution of the form $\lambda\exp(-\lambda t)$. Because of limitations in our stimulus generating system, intervals smaller than 1 ms had to be deleted from the interval distribution. The resulting interval distribution is equivalent to the interval distribution of a Poisson process with a dead-time of 1 ms and is shown in Fig. 1e. The autocorrelation density of the Poisson process is depicted in Fig. 1f, indicating that subsequent clicks are uncorrelated. The arrowhead indicates the expected value λ^2 foran ideal homogeneous Poisson proces with intensity λ. The total stimulus ensemble consisted of a short sequence of 30 s followed by 3 identical sequences of 240 s each, presented immediately after each other. The first short sequence was used to allow the units to reach a steady-state response level. These initial 30 s were discarded from the stimulus-response analysis.

Usually stimuli were presented to the contralateral (with respect to recording side) ear at a peak amplitude corresponding to 100 dB SPL (relative to 20 $\mu N/m^2$).

2.3. Recording Procedure

Ultra-fine or tapered tungsten microelectrodes coated with parylene-c, having a 10-15 µm exposed tip with a 1 kHz impedance of 1.5-2.5 MΩ (Micro Probe Inc) were used for extracellular recording. Two electrodes were advanced independently through the intact dura and lowered into the auditory midbrain using two motorized hydraulic microdrives (Trent-Wells 3-0661 and Frederick Haer & Co). Stepping precision was 1 µm. Electrode signals were am-

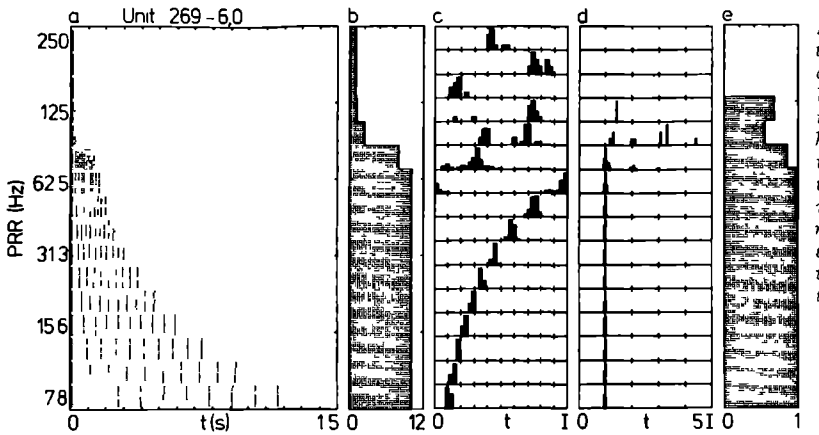

Fig. 2. Illustration of the forward correlation approach in case of a periodic click train stimulus. (a) Dotdisplay. (b) Iso-intensity rate histogram. (c) Period histograms, time-base equals 1 interclick interval (I). (d) Interval histograms, time-base equals 5 interclick intervals. (e) Synchronization index histogram. For reasons of visibility period and interval histograms have been scaled to their own extrema.

plified using Dagan 2400Z extracellular preamplifiers bandpassed between 100 Hz and 10 kHz.

In this configuration simultaneous activity of small neural populations (up to 4 neurons, located within a sphere with a radius of about 25 µm) regularly was recorded on both electrodes. In order to separate the superimposed few-unit activity into the component single-unit spiketrains a pattern recognition technique using the action potential waveform was applied [6]. Waveform features and spike-epochs were stored by a data-acquisition system build around a PDP 11/34 for subsequent off-line analysis on a PDP 11/44. Temporal resolution was 60 µs.

2.4. Stimulus-Event Analysis

2.4.1. Forward Correlation Approach

Temporal sensitivity of units to the periodic click train ensemble was visualized by representing the neural response in several well known forms [15]. The dotdisplay, in which each line shows the neural response to a particular stimulus train, gives an overall impression of temporal sensitivity. The average response rate, defined as the average number of spikes per click train, as a function of click rate was expressed in iso-intensity rate histograms. The degree of locking of neural activity to the clicks was shown in period histograms, which have a timebase equal to the interclick interval. From the period histogram a synchronization index, defined as the vector-strength [16], was derived. The synchronization index has a value between 0, corresponding to a flat period histogram indicating no synchronization, and 1 corresponding to a very peaked period histogram pointing at perfect synchronization. Interspike interval histograms with a timebase equal to 5 interclick intervals showed the degree of entrainment: whether units fired to each click in a time-locked fashion or whether they failed to respond to each click resulting in interspike intervals being multiples of the interclick interval. This type of stimulus event relation analysis, especially suited in case of simple controllable stimuli, may be called a forward correlation or experimenter-centered approach.

The forward correlation procedure is illustrated in Fig. 2 for the periodic click train stimulus. The dotdisplay in Fig. 2a represents the raw neural activity; responses to 10 identical trains have been grouped together and arrayed vertically. The average response rate is expressed in an iso-intensity rate histogram (Fig. 2b). Fine-temporal structure of the neural response has been studied from period (Fig. 2c) and interval (Fig. 2d) histograms with a timebase equal to 1 and 5 interclick intervals respectively. From the collection of period histograms the synchronization index histogram has been constructed. To avoid spurious synchronization values, the synchronization index was set at

0 for PRRs at which the average response rate was < 1. The significance of the synchronization index was not tested statistically. If a period histogram differed by visual inspection not clearly from a flat baseline, the synchronization index was considered insignificant. The unit displayed in Fig. 2a responds to click trains with a PRR up to 62.5 Hz with 1 spike per click in a well synchronized way. At higher PRRs this unit is not able to follow the fine structure of the stimulus. At first for PRRs around 100 Hz the unit does not respond to each individual click anymore, as can most clearly be observed from the interval histograms. For PRRs above 128 Hz the unit responds only to the first click of a burst, a situation for which the synchronization index is not well defined. In the sequel only dotdisplays, iso-intensity and synchronization index histograms will be presented.

2.4.2. Reverse Correlation Approach

An alternative approach, introduced by de Boer and Kuiper [4], is the reverse correlation procedure, which may be called a subject-centered approach. Recently Eggermont et al. [7] have reviewed reverse-correlation methods in auditory research. Each action potential (event) is considered as signalling a stimulus that was of interest to the unit. This view naturally leads to the concept of the pre-event stimulus ensemble (PESE) [19]: the ensemble of signals immediately preceding an event. For this type of approach the stimulus preferably is statistically structured such as Gaussian wideband noise or Poisson distributed click ensembles. Because of the inherent stochastic nature of the neural activity average measures of the PESE have to be determined. Formally this is equivalent to the calculation of crosscorrelation functions of neural activity and various functionals of the stimulus (A functional is a function whose argument is a function and whose value is a number, e.g. the convolution integral is a functional).

Nonlinear systems receiving input of discrete nature can, under certain general assumptions, be characterized by their responses to impulse ensembles with a homogeneous Poisson interval distribution [20]. The method is analogous to the Wiener Volterra expansion of nonlinear systems using a continuous Gaussian wideband noise test-input [32]. The output $y(t)$ of an unknown continuous finite memory nonlinear black box system can be approximated by a series of orthogonal functionals $G_i^P[p_i, x(s), s<t]$ of the Poisson train input $x(t)$ with intensity $\lambda(t)=\lambda$, p_i are the Poisson kernels.

$$y(t) = \sum_{i=0}^{\infty} G_i^P[p_i; x(s), s<t] \qquad (1)$$

and

$$E[G_i^P \cdot G_j^P] = 0, \quad \text{for } i \neq j \qquad (2)$$

The first three functionals are:

$$G_0^P(t) = p_0$$

$$G_1^P(t) = \int_0^{\infty} d\tau\, p_1(\tau)\, [x(t-\tau)-\lambda] \qquad (3)$$

$$G_2^P(t) = \int_0^{\infty}\int_0^{\infty} d\tau\, d\theta\, p_2(\tau,\theta)\, \{[x(t-\tau)-\lambda][x(t-\tau-\theta)-\lambda]\}$$

Following Lee and Schetzen [e.g. 28], Krausz [20] obtained the Poisson kernels $p_n(\tau_1,\ldots,\tau_n)$ by crosscorrelation of input and output. The first three kernels are:

$$p_0 = E[y(t)]$$

$$p_1(\tau) = \lambda^{-1} \cdot E[y(t)x(t-\tau)] - p_0 \quad ; \tau > 0 \qquad (4)$$

$$p_2(\tau,\theta) = \lambda^{-2} \cdot E[y(t)x(t-\tau)x(t-\tau-\theta)]; \ \tau > 0, \ \theta > 0$$

$$-p_1(\tau) - p_1(\tau+\theta) - p_0$$

These kernels may be interpreted as follows. The kernel of order zero p_0 represents the average system response not time-locked to the input. The first-order kernel $p_1(\tau)$ represents the average system response upon a single impulse. When the system is linear, $p_1(\tau)$ is the impulse response. The second-order kernel $p_2(\tau,\theta)$ is

equal to the average facilitation or depression due to a doublet of pulses θ seconds apart, regardless of intervening impulses. When the system is at most quadratic this facilitation or depression is equal to the one measured in a two-pulse experiment.

In case of neural events the output y(t) may be regarded as a train of identical Dirac δ-pulses: $y(t) = \Sigma\, \delta(t-\tau_i)$, i.e. y(t) is a (stochastic) point process.[1] Then the Poisson kernels can be obtained rapidly using first and second-order cross coincidence algorithms. Because of the discrete nature of input and output, especially the second order kernel looks rather noisy. Therefore we applied a two dimensional bell-shaped 5 × 5 point smoothing window to the 128 × 128 binned raw estimate of $p_2(\tau,\theta)$. The kernels were normalized to number of (output) spikes/s. For a more elaborate treatment of the Poisson functional expansion and a comparison with the Wiener-Volterra expansion the reader is referred to [20]. For visualization of the second-order kernel we preferred a gray scale representation to a pseudo 3-D representation. Although a pseudo 3-D representation has greater resolution, its drawback is that certain effects may become hidden.

2.5. Location of Recording Site

Electrode tracks were made approximately orthogonal to the surface of the midbrain in both hemispheres. Position in the rostrocaudal-mediolateral plane was determined by marking the entrance of a track on a photograph made of the surface of the midbrain. All entrances were made within a region extending from 300-1100 μm rostral to the boundary between midbrain and cerebellum and from 600-1100 μm lateral to the midline between the two hemispheres. Dorsal-ventral position was read from the stepping motor devices. All units were recorded on a depth between 800 μm and 1800 μm beneath the surface of the optic lobes. No lesions were made, but because the location of the recording sites as determined above was well within the classical boundaries of the torus semicircularis, as verified by Hermes et al. [18] in an analogous study with histological techniques, we are certain that almost all our auditory units were indeed located inside the torus.

3. Results

Experiments were performed during the entire year, except for the summer season, on a total of 37 male and female grassfrogs. The present study is based on 173 units, from which reliable and stable recordings could be made. Routinely a tonepip stimulus ensemble has been presented to determine the best frequency (BF) of a unit [8,18]. A stimulus response relation to the tonepip stimulus was observed in 89% of the units. A single BF could be assigned to 69% of the units, although some of them had also minor excitatory or inhibitory sidebands at other frequencies. In 20% of the units no single BF could be determined because of about equally strong multiple spectral sensitivity bands or very broad tuning [8]. Spontaneous activity, defined as at least 1 spike per 10 s, was exhibited by 36% of the units.

A stimulus-response relation to one or both click ensembles was observed in 68% of the units. The absence of a stimulus-response relation was not correlated with BF. About half of the units not responsive to tonepips did also not react to clicks. Broadly tuned units always responded to clicks.

3.1. Response to Periodic Click Trains

The periodic click train ensemble was presented to 97 units in 20 frogs. Of these units 77% showed an excitatory response, 4% suppression of spontaneous activity and 19% no response.

3.1.1. Classification of Responses on the Basis of Average Response Rate

On basis of the iso-intensity rate histogram click responsive units were assigned to five different categories.

Low-pass (LP) units (20%). These units responded most strongly at low PRRs, their average

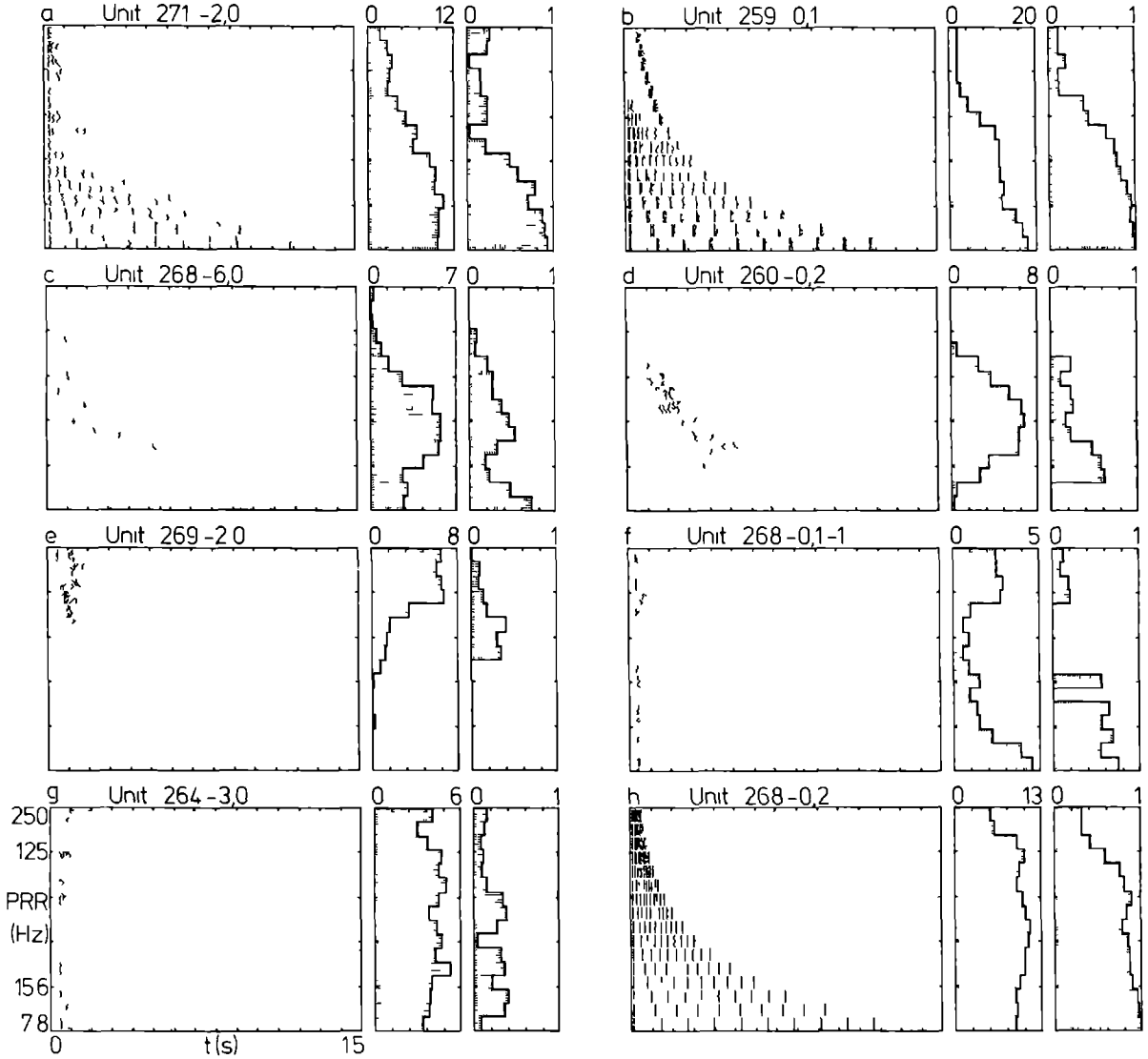

Fig. 3. Examples of 5 different types of units, based on the average response rate. Each figure consists of, from left to right, a dotdisplay, iso-intensity histogram and synchronization index histogram. (a) Low-pass unit. (b) Low-pass unit. (c) Weak band-pass (BPa) unit. (d) Pronounced band-pass (BPb) unit. (e) High-pass unit. (f) Bimodal unit. (g) Non-selective unit. (h) Non-selective unit.

responses rate decreased by at least 50% at higher PRRs. The PRR at which the response has dropped to 50% of maximum is called the cut-off PRR. An example was already shown in Fig. 2. Another low-pass unit is depicted in Fig. 3a, having a cut-off PRR at 62 Hz. In Fig. 3b a low-pass unit is shown that responds with 2 spikes upon a click at very low PRRs. At somewhat higher PRRs the unit responds with only 1 spike per click, especially towards the end of a train. Around a PRR of 62 Hz the unit changes from a sustained firing mode at low PRRs to an off-response mode at high PRRs. This phenomenon was observed in case of 2 low-pass units and might be due to our choice of trains with equal number of

clicks instead of trains of identical duration (see also Discussion).

Band-pass (BP) units (31%). This unit type is characterized by an optimum average response at a specific PRR, the best repetition rate (BRR). The response decreases at least 50% of maximum towards lower and higher PRRs to reach a constant (BPa, weak band-pass, 12%) or even zero level (BPb, pronounced band-pass, 19%). An example of a BPa unit is shown in Fig. 3c. This spontaneous unit responded at all PRRs but optimally at 30 Hz. The histograms have been corrected for the spontaneous activity. In Fig. 3d a BPb unit is represented with a BRR of 30 Hz and no response at low and high PRRs. These BPb units often had long latencies (LT > 50 ms), which were dependent on PRR.

High-pass (HP) units (19%). High-pass units exhibit an increasing average response rate as function of PRR. The maximum response is at least 200% of the minimum response. The cut-off PRR is defined analogously as for LP units. An example of a HP unit is shown in Fig. 3e. This unit has a cut-off PRR at 100 Hz, below which the response drops steadily towards zero.

Bimodal (BI) units (15%). This type of unit combines features of the previous types, resulting in two PRR ranges with high response separated by a region of decreased response. This group of units is rather heterogeneous, because its characteristic may have been shaped by any combination of low-pass, band-pass and high-pass responses. In Fig. 3f a combination of a low-pass and a high-pass type is presented. This unit has a sustained response for low and high PRRs, BRRs are 8 and 150 Hz respectively. At intermediate PRRs this unit behaves transiently, responding with 1 spike at train onset.

Non-selective (NS) units (15%). The average response rates of these units did not reveal any preference (within 50%) for certain PRR values. An example is depicted in Fig. 3g. Most of these units had weak to intermediate synchronization capabilities. Only 1 unit responded in a synchronized way up to 250 Hz (Fig. 3h).

The classification of the units on basis of their average response rates was not always distinct. Some units took an intermediate position between two categories. This is illustrated by the unit in Fig. 3h, which could have been regarded as a low-pass unit with a very high cut-off PRR.

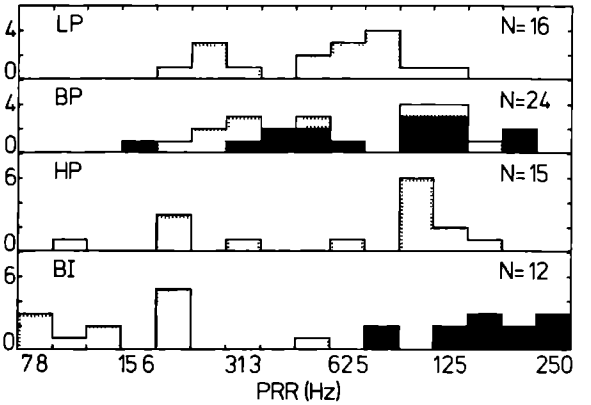

Fig. 4. (a) Distribution of cut-off PRRs of low-pass units. (b) Distribution of BRRs of weak band-pass (shaded) and pronounced band-pass (black) units. (c) Distribution of cut-off PRRs of high-pass units. (d) Distribution of double BRRs at low (shaded) and high (black) PRRs of bimodal units.

No clear correlation was observed between average response rate type and BF nor with spontaneous activity. Units which did respond to clicks but not to tonepips were all band-pass or high-pass units. The distribution of cut-off PRRs and BRRs for the different categories of units is given in Fig. 4. It appears that cut-off PRRs and BRRs are distributed over a broad range. Remarkably band-pass and bimodal units seem to behave antagonistically: BRRs of band-pass units are in the same range as the valley between the two BRRs of bimodal units. This result has already been observed by Walkowiak [30].

3.1.2. Synchronization Capability

In contrast to the diversity of average response rate types, the synchronization capability of units was much more uniform. Of the 79 click responsive units 43% showed a synchronization index histogram with a low-pass character. The synchronization index decreases steadily towards higher PRRs and becomes insignificant for most units. Examples of this type of synchronization behavior are repre-

sented in Fig. 2 and Figs. 3a,b,d,f,g and h. In 3% of the units a bimodal synchronization behavior was observed. The unit in Fig. 3c is an example, it has an optimum synchronization index at a PRR of 8 and 25 Hz. Note that the second optimum coincides with the optimum in the iso-intensity rate histogram. For the other unit with a bimodal synchronization characteristic optima in both types of histograms did not coincide. About half (54%) of the click responsive units had insignificant synchronization indices at all PRRs presented (Fig. 3e).

No clear correlation was observed between synchronization capability and BF. Short latency units had a significantly ($P < 2.5\%$, χ^2-test) better synchronization capability than longer latency units. A clear correlation ($P < 0.05\%$, χ^2-test) was observed between average response rate type and synchronization capability. Low-pass and bimodal units very often ($\pm$ 80%) show significant synchronization indices. Pronounced band-pass and high-pass units, however, mostly ($\pm$ 90%) are not synchronized. Weak band-pass and non-selective units take an intermediate position. The synchronization capability of units is summarized in Fig. 5. It can be concluded that although a large portion of torus units has a diminished synchronization capability, with respect to units of lower auditory nuclei, there still is a considerable fraction ($\pm$ 10%) with high synchronization indices being significant for PRRs larger than 100 Hz.

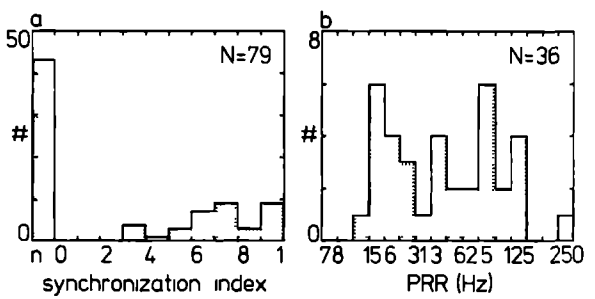

Fig. 5. (a) Distribution of maximum synchronization indices, n: non-significant synchronization. (b) Distribution of ultimate PRRs at which the synchronization index was significant.

3.1.3. Influence of Stimulus Intensity

To investigate whether the stimulus-response relation is invariant to stimulus intensity or not, the periodic click train ensemble was presented to 16 units with intensity decreasing in steps of 10 dB down to threshold. It appeared that 10 units behaved rather invariant (4 units tested over a range of 10 dB, 4 units over a range of 20 dB, 2 units over a range of 30 dB). An example of an invariant unit over a range of 30 dB is shown in Fig. 6a. However, 6 units have been observed that exhibited an alteration of type over a range of 20 to 30 dB. An example of such a unit is presented in Fig. 6b, that changes from a pronounced band-pass unit at 110 dB to a high-pass unit at 80 dB. Moreover, the dependency of latency on PRR becomes less distinct at lower intensities.

3.1.4. Relation between Best Repetition Rate and Best Frequency

Band-pass and bimodal units exhibit the largest selectivity. Of 15 band-pass units and 10 bimodal units a single best frequency could be determined. The position of these units in the spectro temporal BF-PRR plane is indicated in Fig. 7. Of the band-pass units best repetition rate (BRR) is represented. Bimodal units have two BRR-values, which are difficult to picture conveniently. Therefore we have represented the PRR at which the valley between the two peaks in the iso-intensity rate histogram of bimodal units is minimal, inspired by the seemingly antagonistic behavior of band-pass and bimodal units (Fig. 4). For comparison the energy distribution of the 4 most prominent natural vocalizations of the grassfrog [5,12,29,31] has been portrayed as well. No clear correlation is present between BF and PRR. Units do not cluster obviously within regions of high conspecific call energy, but are scattered all over the plane.

3.2. Response to Poisson Distributed Click Ensembles

The Poisson distributed click stimulus was

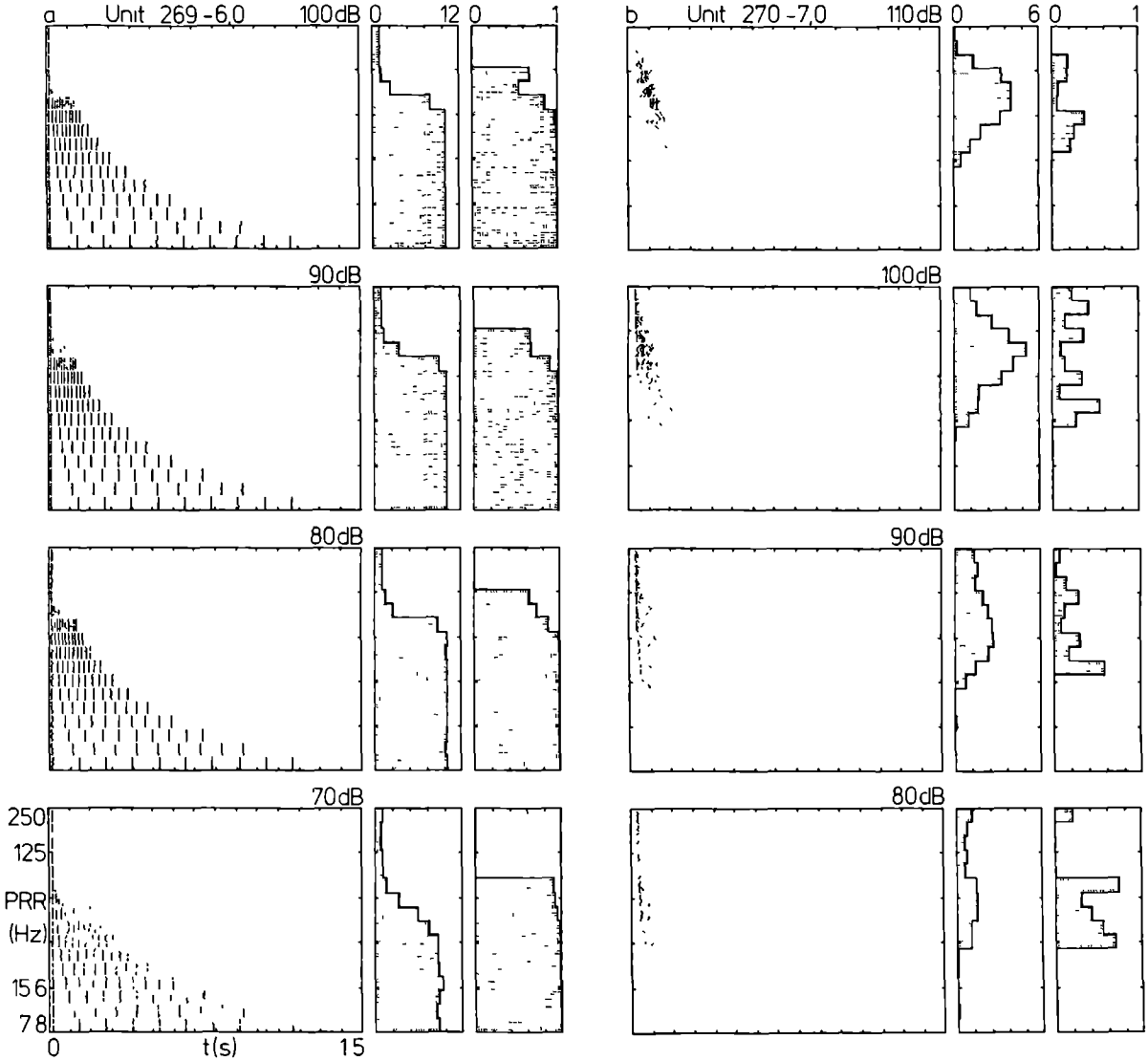

Fig. 6. (a) Unit being invariant to stimulus intensity. (b) Unit having an intensity dependent response. Per unit the iso-intensity rate histograms have been scaled identically.

presented to 138 units in 34 frogs. Of these units 81 (59%) responded stationary, in the sense of average firing rate, after an onset period varying from a few seconds to several minutes. The other 57 units did not respond at all or at least not stationary. The existence of a stimulus-response relation was investigated by means of the existence function which measures the degree of reproducibility of neural activity upon identical stimulus sequences [1,8,18]. Of the 81 stationary responding units 73 (90%) had a clear positive existence function. Of the remaining 8 units 4 were suppressed by the stimulus, 4 other units appeared to respond weakly and loosely bound to the stimulus as became clear from the kernel analysis. The nature of the stimulus-response relation was investigated by com-

putation of first and second-order Poisson system kernels.

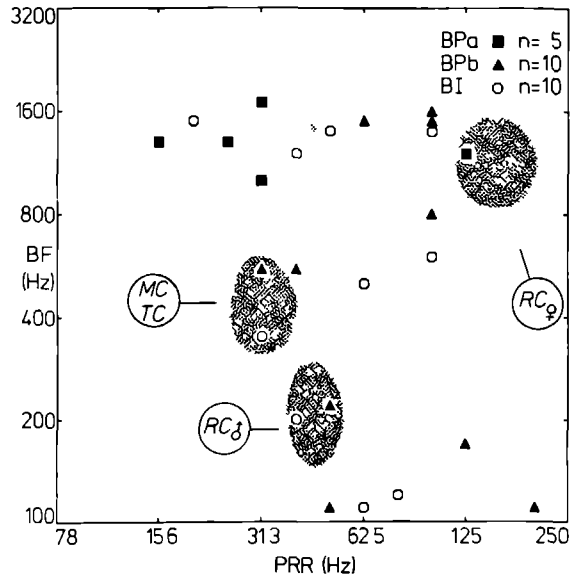

Fig. 7. Relation between characteristic pulse repetition rate (PRR) and best frequency for band-pass (BP) and bimodal (BI) units. In case of band-pass units their best repetition rate is represented, for bimodal units the PRR at which the valley between the two peaks in the iso-intensity rate histogram was at minimum is indicated. For comparison also the energy distribution of the natural vocalizations of the grassfrog is pictured. Dark gray shades indicate regions of high energy. MC: mating call; TC: territorium call; RC: release call.

3.2.1. Classification of Responses on Basis of the First-Order Kernel

The 81 stationary responding units exhibited 6 different types of first-order kernels due to different dynamics of activation and suppression phenomena. The nomenclature was adopted from Bibikov [2].

Type I units (40%). These units were characterized by a positive unimodal peak, pointing at activation. An example is illustrated in Fig. 8a, which had a latency of about 25 ms indicated by the arrowhead. Sometimes also minor sidepeaks, mostly not more than a bend on the flank of the main peak, were observed (Fig. 8b) indicating a more complex mode of behavior. Presumably these more complex units can be regarded as a transition to type V units.

Type II units (23%). In the first-order kernel of these units the positive peak was accompanied by a negative one at the longer latency side. Sometimes the negative deflection could extend beyond 500 ms (Fig. 8c). The relative amplitudes and durations of positive and negative phenomena could vary substantially within this class. In Fig. 8d a unit is shown of which the long lasting negative deflection is hardly discernable.

Type III units (16%). These units have first order kernels in which the course of the dynamics is reversed with respect to type II units. A negative valley is observed at smaller latencies than the positive peak (Fig. 8e). These units are, on average, at first suppressed by a click and later on activated. Again relative amplitudes of positive and negative phenomena could vary to a large extent.

Type IV units (5%). These units combine the features of type II and III units. A positive peak is flanked on both sides by a negative valley. In the example of Fig. 8f the initial suppressive effect was so strong that no activity was present in the latency region 12-24 ms, resulting in a flat first-order kernel at level $-p_0$ for these latencies.

Type V units (10%). The main feature of this category is the presence of two, sometimes even three, clearly separated positive peaks. The unit in Fig. 8g has two positive peaks with latencies of 9 and 15 ms respectively. Most type V units had in addition to a multimodal positive structure also one or more properties of the other categories such as a negative deflection at longer latencies (Fig. 8h).

Type VI units (6%). These units were characterized by one negative valley. This type was observed only in case of spontaneously active units. The interpretation of this phenomenon is that on average a click suppresses the spontaneous activity. An example is shown in Fig. 8i.

No clear relationship was observed between type of first-order kernel and BF, except that all

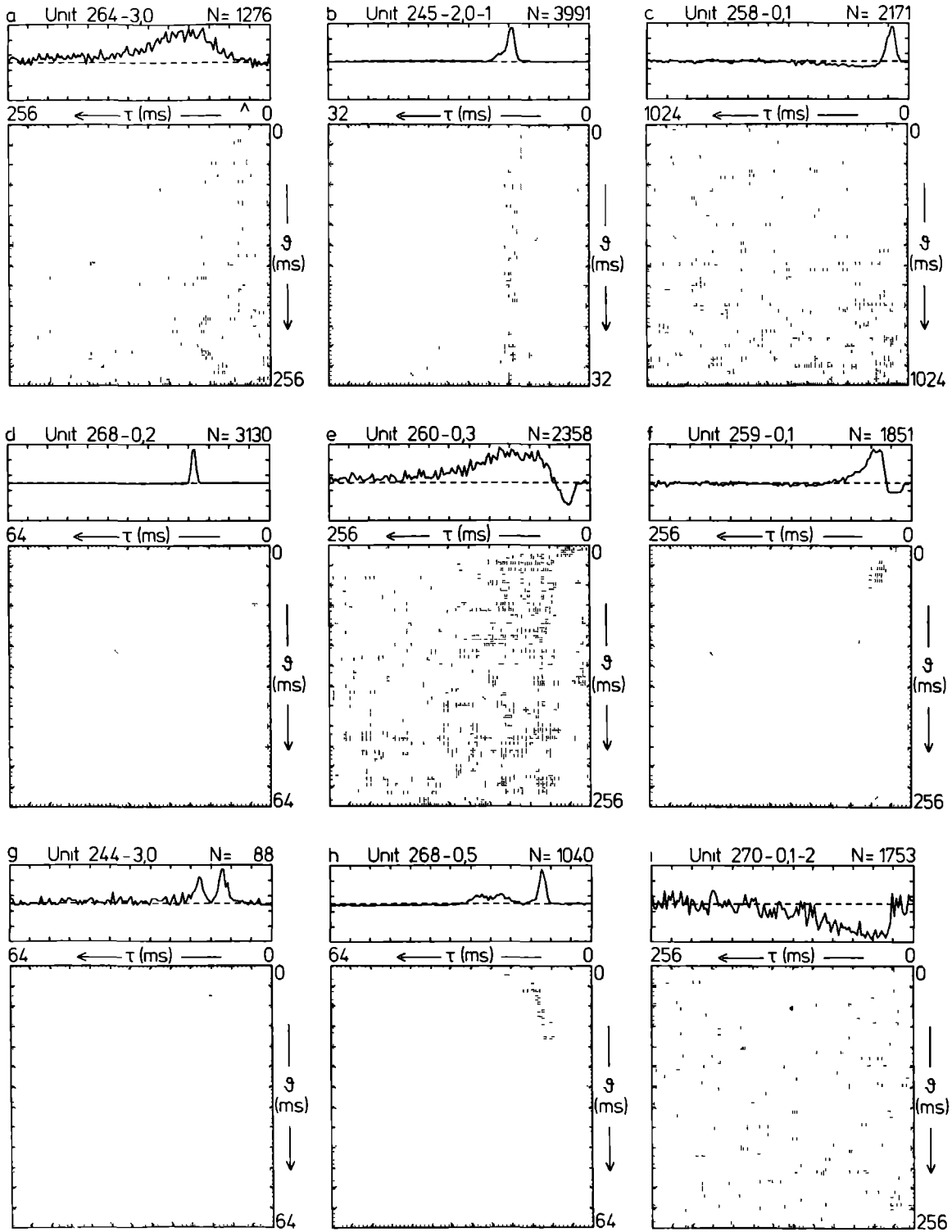
a Unit 264-3,0 N= 1276
256 ⟵ τ (ms) ⟵ 0
ϑ (ms)
256
b Unit 245-2,0-1 N= 3991
32 ⟵ τ (ms) ⟵ 0
ϑ (ms)
32
c Unit 258-0,1 N= 2171
1024 ⟵ τ (ms) ⟵ 0
ϑ (ms)
1024
d Unit 268-0,2 N= 3130
64 ⟵ τ (ms) ⟵ 0
ϑ (ms)
64
e Unit 260-0,3 N=2358
256 ⟵ τ (ms) ⟵ 0
ϑ (ms)
256
f Unit 259-0,1 N= 1851
256 ⟵ τ (ms) ⟵ 0
ϑ (ms)
256
g Unit 244-3,0 N= 88
64 ⟵ τ (ms) ⟵ 0
ϑ (ms)
64
h Unit 268-0,5 N= 1040
64 ⟵ τ (ms) ⟵ 0
ϑ (ms)
64
i Unit 270-0,1-2 N= 1753
256 ⟵ τ (ms) ⟵ 0
ϑ (ms)
256

Fig. 8. First and second-order Poisson kernels for a representative set of units. In the second-order kernel amount of activation is coded along a gray-scale: black corresponds to activation, white to depression. (a), (b) Type I units. (c), (d), Type II units. (e) Type III unit. (f) Type IV unit. (g), (h) Type V units. (i) Type VI unit. Stimulus intensity was 100 dB SPL, except in (c) where it was 80 dB SPL, and click intensity λ was 16/s.

type VI units had BF's below 1000 Hz and therefore presumably receive their input from the amphibian papilla. The distribution of latency, defined as the minimum time at which a positive or negative phenomenon in the first-order kernel deviates distinctly from zero (Fig. 8a), is shown in Fig. 9. This distribution is unimodal around a maximum at 20 ms, minimum LT was 8 ms and maximum LT was 84 ms. No relation was apparent between type of first order kernel and LT.

3.2.2. The Second-Order Kernel

On basis of the first-order kernel only, inferences cannot be made about the influence of interaction of clicks on the neural response. For example it is ambiguous whether the multiple activation and/or suppression effects in types II-V are time-locked to each other, or that these effects are due to independent processes appearing together just because of averaging over time. To be more specific, the type V first-order kernel (Fig. 8g, 8h) may be explained by at least two mechanisms. One mechanism could be that the unit responds with

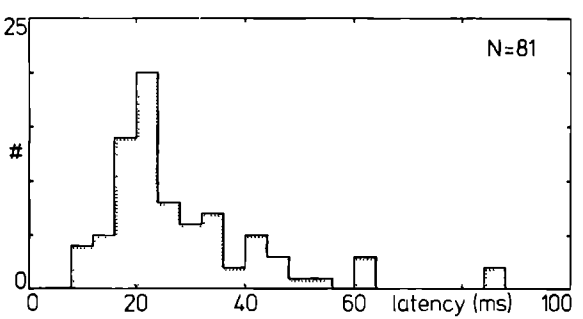

Fig. 9. Latency distribution on basis of the first order Poisson kernel.

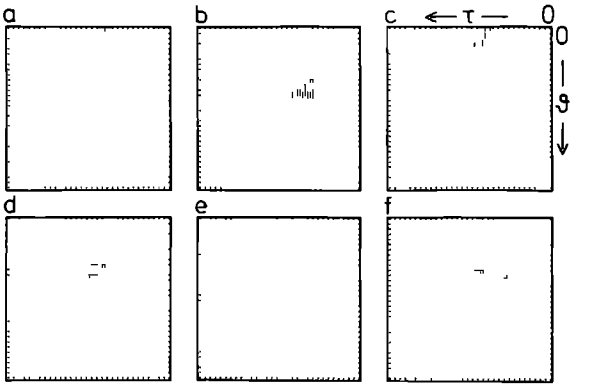

Fig. 10. Stylized examples of different types of second order Poisson kernels. Black corresponds to activation, white to depression.

two spikes to one click. Another explanation might be that the unit reacts selectively with 1 spike to a pair of clicks separated by a certain interval. Clearly extra information is needed to decide between the possible mechanisms. For type V units the interval distribution of neural activity could settle the issue. Evaluation of the second-order kernel, however, is from a system-theoretical point of view a more elegant and more general tool to investigate nonlinear synaptic and spike-generating mechanisms.

Essentially 6 basic types of second-order kernels have been observed. Stylized examples are shown in Fig. 10.

Type A (32%). This kind of second-order kernel is characterized by a positive contribution for click separation intervals θ smaller than a certain θ_m (Fig. 8a, 8i, 10a). It can be interpreted as non-linear facilitation of the neural response to a click, when another click preceded this click by at most θ_m ms. In case of the unit in Fig. 8a this means that the response to a pair or clicks within θ_m ms will be larger than the sum of the responses to two single clicks. The unit in Fig. 8i has kernels of opposite sign, which points to a less depressed activity to a pair of clicks than would be expected from the first-order kernel alone.

Type B (11%). These kernels are positive only for a specific range of θ-values, for smaller and larger θ-values they are zero (Fig. 8g, 10b). This

kind of kernel points at facilitation when a click-pair has a specific temporal separation. With this information the unit with the bimodal first-order kernel of Fig. 8g presumably is best explained by stating that it is sensitive to click pairs separated by a certain interval, instead of firing two spikes in response to one click. This explanation was supported by the unit's interval distribution, in which no optimum interval was present. The selectivity of this unit is underlined by the fact that it responded with only 88 spikes to a stimulus containing more than 10.000 clicks!

Type C (15%). These kernels exhibit facilitation for click separation intervals smaller than a certain value like type A kernels. In addition, however, they have a negative region for larger separation intervals pointing at depression (Fig. 10c).

Type D (14%). Like type B kernels there is facilitation for a specific click separation interval. For smaller intervals, however the response is depressed (Fig. 8b, 10d). Sometimes, this particular combination of facilitation and depression was also observed in more complex kernels (Fig. 8e, 8f, 8h). For example the second-order kernel in Fig. 8h shows facilitation for separation intervals between 5 and 19 ms, and depression for smaller and larger intervals at the same latency τ = 10 ms. This kernel may be interpreted as that a click evokes neural activity with a latency of 10 ms. The response to this click is facilitated if it is preceded by another click by 5-19 ms and depressed at other separation intervals. In addition this kernel shows a negative region at latency τ = 17 ms and separation intervals τ = 3-11 ms. This interplay of facilitatory and depressive phenomena may serve as contrast enhancement.

Type E (10%). These kernels are characterized by one negative region for separation intervals smaller than a specific value (Fig. 8c, 8d, 10e). These kernels in combination with type II first order kernels (Fig. 8c, 8d) indicate that the negative and positive effects of the first-order kernel are time-locked to each other and not due to independent inhibitory and excitatory influences arriving with different latencies. So it may be stated that these units exhibit post-activation suppression. This conclusion could not be drawn from the first-order kernel alone! Note that the suppression effect in Fig. 8d is much more conspicuous in the second-order than in the first-order kernel.

Type F (11%). The main characteristic of this rather heterogeneous type of kernels is a depressive effect at shorter latencies than the facilitatory effect (Fig. 10f). Often also features of the former types were present (Fig. 8e, 8f).

Of the 81 units with a first-order kernel 6 units (7%) did not exhibit a second-order kernel. Of these 6 units 3 had only a weak noisy type I first-order kernel, the other 3 had a weak type VI first-order kernel. So probably the absence of a clear second-order kernel in these 6 units is due to the weak stimulus-response coupling, causing a large variability in the kernel estimates. All units with moderate to strong stimulus-response relations as apparent from existence functions and first-order kernels showed also clear second-order kernels.

Table I. Distribution of first-order and second order Poisson kernels.

	I	II	III	IV	V	VI	total second-order
A	18		4	2		2	26
B	7		1		1		9
C	1	10	1				12
D	3	2			6		11
E		7			1		8
F			7	2			9
no	3					3	6
total first order	32	19	13	4	8	5	81

For definition and illustration of the different types of kernels see text.

The types of first-order and second-order Poisson kernels appeared to be strongly related, see Table I. Unimodal positive first-order kernels (type I) often were accompanied by unimodal posi-

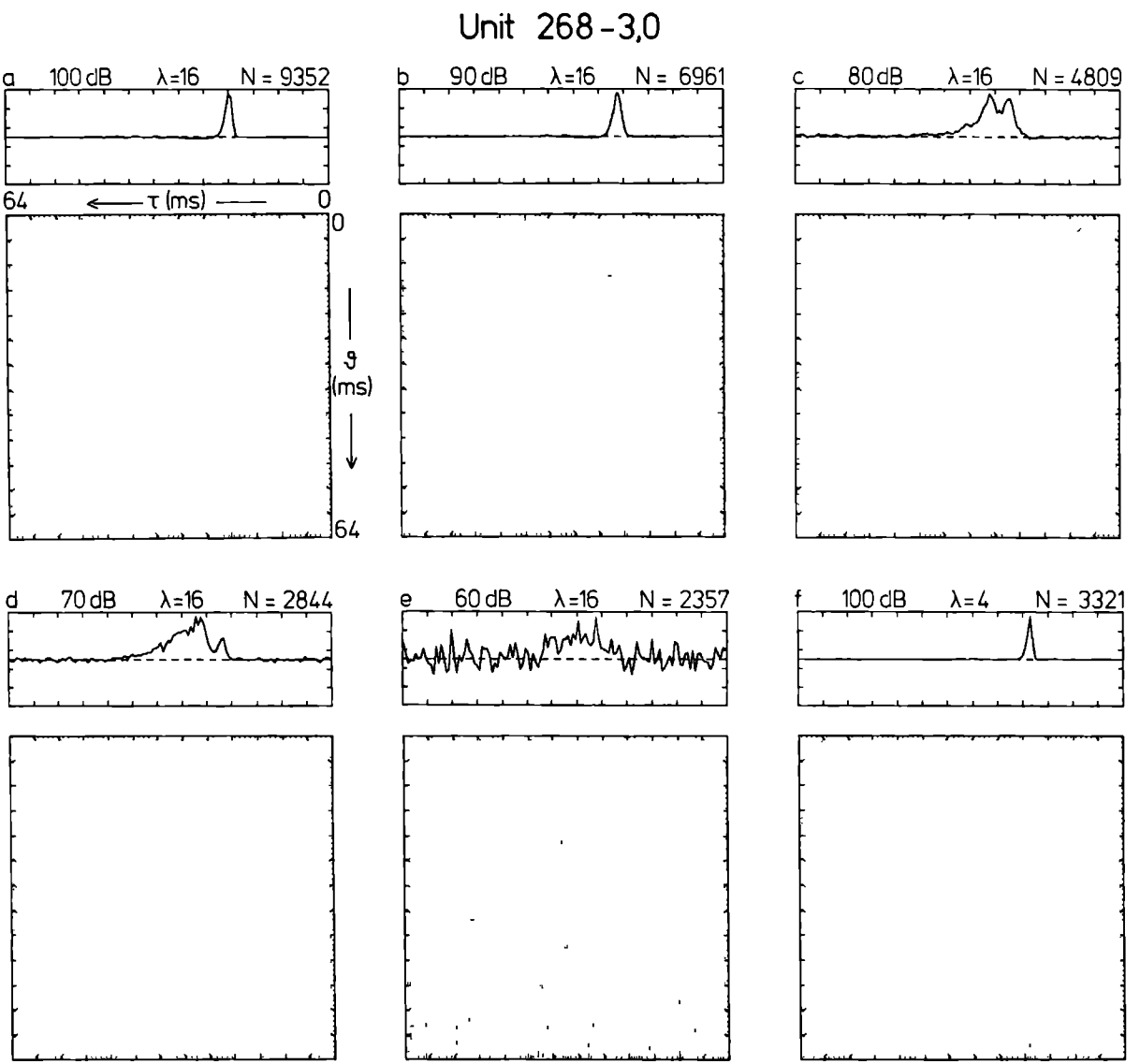

Fig. 11. Influence of stimulus level and average click rate λ on Poisson kernels.(a)-(e) Varying stimulus level, constant click intensity λ = 16. (f) Stimulus level 100 dB, click intensity λ = 4. For reasons of visibility the kernels have been scaled to their own extrema. The extrema of first-order and second-order kernels respectively are: (a) 445, 482; (b) 268, 229; (c) 55, 176; (d) 21, 69; (e) 4, 15; (f) 626, 546.

tive second-order kernels (type A,B). Type II first-order kernels often were coupled to second order kernels with depressive effects for click separations smaller than a certain value (type C,E), indicating post-activation suppression. Type III first-order kernels and type F second-order kernels were regularly observed together. With one exception bimodal positive first-order kernels (type V) were coupled to second-order kernels with facilitation for specific click separation intervals (type B,D), indicating responsiveness to click-pairs. In 2 of the 8 units with bimodal first-order kernels

it appeared that the interval distribution of spontaneous activity had a maximum corresponding to the specific click separation interval. The tight coupling of first- and second-order kernels makes it plausible that these kernels are different manifestations of the same underlying nonlinear process and that they are not due to two independent processes: one linear and e.g. one quadratic process.

3.2.3. Influence of Stimulus Level and Average Click Rate λ

The Poisson distributed click ensemble was presented to 7 units at different stimulus levels, but with an identical click intensity λ. Of these units 3 were invariant to change of stimulus level (2 units over a range of 10 dB, 1 unit over a range of 20 dB). The other 4 units had variable characteristics, e.g. change in latency, temporal spread and type of kernels. An example of a unit not invariant to alteration of stimulus level is shown in Fig. 11. This unit has a post-activation suppression type of behavior at 100 and 90 dB SPL, changes to a broader sensitivity for click pairs with separation of about 4 ms at 80 en 70 dB SPL to become eventually weakly activated without a significant second-order kernel at 60 dB SPL just above threshold (Fig. 11a-e). Note that latency (19 ms) is rather invariant over a range of 40 dB.

Also 7 units have been tested at identical stimulus levels but with varying click intensities λ (4/s, 8/s, 16/s). It appeared that 4 units behaved invariant, while 3 others exhibited changes in latency and/or type of kernels. An example of a unit of which mainly the latency varies is the one already shown above, which has a somewhat shorter latency (17 ms) and a sharper first-order kernel at click intensity λ = 4 (Fig. 11f) than at click intensity λ = 16 (Fig. 11a). The type of kernels of this unit is the same at both click intensities.

3.3. Relation of Characteristics Obtained with Periodic and Poisson Distributed Clicks

Both types of stimulus ensembles were presented to 62 units at the same intensity level. Of these units 41 responded stationary to both stimuli. Of the other 21 units 2 responded not at all to both stimuli, 16 units responded not stationary to the Poisson stimulus and 3 units did not react to the periodic click train ensemble.

It is tempting to explain qualitatively the sensitivity to periodic click bursts on basis of the kernels determined with Poisson distributed click ensembles. For example at first instance one would expect a band-pass unit to have a bimodal first-order and presumably a type B or D second order kernel. However, in the, admittedly small, population of 41 units responsive to both ensembles no obvious relations between type of sensitivity to periodic click trains and kernel types have been observed. We will return to this subject in the discussion.

4. Discussion

In the torus semicircularis of the grassfrog a large variety of response types has been observed both in reaction to periodic click trains as well as to Poisson distributed click ensembles. Taking into account the somewhat different stimulus paradigms used, the results of the present study in general agree well with analogous studies conducted in the auditory midbrain of anurans [2,24,25,30]. The only difference with the study of Walkowiak [30] was the fraction of band-pass units: 31% versus 58%. This difference presumably is explained by the use of trains of equal number of clicks versus trains of equal duration.

4.1. Synchrony Code versus Rate Code

From the studies of Rose and Capranica [24, 25], Walkowiak [30] and the present one it becomes clear that on the level of the auditory midbrain a transformation from a synchrony code to a rate code takes place. In principle these codes are independent, because synchronization capability can be changed without affecting average rate and vice-versa. The synchrony code, in which the fine-temporal structure of sound is coded by synchronization

of neural activity to the envelope, exclusively acts on the level of the auditory nerve [10,25] and also is the dominant code in the two medullary nuclei [11,30]. Up to the level of the superior olivary complex the synchronization capability of most units extends beyond 100 Hz, sometimes even beyond 250 Hz [11].

In the torus semicircularis, however, most units show a drastically reduced synchronization capability, although still about 10% of the units has the same synchronization qualities as observed in lower stations. The reduced synchronization capability, however, is compensated by a large diversity of average rate characteristics containing information about fine-structure of sound, pleading in favour of a rate code.

4.2. Influence of Sound Pressure Level and Average Click Rate λ

About half of the units tested at different sound pressure levels and/or click intensities behaved invariant over a considerable range of values. These units possibly act as temporal filters. The other units, however, have characteristics not exclusively depending on the temporal fine structure of the sound and therefore do not encode this feature unambiguously, at least on the single-unit level. The variation of the Poisson kernels with changes in stimulus characteristics may have at least two causes. The first reason of variation is that the units exhibit non-linearities of order higher than two. The second and presumably most important reason is that these units, considered as nonlinear systems, have parameters which are in itself dependent on overall stimulus characteristics. For example adaptation levels will probably depend on SPL and λ values.

4.3. Relation of PRR Sensitivity and Poisson Kernels

As already discussed by Walkowiak [30] the sensitivity to pulse repetition rate can be accounted for by various mechanisms such as adaptation, temporal summation and the most important: neural interaction. The influence of neural interaction is also apparent in the shape of the more complex Poisson kernels (first-order types III, IV and V and second order type B,D,F), which cannot be explained conveniently by adaptation or temporal summation mechanisms. These neural interaction circuits presumably are located within the torus semicircularis.

In the neural population investigated with both the periodic click trains as well as the Poisson distributed click ensemble no obvious qualitative correspondence was observed between type of PRR sensitivity and Poisson kernel type. There may be several reasons for this finding. The first reason is that no quantitative features of the kernels, such as duration and relative strength of excitatory and inhibitory phenomena have been taken into account. The second reason might be that sensitivity to PRR cannot be explained solely on basis of first- and second-order kernels. A third reason can be that although both stimulus ensembles have been presented at the same peak SPL, adaptation levels might differ drastically due to the long silences between the periodic click trains in contrast to the homogeneous Poisson distributed click ensemble. Presumably this difference of adaptation levels is the most important reason in the light of the variation of neural characteristics with changes in SPL and λ.

A straightforward and elegant way to try to explain PRR sensitivity out of the Poisson kernels is by making quantitative predictions of the response to periodic click trains on basis of the Poisson functional expansion. In a forthcoming paper these response predictions will be described and the sufficiency of the kernel expansion up to second-order will be evaluated.

4.4. Spectro-Temporal Sensitivity and Conspecific Calls

No obvious relation was observed between the spectro-temporal sensitivity of units and the spectro-temporal energy distribution of the conspecific calls of the grassfrog (Fig. 7), at least as determined in this study using acoustic clicks. In fact

the spectral and temporal components of the spectro-temporal sensitivity have been obtained separately. Best frequency was determined with tonepips, whereas optimal pulse repetition rate was based on stimuli containing clicks with a flat spectrum. Thereby it has been observed that a considerable portion of the pronounced band-pass units did not respond to tonepips. It may well be possible that in a combined spectro-temporal sensitivity study neural characteristics and natural vocalizations show a larger correspondence. In the companion paper [9] using AM sound the effect of the spectral content on temporal sensitivity has been investigated. Nevertheless the anuran auditory midbrain probably has a broader spectro-temporal sensitivity than the domain of the conspecific calls.

4.5. General Conclusions

From the present study several general conclusions about the coding of fine-temporal structure of sound in the anuran auditory midbrain can be drawn.

(i) On the level of the torus semicircularis a transformation takes place from a synchrony code to a rate code. Some units, however, still exhibit the same synchronization capability as reported for medullary units. Moreover, selectivity for particular pulse repetition rates is enhanced drastically in the auditory midbrain.

(ii) About half of the units were invariant to changes of sound pressure level. These units are potential feature detectors of fine-temporal structure.

(iii) The Poisson system kernels reveal possible underlying (nonlinear) synaptic and spike generating mechanisms accounting for the observed selectivity for fine-temporal structure of sound.

Acknowledgements

This investigation forms part of the research program "Brain and Behaviour" at the Department of Medical Physics and Biophysics of the University of Nijmegen and was supported by the Netherlands Organization for the Advancement of Pure Research (ZWO). The authors wish to thank Jan Bruijns, Dick Bosman and Wim van Deelen for software development, Koos Braks for the animal preparations and technical assistance, Hans Krijt and his group for electronic support. Ad Aertsen, Henk van den Boogaard, Peter Johannesma and Ivo van Stokkum provided valuable comments on the manuscript, which was put into the wordprocessor carefully by Marianne Nieuwenhuizen.

References

1 Aertsen, A.M.H.J., Smolders, J.W.T. and Johannesma, P.I.M. (1979): Neural representation of the acoustic biotope: on the existence of stimulus-event relations for sensory neurons. Biol. Cybern. 32, 175-185.
2 Bibikov, N. (1981): Cross-correlation analysis of the activity of the auditory neurones on exposure to sound clicks. Biophysics 26, 346-352.
3 Bibikov, N. and Gorodetscaya, O. (1981): Coding of amplitude-modulated tones in the midbrain auditory region of the frog. In: Neuronal Mechanisms of Hearing, pp. 347-352. Editors: J. Syka and L. Aitkin. Plenum Press, London, New York.
4 Boer, E. de, Kuiper, P. (1968): Triggered correlation. IEEE Trans. Biomed. Eng. BME-15, 169-179.
5 Brzoska, J., Walkowiak, W. and Schneider, H. (1977): Acoustic communication in the grass frog (*Rana temporaria* L.): calls, auditory thresholds and behavioral responses. J. Comp. Physiol. 118, 173-186.
6 Eggermont, J.J., Epping, W.J.M. and Aertsen, A.M.H.J. (1983): Stimulus dependent neural correlations in the auditory midbrain of the grassfrog (*Rana temporaria* L.). Biol. Cybern. 47, 103-117.
7 Eggermont, J.J. Johannesma, P.I.M. and Aertsen, A.M.H.J. (1983): Reverse-correlation methods in auditory research. Quarterly Reviews of Biophysics 16, 341-414.
8 Epping, W.J.M. and Eggermont, J.J. (1985): Single-unit characteristics in the auditory midbrain of the immobilized grassfrog. Hearing Res. (in press)
9 Epping, W.J.M. and Eggermont, J.J. (1986): Sensitivity of neurons in the auditory midbrain of the grassfrog to temporal characteristics of sound. II. Stimulation with amplitude modulated sound. (submitted).
10 Frishkopf, L.S., Capranica, R.R. and Goldstein, M.H. (1968): Neural coding in the bullfrog's auditory system, a teleological approach. Proc. IEEE 56, 969-980.
11 Fuzessery, Z.M. and Feng, A.S. (1983): Frequency selectivity in the anuran medulla: excitatory and inhibitory tuning properties of single neurons in the dorsal medullary and superior olivary nuclei. J. Comp. Physiol. A 150, 107-119.
12 Gelder, J.J. van, Evers, P.M.G. and Maagnus, G.J.M. (1978): Calling and associated behaviour of the common frog, *Rana temporaria*, during breeding activity. J. Anim. Ecol. 47, 667-676.
13 Gerhardt, H.C. (1978): Mating call recognition in the green treefrog *(Hyla cinerea)*: the significance of some fine-temporal properties. J. Exp. Biol. 74, 59-73.
14 Gersuni, G.V. and Vartanian, I.A. (1973): Time dependent features of adequate sound stimuli and

the functional organization of central auditory neurons. In: Basic Mechanisms in Hearing, pp. 623-673. Editor: A.R. Møller. Academic Press, New York, London.

15 Gibson, J.M. and Welker, W.I. (1982): Stimulus response profile analysis: a comprehensive, quantitative approach to the study of sensory coding and information processing. J. Neurosci. Meth. 5, 349-368.

16 Goldberg, J.M. and Brown, P.B. (1969): Response of binaural neurons of dog superior olivary complex to dichotic tonal stimuli: some physiological mechanisms of sound localization. J. Neurophysiol. 32, 613-636.

17 Hermes, D.J., Aertsen, A.M.H.J., Johannesma, P.I.M. and Eggermont, J.J. (1981): Spectro-temporal characteristics of single units in the auditory midbrain of the lightly anaesthetised grass frog (*Rana temporaria* L.) investigated with noise stimuli. Hearing Res. 5, 147-178.

18 Hermes, D.J., Eggermont, J.J., Aertsen, A.M.H.J. and Johannesma, P.I.M. (1982): Spectro temporal characteristics of single units in the auditory midbrain of the lightly anaesthetised grass frog (*Rana temporaria* L.) investigated with tonal stimuli. Hearing Res. 6, 103-126.

19 Johannesma, P.I.M. (1972): The pre-response stimulus ensemble of neurons in the cochlear nucleus. In: Proc. of the IPO Symp. on Hearing Theory, pp. 58-69. Editor: B.L. Cardozo. IPO, Eindhoven.

20 Krausz, H.I. (1975): Identification of nonlinear systems using random impulse train inputs. Biol. Cybern. 19, 217-230.

21 Marmarelis, P.Z. and Marmarelis, V.Z. (1978): Analysis of Physiological Systems: The White-Noise Approach, Plenum Press, New York.

22 Møller, A.R. (1969): Unit responses in the rat cochlear nucleus to repetitive, transient sounds. Acta Physiol. Scand. 75, 542-551.

23 Rose, G. and Capranica, R.R. (1983): Temporal selectivity in the central auditory system of the leopard frog. Science 219, 1087-1089.

24 Rose, G.J. and Capranica, R.R. (1984): Processing of amplitude-modulated sounds by the auditory midbrain of two species of toads: matched temporal filters. J. Comp. Physiol. A 154, 211-219.

25 Rose, G.J. and Capranica, R.R. (1985): Sensitivity to amplitude modulated sounds in the anuran auditory nervous system. J. Neurophysiol. 53, 446-465.

26 Rouiller, E., de Ribaupierre, Y., Toros-Morel, A. and de Ribaupierre, F. (1981): Neural coding of repetitive clicks in the medial geniculate body of cat. Hearing Res. 5, 81-100.

27 Rouiller, E. and de Ribaupierre, F. (1982): Neurons sensitive to narrow ranges of repetitive acoustic transients in the medial geniculate body of cat. Exp. Brain Res. 48, 323-326.

28 Schetzen, M. (1980): The Volterra and Wiener theories of nonlinear systems. Wiley, New York.

29 Walkowiak, W. (1980): The coding of auditory signals in the torus semicircularis of the fire-bellied toad and the grass frog: responses to simple stimuli and to conspecific calls. J. Comp. Physiol. A 138, 131-148.

30 Walkowiak, W. (1984): Neuronal correlates of the recognition of pulsed sound signals in the grass frog. J. Comp. Physiol. A 155, 57-66.

31 Walkowiak, W. and Brzoska, J. (1982): Significance of spectral and temporal call parameters in the auditory communication of male grass-frogs. Behav. Ecol. Sociobiol. 11, 247-252.

32 Wiener, N. (1958): Nonlinear problems in random theory. Wiley, New York.

33 Wilczynski, W. and Capranica, R.R. (1984): The auditory system of anuran amphibians. Progress in Neurobiol. 22, 1-38.

SENSITIVITY OF NEURONS IN THE AUDITORY MIDBRAIN OF THE GRASSFROG TO TEMPORAL CHARACTERISTICS OF SOUND

II. Stimulation with Amplitude Modulated Sound

Willem J.M. Epping and Jos J. Eggermont

Department of Medical Physics and Biophysics, University of Nijmegen, Geert Grooteplein Noord 21
NL-6525 EZ Nijmegen, The Netherlands

The coding of fine-temporal structure of sound, especially of frequency of amplitude modulation, was investigated on the single-unit level in the auditory midbrain of the grassfrog. As stimuli sinusoidally amplitude modulated sound bursts, and continuous sound with low-pass Gaussian noise amplitude modulation have been used. Both tonal and wideband noise carriers have been applied. The response to sinusoidally AM sound bursts was studied in two aspects focussing on two types of possible codes: a rate code and a synchrony code. From the iso-intensity rate histogram five basic average response characteristics as function of modulation frequency have been observed: low-pass, band-pass, high-pass, bimodal and non-selective types. The synchronization capability, expressed in a synchronization index, was non-significant for 38% of the units and a low-pass function of modulation frequency for most of the other units. The stimulus-response relation to noise AM sound was investigated by a nonlinear system theoretical approach. On basis of first and second-order Wiener-Volterra kernels possible neural mechanisms accounting for temporal selectivity were obtained. About one quarter of the units had response characteristics that were invariant to changes in sound pressure level and spectral content of the carrier. These units may function as feature detectors of fine-temporal structure of sound. The spectro-temporal sensitivity range of the auditory midbrain of the grassfrog appeared not to be restricted to and showed no preference for the spectro-temporal characteristics of the ensemble of conspecific calls. Comparison of response characteristics to periodic click trains as studied in the companion paper [7] and sinusoidally AM sound bursts revealed that the observed temporal sensitivity is due to a combination of sensitivities to sound periodicity and pulse duration. It was found that for most units the first-order kernels for Gaussian AM stimuli and Poisson distributed click stimuli were alike. In contrast second-order kernels for the Gaussian AM stimuli often represented only static nonlinearities, while second-order kernels for Poisson distributed clicks [7] mostly revealed dynamic nonlinearities.

amplitude modulation, anuran, auditory midbrain, Gaussian noise, nonlinear systems, Wiener-Volterra expansion

1. Introduction

The ensemble of natural vocalizations of the grassfrog (Rana temporaria L.) consists of sequences of calls with a distinct amplitude modulated (AM) structure. In the companion paper [7] the coding of sound-pulse repetition rate in the auditory midbrain of the grassfrog was investigated with discrete clicktrain ensembles.

The aim of the present study is to investigate the coding of envelope periodicity in the auditory midbrain with continuous modulated sounds. As stimuli both sinusoidally amplitude modulated sound bursts as well as long duration sound ensembles with a Gaussian noise envelope have been used. Loosely speaking these ensembles mimic a calling frog in isolation and a large chorus of calling frogs respectively. Both narrowband (tonal) and wideband (Gaussian noise) carriers were applied. The sinusoidally AM stimulus is common in the investigation of neural sensitivity to fine-temporal characteristics (e.g. [3,11,15,19,22,23]). The Gaussian noise modulated stimulus is in use as test

---

Abbreviations: AM amplitude modulation; BF best frequency; BI bimodal; BMF best modulation frequency; BP band-pass; BRR best repetition rate; HP high-pass; LP low-pass; LT latency; MF modulation frequency; NS non-selective; PESE pre-event stimulus ensemble; SPL sound pressure level

signal in the theory of non-linear systems with continuous inputs (e.g. [17,25,29]), and has been used for describing the linear part of the response of auditory units by determining the first-order system kernel with respect to sound envelope [18, 20]. In addition to the first-order kernel we have also determined the second-order kernel, which gives an approximative description of the nonlinear neural response characteristics. This system-theoretical approach might reveal underlying neural mechanisms accounting for the temporal sensitivity as observed in sinusoidally AM sound burst experiments. By comparing the responses to the different types of stimuli, as described in the present and the companion paper, influence of fine-structure of the envelope (discrete click versus continuous amplitude modulation) on temporal sensitivity has been determined.

2. Materials and Methods

Details of animal preparation, acoustic stimulus presentation and recording procedure have been described extensively in previous papers[6,13,14]. Of these subjects a brief description has been given in the companion paper [7].

2.1. Acoustic Stimulus Ensembles

Sinusoidally amplitude modulated sound bursts with a duration of 500 ms, 100 ms rise and fall time, and repeated once per 3 s were used (Fig. 1a). The depth of modulation was 100% peak. AM rates were selected from 16 logarithmically equidistant values in the 5 octave range 7.8-250/s, in addition to one unmodulated burst. One stimulus sequence was composed of 17 bursts with pseudorandomly varied AM rates. The total stimulus ensemble consisted of 10 identical sequences, resulting in a total duration of 510 s. The carrier either was Gaussian wideband noise or a pure tone, mostly at BF. In case of sinusoidally modulated sound the depth of modulation is asymmetrical on a logarithmic dB-scale. For 100% AM the maximum is 3 dB above average and the minimum $-\infty$ dB below average. Therefore also a modified stimulus ensemble was presented, which was in all aspects identical to the former stimulus ensemble except that the original sinusoidally shaped modulator was multiplied by an exponential function (Fig. 1b). The modulator of the modified ensemble is sinusoidal on a logarithmic dB-scale, its modulation depth was 16 dB (maximum 8 dB above average, minimum -8 dB below average).

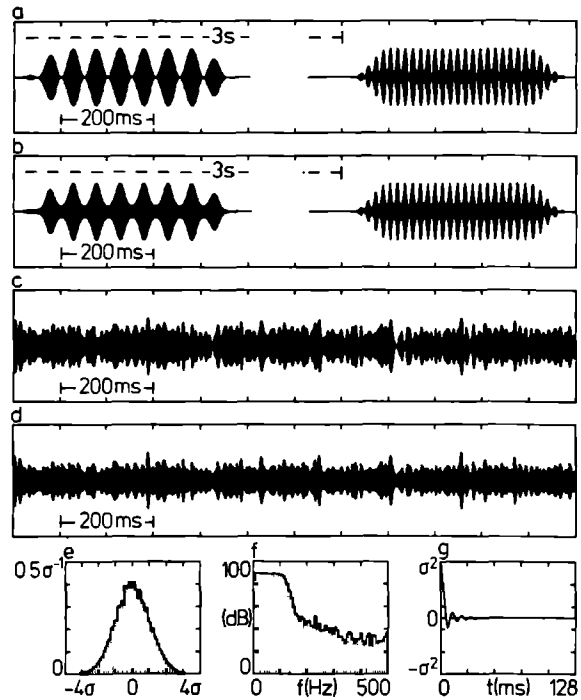

Fig. 1. Characteristics of amplitude modulated stimulus ensembles. (a) Fragment of the sinusoidally amplitude modulated sound burst ensemble. (b) Fragment of an AM sound burst ensemble of which the modulator was a sinus multiplied by an exponential function. (c) Fragment of noise modulated sound. (d) Fragment of sound of which the modulator was noise multiplied by an exponential function. (e) Amplitude distribution of the noise modulator. (f) Power spectrum of the noise modulator. (g) Autocorrelation density of the noise modulator.

Pseudorandomly amplitude modulated sound was constructed by multiplying a Gaussian wideband noise or tonal carrier with a pseudorandom envelop $a(t) = 1 + n(t)$, (Fig. 1c). The ac-component $n(t)$ of the envelope was obtained by low-pass filtering (48 dB/octave, cut-off frequency at 120 Hz) a pseu-

dorandom binary noise sequence (Hewlett-Packard HOI 3722A, clock period 10 μs, sequence length 1,048,575 points). The peak factor of the noise was smoothly compressed to 3σ. The approximate Gaussian amplitude distribution, the power spectrum and the auto-correlation density of n(t) are shown in Fig. 1e, f and g respectively. The depth of amplitude modulation was 100% peak, which corresponds to 33% r.m.s. The total stimulus ensemble consisted of 5 identical sequences and lasted about 525 s. For the same reason mentioned before in case of sinusoidally AM sound, a modified ensemble was also presented with a noise modulator which was symmetrical on a logarithmic dB-scale. This was obtained by multiplying n(t) by an exponential function (Fig. 1d). The modulation depth of the modified ensemble was 30 dB peak (maximum at 15 dB, minimum at -15 dB relative to average).

Usually stimuli were presented to the contralateral (with respect to recording side) ear at a peak amplitude corresponding to 90 dB SPL (relative to 20 $\mu N/m^2$).

2.2. Stimulus-Event Analysis

The stimulus-event relation has been investigated in a way very much analogous to the analysis described in the companion paper [7]. In case of sinusoidally AM sound burst ensembles the stimulus event relation was visualized in dot displays, isointensity rate histograms, period histograms and interspike interval histograms. From the period histogram a synchronization index, defined as the vector-strength [12], was derived. The significance of the synchronization index was not tested statistically. If a period histogram differed by visual inspection not clearly from a flat baseline, the synchronization index was considered insignificant. An illustration of this procedure is presented in the companion paper [7].

Nonlinear systems receiving input of continuous nature can, under certain general assumptions, be characterized by their responses to a continuous Gaussian wideband noise test-input [29]. The output y(t) of an unknown continuous finite memory nonlinear black box system can be approximated by a series of orthogonal functionals $G_i^W[w_i;x(s),s<t]$ of the Gaussian wideband noise input x(t) with power density P_a, w_i are the Wiener-Volterra kernels. This expansion is known as the Wiener-Volterra expansion.

$$y(t) = \sum_{i=0}^{\infty} G_i^W[w_i;x(s),s<t] \tag{1}$$

and

$$E[G_i^W \cdot G_j^W] = 0 \quad , \quad \text{for } i \neq j \tag{2}$$

The first three functionals are:

$$G_0^W(t) = w_0 \tag{3}$$

$$G_1^W(t) = \int_0^{\infty} d\tau\, w_1(\tau)x(t-\tau)$$

$$G_2^W(t) = \int_0^{\infty}\int_0^{\infty} d\tau d\theta\, w_2(\tau,\theta)[x(t-\tau)x(t-\tau-\theta) - \Phi_{xx}(\theta)]$$

In this formula $\Phi_{xx}(\theta)$ is the autocorrelation density of the input (cf. Fig. 1g).

$$\Phi_{xx}(\theta) = E[x(t)\cdot x(t+\theta)] \tag{4}$$

By crosscorrelation of input and output the Wiener-Volterra kernels $w_n(\tau_1,\ldots,\tau_n)$ are obtained (e.g. [25]). The first three kernels are:

$$w_0 = E[y(t)] \tag{5}$$

$$w_1(\tau) = P_a^{-1} E[y(t)x(t-\tau)] \quad ; \quad \tau > 0$$

$$w_2(\tau,\theta) = q(\theta)\, P_a^{-2}\{E[y(t)x(t-\tau)x(t-\tau-\theta)] - w_0\Phi_{xx}(\theta)\} \quad ; \quad \tau > 0$$

$$\text{where } q(\theta) = \begin{cases} 1 & \text{for } \theta > 0 \\ 0.5 & \text{for } \theta = 0 \end{cases}$$

In these equations the power density P_a is:

$$P_a = \int_{-\infty}^{\infty} d0\, \Phi_{xx}(0) \tag{6}$$

Note that the expressions for functionals and kernels as presented here differ slightly from the equations given by most textbooks (e.g. [17]). The reasons for this deviation are the non-whiteness of the input and a transformation of the second argument of the second-order kernel. Due to the non-whiteness of the stimulus the first and second order Wiener kernels are not exactly estimated by the crosscorrelation functions of input and output. The formulae of these kernels as given here are approximations under the assumption that these kernels are smooth functions of their arguments. Because of the transformation of the second argument of the second-order kernel ($\tau+\theta \rightarrow \theta$) the first row of the kernels represent what is usually called the diagonal contribution. The Wiener kernels may be interpreted in the same way as the Poisson kernels of the companion paper [7]. The kernel of order zero w_0 represents the average system response not time-locked to the input. The first-order kernel $w_1(\tau)$ represents the average system response upon a single impulse. When the system is linear, $w_1(\tau)$ is the impulse response. The second-order kernel $w_2(\tau,\theta)$ is equal to the average facilitation or depression due to a doublet of pulses θ seconds apart, regardless of intervening impulses. When the system is at most quadratic this facilitation or depression is equal to the one measured in a two-pulse experiment.

In case of neural events the output y(t) may be regarded as a train of identical Dirac δ-pulses: $y(t) = \Sigma\, \delta(t-\tau_1)$. Then the estimation of the Wiener kernels by crosscorrelation of neural activity and various functionals of the stimulus is formally equivalent to the determination of the corresponding moments of the pre-event stimulus ensemble (PESE) [16]. The kernels were normalized to number of (output) spikes/s. Additional smoothing has not been applied.

3. Results

Sinusoidally and/or noise modulated sound was presented to 124 units of 17 frogs. Of these units 82% responded with a sufficient number of spikes to at least one of the stimulus ensembles. Of the remaining 18% of the non or very weakly responding units 86% was tested only with a wideband noise carrier. There appeared to be no relation between best frequency and the responsiveness of units.

3.1. Response to Sinusoidally AM Sound

The sinusoidally amplitude-modulated stimulus ensemble was presented to 123 units. Of these units 60 have been tested with only a wideband noise carrier, 36 with only a tonal carrier mostly near BF and 27 units have been stimulated with both noise and tonal carriers. Reliable responses were obtained in the case of 101 (82%) units.

3.1.2. Classification of Responses Based on the Iso-Intensity Rate Histogram

On basis of the form of the iso-intensity rate histogram the 101 responsive units have been classified into 5 categories. When responses were obtained to both wideband noise and tonal carriers, the histogram coresponding to the tonal carrier at BF was considered. The nomenclature of the companion paper has been adopted.

Low-Pass (LP) units (6%). These units are characterized by a decreasing average response rate as a function of modulation frequency (MF). The average response rate at high modulation frequencies is at most 50% of the response rate at low mo-

Fig. 2. Examples of response types based on the iso-intensity rate histogram. Each figure shows from left to right: dotdisplay, iso-intensity histogram and synchronization index histogram. The response to unmodulated sound (un) is indicated by the differently shaded lowest bin in the iso-intensity histogram. (a) Low pass unit, carrier was wideband noise. (b) Weak band-pass unit, carrier 1250 Hz. (c) Weak band-pass unit, carrier 2200 Hz. (d) Pronounced band-pass unit exhibiting synchronization, carrier 250 Hz. (e) Pronounced band-pass unit with no synchronization, carrier 550 Hz. (f) High-pass unit, carrier was 600 Hz. (g) Bimodal unit with a double band-pass characteristic, carrier 500 Hz. (h) Bimodal unit with a combined low-pass and high-pass characteristic, carrier 315 Hz. (i) Non-selective unit with no response synchronization, carrier wideband noise. (j) Non-selective unit exhibiting synchronization, carrier 630 Hz.

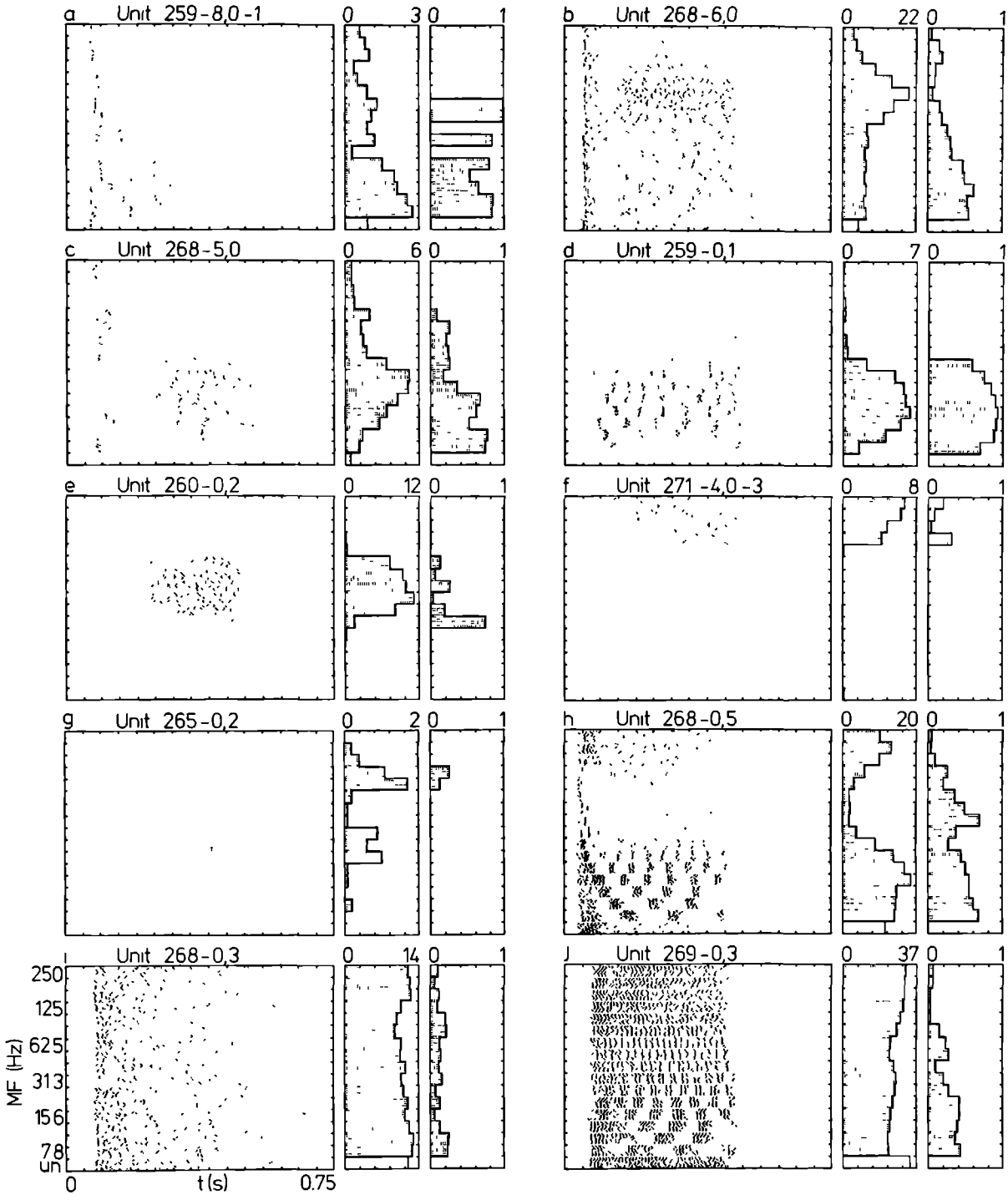
a Unit 259-8,0-1
0 3 0 1
b Unit 268-6,0
0 22 0 1
c Unit 268-5,0
0 6 0 1
d Unit 259-0,1
0 7 0 1
e Unit 260-0,2
0 12 0 1
f Unit 271-4,0-3
0 8 0 1
g Unit 265-0,2
0 2 0 1
h Unit 268-0,5
0 20 0 1
i Unit 268-0,3
0 14 0 1
J Unit 269-0,3
0 37 0 1
MF (Hz)
250
125
625
313
156
78
un
0
t (s)
0.75

dulation frequencies. The modulation frequency at which the response rate is 50% of maximum is called cut-off modulation frequency. These units respond moderately to unmodulated sound. An example is shown in Fig. 2a. This unit has a cut-off MF of 20 Hz and has an onset response to unmodulated sound.

Band-Pass (BP) units (33%). These units respond optimally to intermediate modulation frequencies. At lower and higher MF's the response is at most 50% of maximum (weak band-pass BPa, 18%) or totally absent (pronounced band-pass BPb, 15%). In general these units respond little (BPa units) or not at all (BPb units) to unmodulated sound bursts. Two examples of weak band-pass units are illustrated in Fig. 2b and 2c. The unit in Fig. 2b has a sustained response at all MF's and to unmodulated sound. Its average response rate reaches a clear maximum at best modulation frequency (BMF) = 80 Hz. The units in Fig. 2c fires only sustainedly to intermediate MF's and has a BMF of 30 Hz. At lower and higher modulation frequencies this unit has a transient response. Two examples of pronounced band-pass units are presented in Fig. 2d and 2e. The unit in Fig. 2d shows synchronized behavior and has an optimal MF of 15 Hz. The other BPb unit in Fig. 2e is not synchronized and attains a maximum at MF = 40 Hz.

High-Pass (HP) units (10%). High-pass units are the counterpart of low-pass units, because they exhibit an increasing average response rate as a function of MF. In general they respond moderately to unmodulated sound bursts. An example is the unit in Fig. 2f, which has a cut-off MF at 125 Hz and hardly reacts to unmodulated sound bursts.

Bimodal (BI) units (21%). These units form quite an inhomogeneous group and combine features of the former three categories. The iso-intensity rate histogram can be build up of all possible combinations of low-pass, band-pass or high-pass combinations. An example of a unit exhibiting a double band-pass characteristic is shown in Fig. 2g. This unit has maxima at MF = 30 Hz and 100 Hz and is not responsive to unmodulated sound. Another unit combining a low-pass and a high-pass characteristic is presented in Fig. 2h. This unit synchronizes in the low-pass region which has a cut-off MF at 30 Hz and is not synchronized in the high-pass region which has a cut-off MF at 150 Hz. Its response to unmodulated sound bursts is good, after an initial onset the firing rate reaches a steady-state level. On the whole the responsiveness to unmodulated sound bursts of this class of units depends on the particular combination of low-pass, band-pass or high-pass features. Units having solely band-pass characteristics react little or not at all to unmodulated sound. The other units, on the contrary, are moderately to well responsive to unmodulated sound bursts.

Non-Selective (NS) units (30%). A large class of units did not exhibit any preference (within 50% of the average response rate) to a particular range of modulation frequencies. These units invariably respond very well to unmodulated sound. An example without any sign of synchronization capability is presented in Fig. 2i. Another example with response synchronization at low modulation frequencies is given in Fig. 2j.

No clear relation was observed between the above defined categories with best frequency (BF) nor with latency (LT) as determined with a tonepip stimulus ensemble. Many pronounced band-pass units, however, were not responsive to single tonepips. A

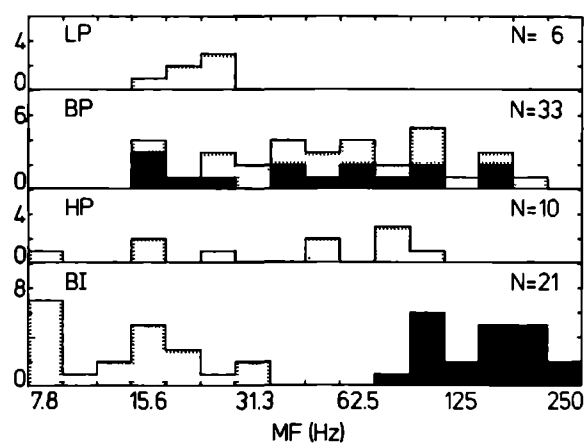

Fig. 3. Cut-off and best modulation frequencies for the various categories. (a) Cut-off MF's for low pass units. (b) BMF's for weak band-pass (shaded) and pronounced band-pass (black) units. (c) Cut-off MF's for high-pass units. (d) BMF's for the lower frequency (shaded) and higher frequency region (black) of bimodal units.

summary of cut-off modulation frequencies and best modulation frequencies is given in Fig. 3. It appears that these characteristic modulation frequencies are distributed over a wide range. As in the case of periodic click trains [7] it seems that band-pass and bimodal units behave antagonistically, especially in the MF-region 30-80 Hz.

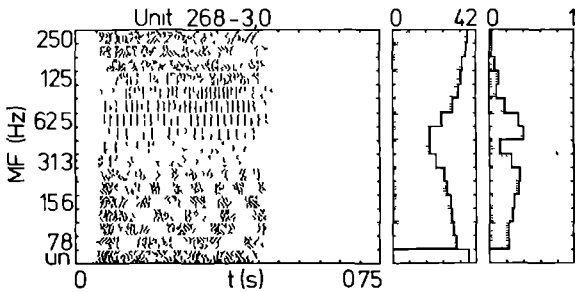

Fig. 4. Unit having a bimodal synchronization characteristic. Its iso-intensity rate histogram is an intermediate between a bimodal and a non-selective type. Carrier was a 400 Hz tone.

3.1.3. Synchronization Capability

From the period histograms a synchronization index histogram was computed. Of the 101 responsive units 56% had a low-pass synchronization behavior, i.e. synchronization capability deteriorates towards higher modulation frequencies (Fig. 2a,b,c, d,e). Some units (3%) exhibited a weak band-pass synchronization behavior, they had a maximal synchronization index at particular MF's, which were always below 20 Hz. Three units (3%) even exhibited a bimodal synchronization capability they had a maximal synchronization index at two separate MF regions (Fig. 2h,2j,4). A large fraction (38%) of units had insignificant synchronization indices at all modulation frequencies tested (Fig. 2f,g,i).

Synchronization capability appeared to be significantly correlated with average response rate characteristic ($P < 2.5\%$, χ^2-test). Weak band-pass, bimodal and non-selective units often showed high synchronization indices. Pronounced band-pass units, on the contrary, mostly were badly synchronized. The other categories took an intermediate position. Synchronization capability was also correlated with BF ($P < 0.1\%$, χ^2-test) and LT ($P < 0.5\%$, χ^2-test), as measured with tonepips. Units with basilar papilla input or short latencies on average synchronized better than units with amphibian papilla input or having long latencies.

The synchronization capability of torus units is summarized in Fig. 5. It appears that in the torus a small fraction of units has a high synchronization capability, which sometimes is maintained beyond a modulation frequency of 100 Hz.

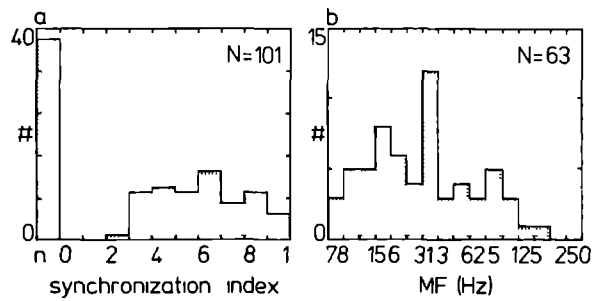

Fig. 5. Synchronization capability of torus units. (a) Distribution of maximal synchronization indices. (b) Distribution of ultimate modulation frequencies at which the synchronization index was significant.

3.1.4. Influence of Sound Pressure Level

To investigate whether the response to sinusoidally modulated sound is invariant to changes of sound pressure level, 25 units have been tested over a range of stimulus intensities, decreasing in steps of 5 or 10 dB from 90 dB SPL down to threshold. An invariant response was exhibited by 16 units (6 units tested over a range of 10 dB, 4 units over 20 dB, 4 units over 30 dB and 2 units over 35 dB). An example of a unit with an invariant response is shown in Fig. 6a. This unit has a pronounced band-pass characteristic, which is maintained over a range of 30 dB. The remaining 9 units had intensity dependent response characteristics over a range of 10-40 dB. An example of such a unit is shown in Fig. 6b. This unit has a non-selective characteristic at 90 and 80 dB SPL, that changes

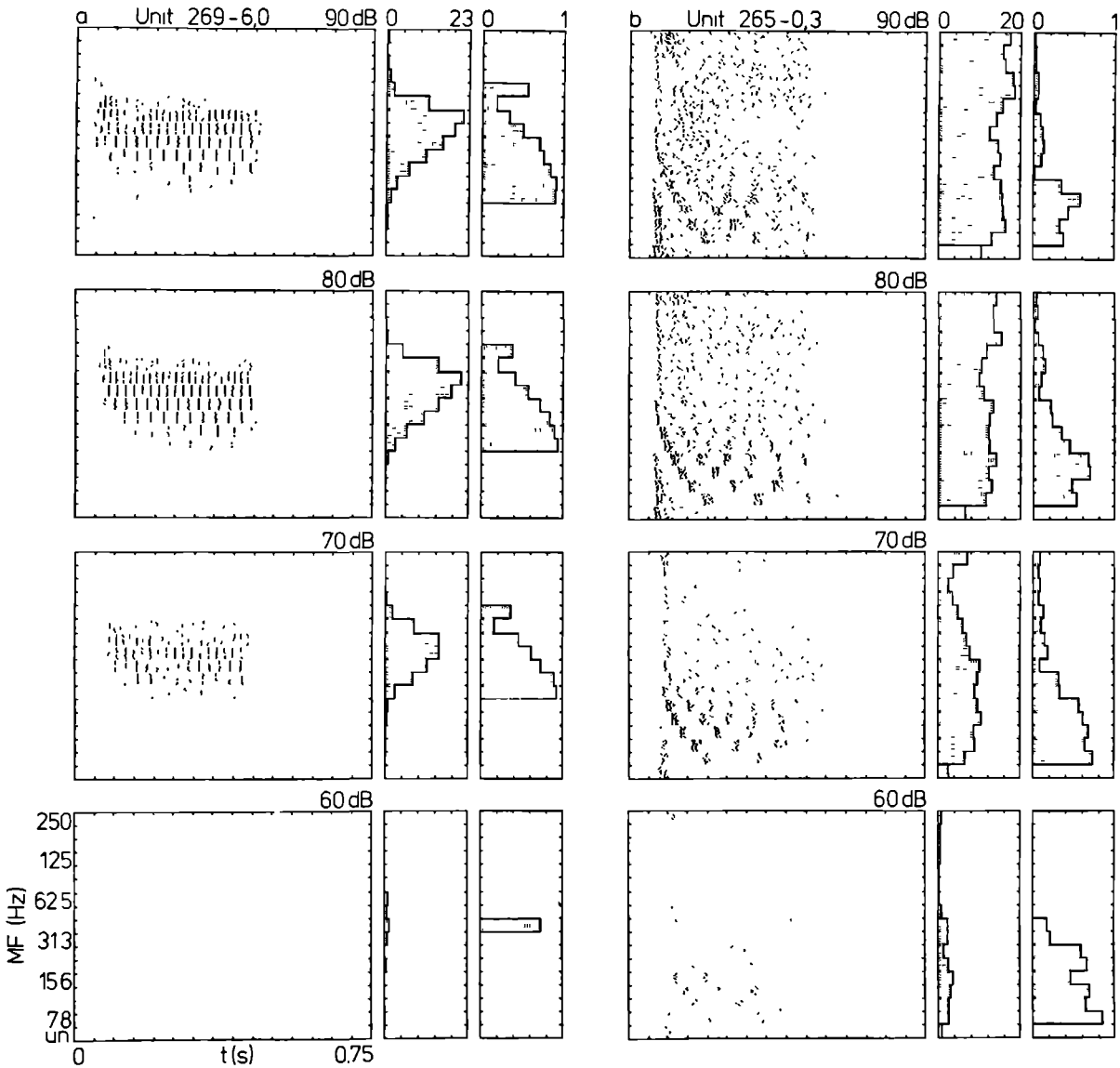

Fig. 6. (a) Unit being invariant to stimulus intensity, carrier was 800 Hz. (b) Unit having a stimulus dependent response characteristic, carrier was 1000 Hz. For each unit the iso-intensity histograms have been scaled identically.

into a weak band-pass characteristic at 70 and 60 dB SPL. Note that this change is due to an alteration of a sustained response to high modulation frequencies at high stimulus intensities to a transient response at lower stimulus intensities. The response to low modulation frequencies remaines sustained. In general the synchronization capability of units is invariant (e.g. Fig. 6a) or increases (e.g. Fig. 6b) with decreasing stimulus intensity.

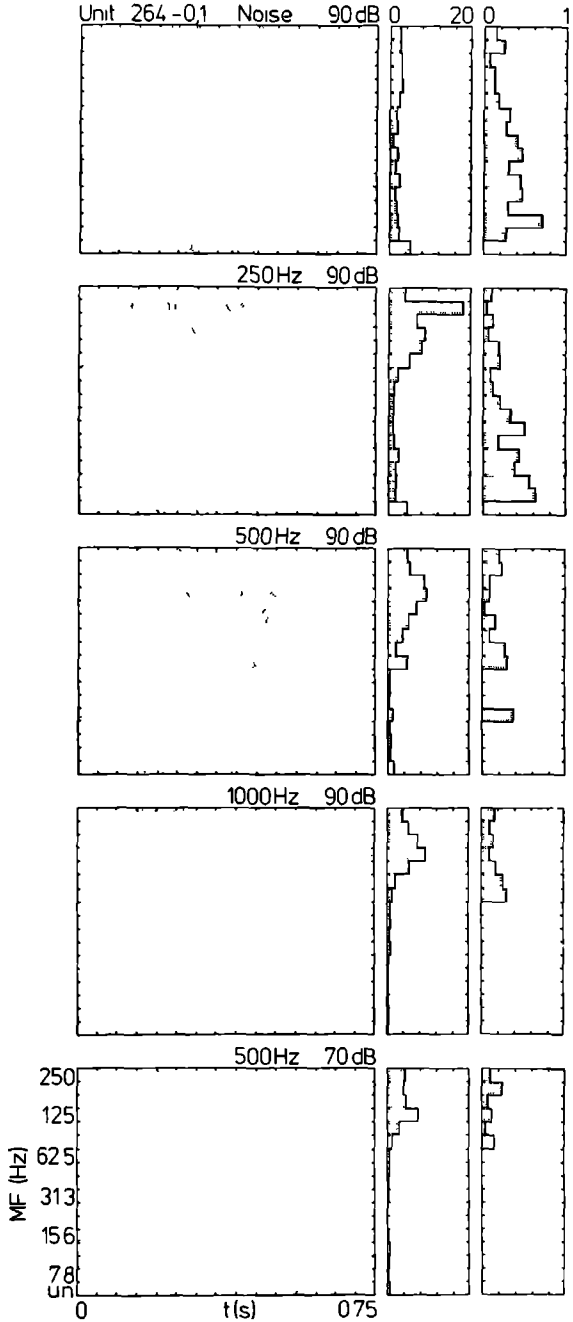

Fig. 7. Response characteristics of a unit with a BF of 120 Hz to sinusoidally AM sound with different carriers.

3.1.5. Influence of Sound Carrier

To study the influence of the spectral content of the sound carrier on the response characteristics both wideband noise carriers and tonal carriers near BF and at other frequencies at the same SPL have been applied. In 29 units reliable responses to at least two different carriers have been obtained. Of these 29 units 12 units exhibited carrier-invariant response characteristics. The remaining 17 units showed response characteristics not invariant to change of carrier. In 10 of these 17 units it could be excluded that the changes were due to different levels of the carriers above threshold, because the response characteristics to different carriers remained incompatible when the level of one of the carriers was varied over some range. An example is provided in Fig. 7. This unit with a spectral sensitivity below 800 Hz for tone-pips and a BF of 120 Hz, but with a broader spectral sensitivity for AM tones, is non-selective when a wideband noise carrier is applied and exhibits a weak band-pass or high-pass characteristic in case of tonal carriers of different frequencies over a range of 20 dB. Note that this unit has a very pronounced response at MF = 200 Hz when the carrier is 250 Hz. Presumably this can be accounted for by the spectral sensitivity of the unit in regard to its low BF. In general temporal selectivity and synchronization capability were better with tonal carriers than with wideband noise carriers.

3.1.6. Influence of Envelope Shape

Stimulus ensembles with sinusoidal envelopes and envelopes being products of sinusoidal and exponential functions (see Materials and Methods) have been presented to 7 units at the same SPL. All these 7 units responded identically to these two ensembles.

3.1.7. Relation between Best Modulation Frequency and Best Frequency

Band-pass and bimodal units show the most selective responses. Of 25 band-pass units and 17 bi-

modal units a single best frequency could be determined. The position of these units in the spectro temporal BF-MF plane is indicated in Fig. 8. Band-pass units have been represented by their best modulation frequency (BMF). Bimodal units have two BMF-values, which are difficult to picture conveniently. Therefore we have represented the MF at which the valley between the two peaks in the iso-intensity rate histogram of bimodal units is minimal, inspired by the seemingly antagonistic behavior of band-pass and bimodal units (Fig. 3). For comparison the energy distribution of the 4 most prominent natural vocalizations of the grassfrog [4,10,26,28] has been portrayed as well. No clear correlation is present between BF and MF. Units do not cluster obviously within regions of high conspecific call energy, but are scattered all over the plane.

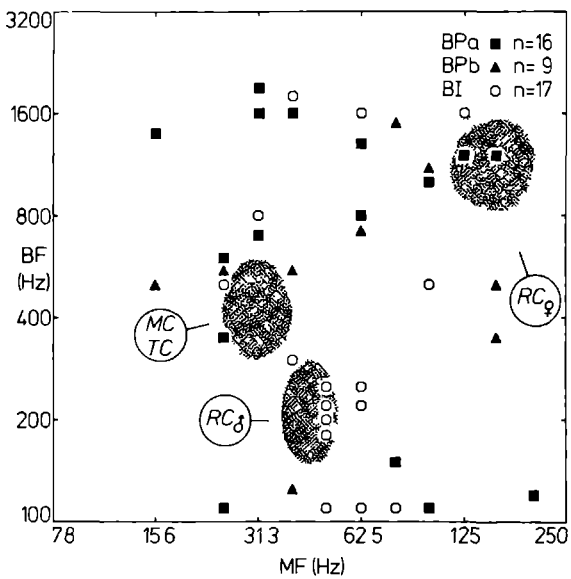

Fig. 8. Relation between characteristic modulation frequency (MF) and best frequency for band-pass (BP) and bimodal (BI) units. In case of band-pass units their best modulation frequency is represented, for bimodal units the MF at which the valley between the two peaks in the iso-intensity rate histogram was at minimum is indicated. For comparison also the energy distribution of the natural vocalizations of the grassfrog is pictured. Dark gray shades indicate regions of high energy. MC: mating call; TC: territorium call; RC: release call.

3.2. Responses to Noise AM Sound

Noise modulated stimulus ensembles were presented to 51 units in 12 frogs. Of these units 31 (61%) responded stationary, in the sense of average firing rate, after a transient period varying from a few seconds to several minutes. The other 20 units did not respond stationary. No relation was noticed between BF and responsiveness to noise modulated sound. All units which did not respond to the tonepip ensemble were also unresponsive to noise modulated sound. The existence of a stimulus response relation was investigated by means of the existence function which measures the degree of reproducibility of neural activity upon identical stimulus sequences [1,6,14]. Of the 31 stationary responding units 23 (74%) had a clear positive existence function. The firing pattern of the remaining 8 units was loosely bound to the stimulus as became clear from the kernel analysis. The nature of the stimulus-response relation was investigated by computation of first and second-order Wiener Volterra system kernels.

3.2.1. Classification of Responses on Basis of the First-Order Kernel

The 31 stationary responding units exhibited 5 different types of first-order kernels expressing different dynamics of activation and suppression phenomena. The nomenclature of the companion paper [7] has been adopted.

Type I units (35%). These units had a positive unimodal first-order kernel, pointing at activation. An example is presented in the upper part of Fig. 9a, which had a latency of about 22 ms indicated by the arrowhead.

Type II units (35%). In the first-order kernel of these units the positive peak was accompanied by a negative one at the longer latency side. The relative amplitudes and durations of positive and negative phenomena could vary substantially within this class. An example with a latency of 48 ms and a kernel duration of about 200 ms is shown in the upper part of Fig. 9b. Another type II unit with a latency of 16 ms and a kernel duration of about 25

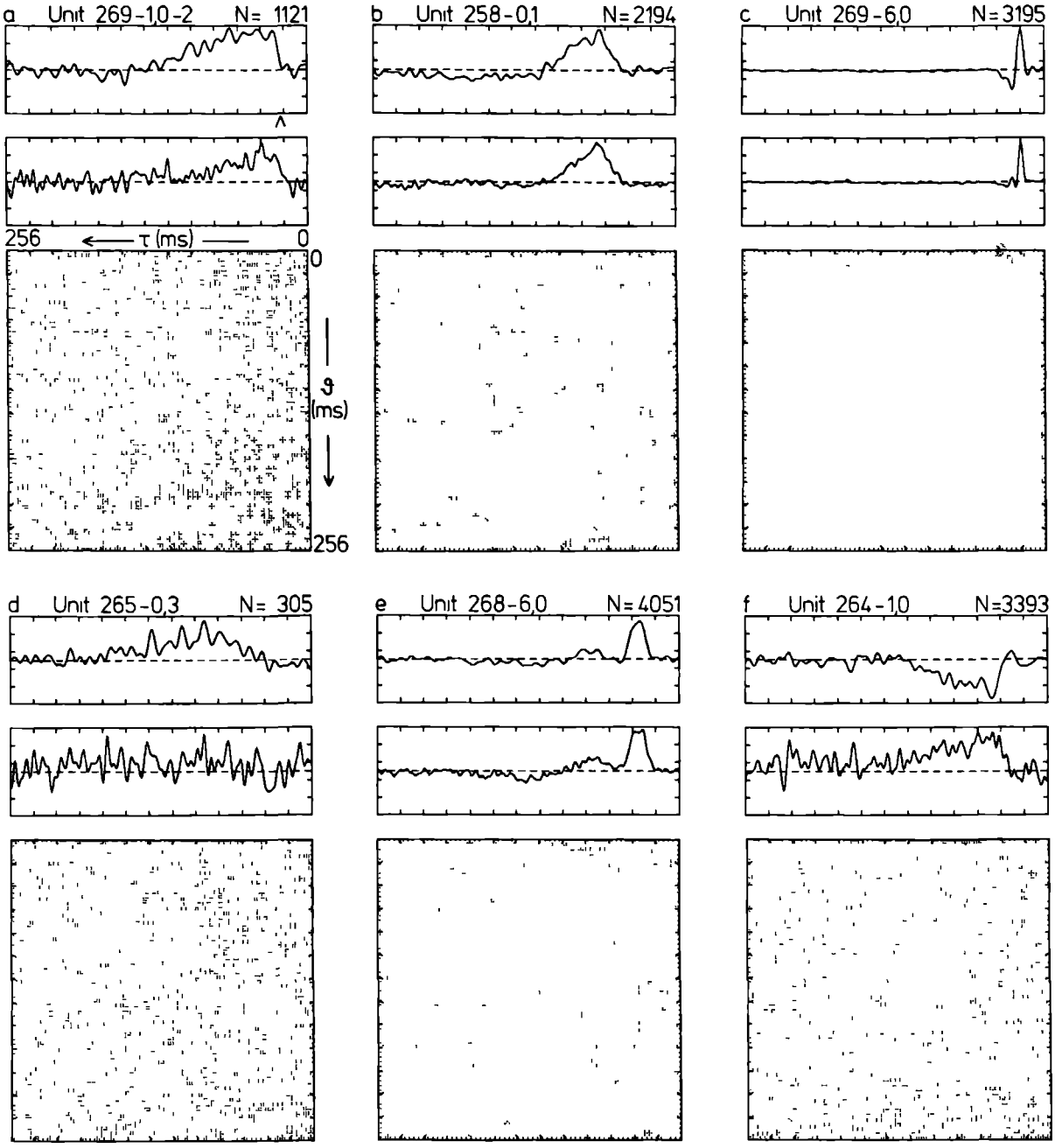

Fig. 9. First and second-order Wiener-Volterra kernels for a representative set of units. The upper part of each figure shows the first-order kernel, the middle part expresses the first row (θ=0) of the second-order kernel and the lower part shows the entire second-order kernel. In the second-order kernel amount of activation is coded along a gray-scale: black corresponds to activation, white to depression. Duration of τ and θ was in all cases 256 ms. (a) Type I unit, carrier was wideband noise. (b), (c) Type II units, carriers were 1600 and 800 Hz respectively. (d) Type III unit, wideband noise carrier. (e) Type V unit, 1250 Hz carrier. (f) Type VI unit, 500 Hz carrier. Stimulus intensity was 90 dB SPL, except in (c), where it was 80 dB SPL. For reasons of visibility the kernels have been scaled to their own extrema. The extrema for first and second-order kernels respectively are: (a) 0.16,0.017; (b) 0.31, 0.065; (c) 3.0, 0.45; (d) 0.065, 0.005; (e) 0.65, 0.07; (f) 0.25, 0.02.

ms is presented in the upper part of Fig. 9c. The oscillation at the short latency side of the peak of the kernel of the latter unit is due to the autocorrelation structure of the stimulus envelope (Fig. 1g).

Type III units (7%). These units have first order kernels in which the course of the dynamics is reversed with respect to type II units. A negative valley is observed at smaller latencies than the positive peak. In the 2 type III units observed the negative valley was not very pronounced (Fig. 9d). These units are, on average, at first suppressed by the stimulus and later on activated or show a type of rebound recovery from the suppression.

Type IV units (0%). This category combines the features of type II and III units. A positive peak is flanked on both sides by a negative valley. This type of unit was observed in response to Poisson distributed click ensembles described in the companion paper [7] but not in response to noise AM sound.

Type V units (7%). The dominant feature of this category is the presence of two clearly separated positive peaks. Mostly also a negative deflection at longer latencies was observed. An example is shown in Fig. 9e, which has two positive peaks with latencies of 24 and 64 ms respectively.

Type VI units (16%). The first-order kernel of this type of units exhibited one negative valley (Fig. 9f). These units all were spontaneously active. The interpretation of this phenomenon is that on average the stimulus suppresses the spontaneous activity.

No clear relationship was noticed between type of first-order kernel and BF, except that all type VI units had BF's below 1000 Hz and therefore presumably receive their input from the amphibian papilla.

3.2.2. The Second-Order Kernel

As already discussed more elaborately in the companion paper [7] the first-order kernel on itself does not provide evidence about nonlinear interactions of different components of the stimulus. For example it is ambiguous whether the multiple activation and/or suppression effects in types II, III and V first-order kernels are time-locked to each other or that these effects are due to independent processes appearing together just because of the averaging over time. The second-order system kernel, however, gives information about nonlinear interactions of different stimulus components indicating a.o. nonlinear synaptic and spike-generating mechanisms. Knowledge of second-order kernels therefore might restrict the class of possible models accounting for the observed phenomena in the first-order kernel.

Of the 31 units with a clear first-order kernel 22 units (71%) exhibited a second-order kernel. Some examples are shown in Fig. 9, where in addition to the entire second-order kernel its first row corresponding with $\theta=0$ is also displayed separately in the middle part of the figure. Most units (55%) had a second-order kernel with only a non-zero contribution in the first-row, pointing at an algebraic or static nonlinearity. This static nonlinearity was in 49% of the units predominantly expansive (Fig. 9b,e,f), while it was in 6% of saturating nature. The remaining 16% of the units with a second-order kernel had also contributions at larger θ-values indicating nonlinear interactions of dynamic nature. Following the nomenclature of the companion paper [7] 10% of the units exhibited a type A second-order kernel (Fig. 9a,d). A type A second-order kernel is characterized by a facilitatory positive contribution for stimulus component intervals θ smaller than a certain θ_m. A type E second-order kernel (Fig. 9c), i.e. a depressive negative contribution for separation intervals $0<\theta<\theta_m$, was observed in 6% of the units. On basis of this second-order kernel it may be concluded that the positive and negative phenomena in the first-order kernel of this unit (Fig. 9c) are time-locked to each other and not due to independent excitatory and inhibitory pathways with different latencies. So it may be stated that the unit of Fig. 9c exhibits really post-activation suppression. The other types of second-order kernels encountered in the companion paper on basis of Poisson distributed click ensembles were not noticed in this study. The time-course of the first

order kernel and of the θ=0 contribution of the second-order kernel always were similar (Fig. 9). Mostly (82%) these two kernel contributions had the same sign (Fig. 9a-e), which indicates a nonlinear enhancement of the linear response. Some units (16%) had a first-order kernel and a θ=0 contribution of the second-order kernel of opposite sign (Fig. 9f), pointing at a nonlinear reduction of the first-order contribution to the response.

3.2.3. Influence of Carrier and Stimulus Level

A total of 15 units has been tested with both tonal and wideband noise carriers. Of these units 5 showed kernels independent of the spectral content of the carrier. In the other 10 units no invariant responses were obtained mainly due to adaptation for a tonal carrier or the absence of clear kernels in case of a noise carrier. The absence of clear kernels in case of a noise carrier often could be ascribed to a stimulus lock (as revealed by existence-functions) which was predominantly to the wideband noise carrier and not to the low-pass noise envelope,.

Dependency of stimulus level was studied in only 1 type VI unit, which appeared to be invariant over a range of 20 dB SPL.

3.3. Relation of Characteristics Obtained with Sinusoidally and Noise AM Stimulus Ensembles

Both types of stimulus ensembles were presented to 46 units at the same peak intensity level and with the same carrier. Of these units 28 responded stationary to both stimuli. Of the other 18 units 4 responded not at all to both stimuli while 14 units, including most of the pronounced band-pass units, did not respond stationary to noise AM sound.

In the population of 28 units stationary responsive to both ensembles no obvious relations between type of sensitivity to sinusoidally AM sound and kernel type has been observed.

3.4. Relation of Response Characteristics Obtained with Clicks and AM Stimuli

By comparing the response characteristics obtained with discrete click ensembles, described in the companion paper [7], and amplitude modulated stimuli as presented in this paper, the influence of fine-temporal structure of the stimulus envelope was studied.

3.4.1. Periodic Click Trains versus Sinusoidally AM Sound

Both types of stimulus ensembles have been presented to 66 units. Of these units 3 did not respond to both stimulus ensembles, 8 units were responsive only to the AM ensemble, 1 unit reacted only to the click ensemble and 54 units responded to both ensembles. Of these 54 units only 14 (26%) had an average rate response characteristic that was equal for both types of stimuli. An example of a unit with an identical average response rate characteristic for both ensembles is unit 260-0,2 (Fig. 2e, compare with Fig. 3d of the companion paper). This unit is pronounced band-pass with a preferred periodicity rate at 40 Hz and hardly synchronized for both types of stimuli. The majority of units (74%) responsive to both ensembles, however, have different response characteristics for periodic click and AM ensembles, beit with respect to average rate, synchronization capability or both. Examples are units 268-6,0 (Fig. 2b, compare with Fig. 3c of the companion paper), unit 259-0,1 (Fig. 2d, compare with Fig. 3b of the companion paper) and unit 269-6,0 (Fig. 6a, compare with Fig. 6a of the companion paper). Unit 268-6,0 has a weak band-pass response for both stimulus ensembles but at different periodicity rates: 80 Hz for AM sound and 40 Hz for clicks. Units 259-0,1 and 269-6,0 have a synchronized pronounced band-pass characteristic for AM sound but a synchronized low-pass characteristic for periodic click trains. The opposite was also observed namely that a pronounced band-pass characteristic for periodic click trains changed into another characteristic for sinusoidally AM sound. On average units were somewhat better

($P < 5\%$, χ^2-test) synchronized to periodic click trains than to sinusoidally AM sound bursts.

3.4.2. Poisson Distributed Click Ensembles versus Gaussian Noise AM Sound

Both types of stimulus ensembles were presented to 31 units, the Poisson distributed clicks mostly at 100 dB SPL peak and the noise modulated AM sound mostly at 90 dB SPL peak. Of these units 2 did not respond in a stationary way to both types of stimuli and 3 units were not responsive to clicks.

Table I. Relation of First-Order Poisson and Wiener-Volterra Kernels.

		Wiener-Volterra							
		I	II	III	IV	V	VI	no	total
P	I	10					1	1	12
o	II		5						5
i	III		3	2			1	1	7
s	IV							1	1
s	V					2	1		3
o	VI						1		1
n	no							2	2
	total	10	8	2	0	2	4	5	31

For definition and illustration of the different kernel types see text. no: first-order kernel was not clearly different from zero.

The distribution of types of first-order kernels obtained with both stimulus ensembles is represented in Table I. It appears that of the 26 units responsive to both stimuli 20 units have the same type of first-order kernel for both ensembles, which is highly significant ($P < 0.05\%$, χ^2 test). Examples are the units of which Figs. 9 and 10 show both Wiener-Volterra and Poisson kernels respectively. Units a,b,d,e and f shown in Figs. 9 and 10 have even kernels with a near identical time-course. Unit c has a somewhat broader Wiener Volterra first-order kernel, presumably due to the autocorrelation structure of the low-pass noise envelope (Fig. 1g). Unit f has first-order kernels of opposite sign, but similar time course.

Comparison of second-order Wiener-Volterra and Poisson system kernels revealed that all units with Wiener-Volterra kernels containing dynamic nonlinearities had the same type of second-order Poisson system kernel. The Wiener-Volterra second-order system kernel often had a larger variance than the Poisson kernel. Examples of two type A and one type E second-order kernel are shown in Figs. 9, 10a, d and c respectively. However, most units with a clear second-order Poisson kernel had a second order Wiener-Volterra kernel, which had only a contribution for $\theta=0$ (Fig. 9,10 b,e). This finding often could not be ascribed to a large difference in number of spikes, nor to a weaker time-locking to the noise envelope as compared to clicks. In some of these units the existence-function even was sharper for the noise AM sound.

4. Discussion

In the torus semicircularis of the grassfrog a large variety of response types has been observed both in reaction to sinusoidally amplitude modulated sound bursts and noise amplitude modulated continuous sound ensembles. The results of the present study based on sinusoidally AM sound in general agree with analogous studies of Rose and Capranica [23,24]. The small differences, a somewhat larger fraction of bimodal units and a somewhat smaller fraction of non-selective units in the present study, possibly are due to the use of tonal carriers versus wideband noise carriers.

4.1. Synchrony Code versus Rate Code

As already discussed in the companion paper [7], and corroborated by the results of the present study, on the level of the auditory midbrain a transformation from a synchrony code to a rate code takes place. The synchrony code, in which the fine temporal structure of sound is coded by synchronization of neural activity to the envelope, exclusively acts on the level of the auditory nerve [8,24]

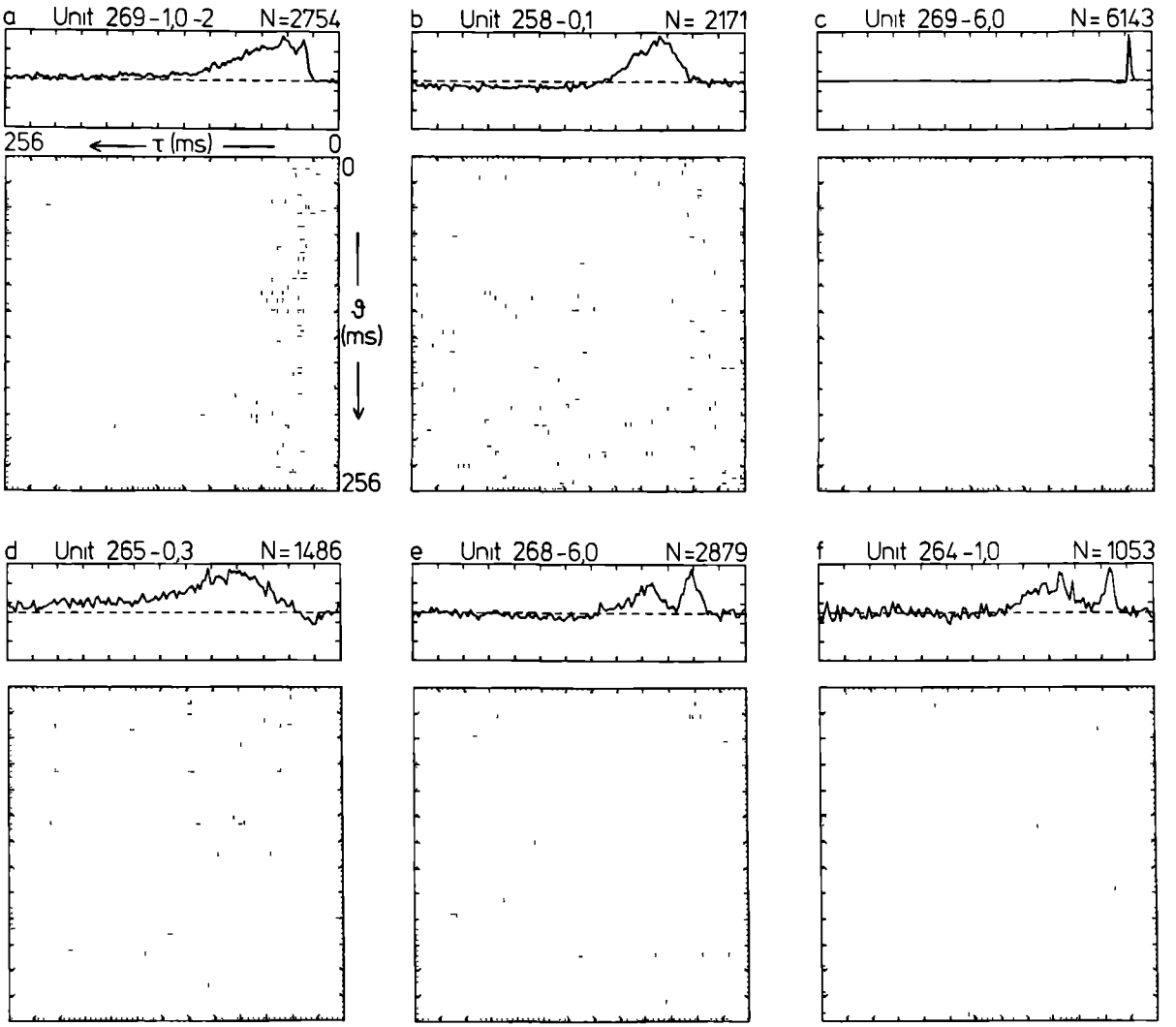

Fig. 10. First and second-order Poisson kernels of the same set of units of which the Wiener-Volterra kernels are displayed in Fig. 9. Duration of τ and θ was in all cases 256 ms. Stimulus intensity was 110 dB SPL in (f), 100 dB SPL in (a), (d), (e), 90 dB SPL in (c) and 80 dB SPL in (b). Average click rate was 16/s. For reasons of visibility the kernels have been scaled to their own extrema. The extrema for first and second-order kernels respectively are: (a) 11,8; (b) 7,2; (c) 230,50; (d) 5,6; (e) 7,6; (f) 2.6,2.0.

and also is the dominant code in the two medullary nuclei [9,27]. Large changes of average firing rate as function of sound periodicity have not been reported in these lower stations [24,27].

In the torus semicircularis, however, most units have a largely diminished synchronization capability as expressed in reduced synchronization indices and cut-off MF's, indicating a minor role of the synchrony code. However, a large diversity of average firing rate characteristics emerges on

the level of the midbrain. This points to a dominant role of the rate code, which carries information of fine-temporal structure of sound by the average firing rate without a need for synchronization.

4.2. Influence of Sound Pressure Level and Carrier

In general response characteristics were not invariant to change of sound pressure level or of spectral content of the carrier. A considerable portion (about one fourth) of units, however, showed invariant characteristics to variation of both stimulus parameters and therefore may be called temporal filters. The dependency on SPL was also observed using clicks with a flat spectrum [7] and thus in most cases presumably is a pure intensity effect and not due to the complex spectral tuning properties of many torus units [6,26].

The dependency on carrier may have two causes. The first obvious one is the complex interplay between spectral content of sound and the tuning properties of units (cf. Fig. 7). A second origin of variation especially apparent comparing tonal and noise carriers may be that a tonal carrier is a constant signal, but a noise carrier is not. Hardly any torus unit does show phase-locking to a tonal carrier [6,13] and therefore the time-lock to an amplitude-modulated tone will entirely be due to the modulator. In case of a stationary wideband noise carrier, although its statistical properties are constant over time, a particular realization will exhibit variations in both amplitude and spectrum over time, thereby providing clues for locking of neural firings [6,13]. Thus in case of amplitude modulated wideband noise the influence of the variations of the modulator may get drowned in the variability due to the noise carrier. Actually, in this study it has been observed that especially sharply tuned units lock better to the noise carrier than to the modulator. As a result units which are selective to modulation frequency using a tonal carrier may appear non-selective when a wideband noise carrier is applied. This finding argues against the exclusive use of wideband noise carriers in the investigation of temporal sensitivity of anuran auditory units [22,23], the more so as these animals in every-day life have to cope with sounds having band-limited carriers.

4.3. Relation of MF Sensitivity and Wiener-Volterra Kernels

Various neural mechanisms may shape the sensitivity to amplitude modulation frequency: adaptation, temporal summation, spectral tuning and neural interaction [27]. The influence of neural interaction is also apparent in the shape of the more complex Wiener-Volterra kernels (first-order types III and V), which cannot be explained conveniently by the other mechanisms. Because the more complex response characteristics have been observed in the torus and not in lower stations [9,24,27], it is likely that the responsible neural interaction circuits are located in the torus semicircularis.

In the neural population investigated with both sinusoidally AM sound bursts as well as noise AM continuous sound no obvious qualitative correspondence was observed between type of MF sensitivity and Wiener-Volterra kernel type. An analogous result was obtained in the corresponding study using clicks [7]. For a discussion of this finding, the major reason presumably being a different level of adaptation due to the long silences between sinusoidally AM bursts as opposed to the continuous noise AM sound ensemble, the reader is referred to the companion paper [7].

In a forthcoming paper the relation between MF sensitivity and Wiener-Volterra kernels will be investigated more quantitatively. In that paper response predictions to sinusoidally AM sound bursts on basis of the Wiener-Volterra functional expansion will be described and the sufficiency of the kernel expansion up to second-order will be evaluated.

4.4. Spectro-Temporal Sensitivity and Conspecific Calls

The spectro-temporal sensitivity of auditory midbrain units, on basis of BF and BMF, and the

spectro-temporal energy distribution of the conspecific calls of the grassfrog are not very related (Fig. 8). Actually the spectro-temporal sensitivities are scattered all over the BF-BMF plane, without a relation between BF and BMF, and are not confined to the conspecific call regions. Although many of the pronounced band-pass units do not have a BF, because they are not responsive to tonepips, it is unlikely that the anuran auditory midbrain is specifically tuned to its natural vocalizations. In a forthcoming paper we will address this question by the use of natural and synthetic vocalization ensembles.

4.5. Relation of Response Characteristics to Click and AM stimuli

On average no clear relation was observed between response types based on the iso-intensity rate histograms obtained by periodic click train and sinusoidally AM sound burst stimulation. In some cases this might have been due to differences in intensity level, spectral content and duration of the two kinds of stimuli. The major cause, however, might be that stimulus periodicity (PRR or MF) is not the only stimulus parameter accounting for the observed response types. In fact the response types presumably are shaped by a combination of neural sensitivity to periodicity as well as pulse duration. Pulse duration was about 1 ms independent of PRR in case of periodic click trains but inversely proportional to MF in case of sinusoidally AM sound. It has been reported that anuran auditory midbrain units show a sensitivity for sound pulse duration, the most effective duration being about 10 ms in case of the grassfrog [2].

In contrast to the comparison of periodic click trains with sinusoidally modulated sound it was found that first-order Wiener-Volterra and Poisson kernels in most units were very much alike. This means that the linear part of the neural response is not very dependent on the particular stimulus ensemble used, provided that sound pressure levels and thereby adaptation levels are not too far apart. Nonlinearities of dynamic nature, however, were much better revealed using clicks instead of continuous sound. This difference cannot be ascribed entirely to different adaptation levels, because the first-order kernels often were similar for both ensembles. Perhaps the influence of adaptation is larger on nonlinear mechanisms of dynamic nature than on the mechanisms accounting for the linear part of the response and the static nonlinearities, although also the first-order kernel has been shown to be sensitive to SPL changes [7]. Another reason for difference might be that the temporal resolution in a relatively sparsely packed click ensemble is intricately sharper than in an ensemble with a low-pass noise envelope, although this generally did not result in a larger degree of time-lock to the click ensemble at least as estimated by way of the existence function [1].

4.5. General Conclusions

From the studies reported in the companion [7] and the present paper several general conclusions about the coding of fine-temporal structure of sound in the anuran auditory midbrain can be drawn.

(i) On the level of the torus semicircularis a transformation takes place from a synchrony code to a rate code. Some units, however, still exhibit the same synchronization capability as reported for medullary units.

(ii) About one quarter of the units were invariant to changes of sound pressure level and spectral content. These units may be called feature detectors for fine-temporal structure of sound.

(iii) The observed response characteristics are caused by an interplay of sensitivities to stimulus periodicity, sound pulse duration and spectral content.

(iv) The Poisson and Wiener-Volterra system kernels reveal possible underlying (nonlinear) synaptic and spike generating mechanisms accounting for the observed selectivity for fine-temporal structure of sound.

(v) The torus semicirularis of the grassfrog is not specifically tuned to artificial sounds mimicking with respect to spectral content and periodicity the repertoire of conspecific calls. A similar conclusion was arrived at by Walkowiak [27] for

the same species and by Rose and Capranica 24 for Rana pipiens. The auditory midbrains of these two Ranidae seem to behave similarly. Therefore it is not probable that so-called mating-call detectors are present on the single-unit level. This implies that if mating-call detectors do exist, they are located at the thalamus or even the telencephalon; or that they do exist only on multi-unit level at which a possible call is represented by ensemble coding. Perhaps this conclusion may be extended to all Ranidae. However, Rose and Capranica 25 presented evidence that auditory midbrain units may favour conspecific calls in Bufonidae.

Acknowledgements

This investigation forms part of the research program "Brain and Behaviour" at the Department of Medical Physics and Biophysics of the University of Nijmegen and was supported by the Netherlands Organization for the Advancement of Pure Research (ZWO). The authors wish to thank Jan Bruijns, Dick Bosman and Wim van Deelen for software development, Koos Braks for the animal preparations and technical assistance, Hans Krijt and his group for electronic support. Ad Aertsen, Peter Johannesma and Ivo van Stokkum provided valuable comments on the manuscript, which was put into the wordprocessor carefully by Marianne Nieuwenhuizen.

References

1 Aertsen, A.M.H.J., Smolders, J.W.T. and Johannesma, P.I.M. (1979): Neural representation of the acoustic biotope. On the existence of stimulus-event relations for sensory neurons. Biol. Cybern. 32, 175-185.

2 Bibikov, N.G. (1980): The reaction of the torus semicircularis units of *Rana temporaria* to the signals simulating the mating call temporal characteristics. Zool. Zh. 59: 577-586.

3 Bibikov, N. and Gorodetscaya, O. (1981): Coding of amplitude-modulated tones in the midbrain auditory region of the frog. In: Neuronal Mechanisms of Hearing, pp. 347-352. Editors: J. Syka, and L. Aitkin. Plenum Press, London, New York.

4 Brzoska, J., Walkowiak, W. and Schneider, H. (1977): Acoustic communication in the grass frog (*Rana t. temporaria* L.): calls, auditory thresholds and behavioral responses. J. Comp. Physiol. A. 118, 173-186.

5 Brzoska, J. (1984): The electrodermal response and other behavioural responses of the grass frog to natural and synthetic calls. Zool. Jb. Physiol. 88, 179-192.

6 Epping, W.J.M. and Eggermont, J.J. (1985): Single-unit characteristics in the auditory midbrain of the immobilized grassfrog. Hearing Res. (in press).

7 Epping, W.J.M. and Eggermont, J.J. (1986): Sensitivity of neurons in the auditory midbrain of the grassfrog to temporal characteristics of sound. I. Stimulation with acoustic clicks. (submitted)

8 Frishkopf, L.S., Capranica, R.R. and Goldstein, M.H. (1968): Neural coding in the bullfrog's auditory system, a teleological approach. Proc. IEEF 56, 969-980.

9 Fuzessery, Z.M. and Feng, A.S. (1983): Frequency selectivity in the anuran medulla: excitatory and inhibitory tuning properties of single neurons in the dorsal medullary and superior olivary nuclei. J. Comp. Physiol. A 150, 107-119.

10 Gelder, J.J. van, Evers, P.M.G. and Maagnus, G.J.M. (1978): Calling and associated behaviour of the common frog, *Rana temporaria*, during breeding activity. J. Anim. Ecol. 47, 667-676.

11 Gersuni, G.V. and Vartanian, I.A. (1973): Time dependent features of adequate sound stimuli and the functional organization of central auditory neurons. In: Basic Mechanisms in Hearing, pp. 623-673. Editor: A.R. Møller. Academic Press, New York, London.

12 Goldberg, J.M. and Brown, P.B. (1969): Response of binaural neurons of dog superior olivary complex to dichotic tonal stimuli: some physiological mechanisms of sound localization. J. Neurophysiol. 32, 613-636.

13 Hermes, D.J., Aertsen, A.M.H.J., Johannesma, P.I.M. and Eggermont, J.J. (1981): Spectro-temporal characteristics of single units in the auditory midbrain of the lightly anaesthetised grass frog (*Rana temporaria* L.) investigated with noise stimuli. Hearing Res. 5, 147-178.

14 Hermes, D.J., Eggermont, J.J., Aertsen, A.M.H.J. and Johannesma, P.I.M. (1982): Spectro temporal characteristics of single units in the auditory midbrain of the lightly anaesthetised grass frog (*Rana temporaria* L.) investigated with tonal stimuli. Hearing Res. 6, 103-126.

15 Hirsch, H.R. and Gibson, M.M. (1976): Responses of single units in the cat cochlear nucleus to sinusoidal amplitude modulation of tones and noise: linearity and relation to speech perception. J. Neurosci. Res. 2: 337-356.

16 Johannesma, P.I.M. (1972): The pre-response stimulus ensemble of neurons in the cochlear nucleus. In: Proc. of the IPO Symp. on Hearing Theory, pp 58-69. Editor: B.L. Cardozo. IPO, Eindhoven.

17 Marmarelis, P.Z. and Marmarelis, V.Z. (1978): Analysis of Physiological Systems: The White Noise Approach, Plenum Press, New York.

18 Møller, A.R. (1973): Statistical evaluation of the dynamic properties of cochlear nucleus units using stimuli modulated with pseudorandom noise. Brain Res. 57: 443-456.

19 Møller, A.R. (1974): Responses of units in the cochlear nucleus to sinusoidally amplitude-modulated tones. Exp. Neurol. 45, 104-117.

20 Møller, A.R. (1974): Use of stochastic signals in evaluation of the dynamic properties of a neuronal system. Scand. J. Rehab. Med., Suppl. 3: 37-44.

21 Rees, A. and Møller, A.R. (1983): Responses of neurons in the inferior colliculus of the rat to AM and FM tones. Hearing Res. 10, 301-330.

22 Rose, G. and Capranica, R.R. (1983): Temporal selectivity in the central auditory system of the leopard frog. Science 219, 1087-1089.
23 Rose, G.J. and Capranica, R.R. (1984): Processing of amplitude-modulated sounds by the auditory midbrain of two species of toads: matched temporal filters. J. Comp. Physiol. A. 154, 211-219.
24 Rose, G.J. and Capranica, R.R. (1985): Sensitivity to amplitude-modulated sounds in the anuran auditory nervous sytem. J. Neurophysiol. 53, 446-465.
25 Schetzen, M. (1980): The Volterra and Wiener theories of nonlinear systems. Wiley, New York.
26 Walkowiak, W. (1980): The coding of auditory signals in the torus semicircularis of the firebellied toad and the grassfrog: responses to simple stimuli and to conspecific calls. J. Comp. Physiol. A 138, 131-148.
27 Walkowiak, W. (1984): Neuronal correlates of the recognition of pulsed sound signals in the grass frog. J. Comp. Physiol. A 155, 57-66.
28 Walkowiak, W. and Brzoska, J. (1982): Significance of spectral and temporal call parameters in the auditory communication of male grass frogs. Behav. Ecol. Sociobiol. 11, 247-252.
29 Wiener, N. (1958): Nonlinear problems in random theory. Wiley, New York.

COHERENT NEURAL ACTIVITY IN THE AUDITORY MIDBRAIN OF THE GRASSFROG

Willem J.M. Epping and Jos J. Eggermont

Department of Medical Physics and Biophysics University of Nijmegen, Geert Grooteplein Noord 21, NL-6525 EZ Nijmegen, The Netherlands

With a dual-electrode configuration separable few-unit activity was recorded both on one electrode as well as on two electrodes in the auditory midbrain of the grassfrog to a large variety of stimuli. Activity recorded on one electrode was separated by a pattern recognition technique using features of the action potential waveform. Functional connections between units were established on basis of crosscoincidence histograms of pairs of simultaneously recorded units. A hierarchical scheme was adopted to describe the various manifestations of neural coincidence. If a peak or trough was observed in the simultaneous crosscoincidence histogram, irrespective of stimulus conditions, this was called neural synchrony. If this peak or trough was not equal to its shift predictor based on non-simultaneous activity estimating the stimulus contribution, neural correlation was considered to be present. About 60% of the pairs exhibited neural synchrony, mostly due to shared stimulus influences, independent of mutual distance of units. About 15% of the unit pairs showed neural correlation indicating a functional neural connection. Neural correlation was observed only in units with a mutual distance < 300 µm. The majority (~ 85%) of the neural correlation could be ascribed to neural common input. Unidirectional excitation was observed only in unit pairs recorded on the same electrode. Unidirectional inhibition was not apparent. The dependency of occurrence of neural correlation on unit distance has implications for the functional organization of the auditory midbrain. About half of the neurally correlated pairs showed stimulus dependencies of their functional connections. Together with the observed lack of stimulus invariance of single-unit spectro-temporal sensitivities this may indicate a dynamic, stimulus and context dependency of neuronal connectivity in the auditory midbrain of the grassfrog.

1. Introduction

Acoustic communication plays a crucial role in the reproductive behavior of anuran amphibians. During the mating season males produce species-specific calls which serve to attract females of their own species and to maintain breeding aggregations. Both spectral and temporal characteristics of the vocalizations are used in order to identify [6,25,26,27,57] and localize [47] a sound source correctly.

The torus semicircularis, the anuran large auditory midbrain nucleus, which presumably is the homologue of the inferior colliculus in higher vertebrates, is supposed to play a major role in identification and localization of sound [e.g. 60]. On basis of mainly single-unit recordings but also of multi-unit and evoked potential data a wealth of knowledge has been gained about spectral [3,14,23, 32,33,55], temporal [4,16,17,34,48,56] and spatial coding [15,19,43] in the auditory midbrain. For a recent review the reader is referred to [60]. On one hand it appeared that spectral and temporal tuning properties are diverse and for many units complex, in the sense that these units are sensitive to multiple and not contiguous frequency and periodicity ranges respectively [14,16,17,23,48, 55,56]. On the other hand it became clear that the neural representations of the various aspects - spectral, temporal and spatial - of sound are intricately coupled. Variation of the sound in one aspect influences the coding of the other aspects, e.g. neural representations of both temporal and spatial features are in general dependent on the

---

Abbreviations: DCH difference crosscoincidence histogram; NCH non-simultaneous crosscoincidence histogram; SCH simultaneous crosscoincidence histogram; SPL sound pressure level; STS spectro-temporal sensitivity.

spectral content of sound [11,14,15,48]. As a consequence of these findings spectro-temporal sensitivities of neurons determined with artificial sounds as tonepips and continuous wideband noise and with natural vocalizations cannot be brought into register with one another [2]. Response predictions of firing patterns to conspecific calls on basis of those obtained for tonepips and noise frequently fail [13].

In contrast to the large amount of information about function of the anuran auditory midbrain relatively little is known about its anatomical structure. Potter [44] subdivided the torus semicircularis into five cytoarchitectural different regions, three of which have been shown to be sensitive to auditory stimulation. Recently Feng [20] provided evidence that besides the nucleus laminaris also the nucleus principalis has a laminated structure. Several morphological different classes of cells have been reported [5,20,45], but hardly anything is known about their intrinsic connections and local circuits. Even less is known about the relation of structure and function. On basis of evoked potentials Pettigrew et al. [43] claimed a coupled tonotopic and spatiotopic organization of the auditory midbrain. A weak tonotopic organization was also observed by Mohneke [39] in a gross multi-unit study, but was not corroborated by Walkowiak et al. [58] in an analogous investigation. Single-unit studies [14,15,33] have not excluded a possible tonotopy or spatiotopy but indicated that if it exists the organization probably is not clear and simple. Frequently neighbouring units have very different functional properties, which sometimes even are conjoined in complex single-units.

The abundance of complex functional properties in the auditory midbrain has not been reported for the lower auditory stations [24,48,56]. This finding provides indirect evidence for the presence of interneuronal connections - be it convergent, divergent or recurrent - in the auditory midbrain, which are responsible for the observed phenomena. The aim of the present study was to investigate these functional relationships between neurons by determining crosscorrelation functions of simultaneously recorded individual spiketrains of a small number ($2 \leq n \leq 7$) of neurons. Possible stimulus influences on these functional relationships were established by comparing crosscoincidence functions of spontaneous activity and activity evoked by a large variety of stimulus ensembles, ranging from tonepips, continuous wideband noise via periodic click trains and amplitude modulated sound to natural vocalizations. Thereby our focus was on the aspect of identification of sound, implying that only influences of spectral and temporal sound characteristics have been studied. Preliminary results on this subject have been published elsewhere [12]. By the use of a configuration of two independent electrodes, each of which was able to record the activity of up to four neurons, both populations of proximate (within about 50 µm) and more distant (100-400 µm) neurons could be sampled. Thus information was obtained about the influence of spatial separation of neurons on their functional interrelation.

2. Materials and Methods

2.1. Animal Preparation

Adult grassfrogs (Rana temporaria L.) from Ireland were anesthetized by a 0.05% solution of MS-222. After the loss of all reflexes an incision was made and the skin overlying the upper part of the skull was folded away. A screw for fixing the head was glued upside down to the frontal bones with dental resin (Palacav). A small hole of about 7 mm^2 was drilled into the parietal bones covering the tectum mesencephali, the dura was left intact. Afterwards the skinflap was refolded and the animals were allowed to recover for two days.

Before the experimental session local anesthetic (Xylocaine 4%) was applied to the wound margins and the animal was immobilized with an intralymphatic injection of Buscopan (0.16 mg per gram bodyweight). The animal was placed onto a damped vibration isolated frame in a sound attenuated room (IAC type 1202 A). Temperature was kept constant (± 1° C) around 16° C and the skin was kept moist by a

thin layer of cotton gauze to ensure skin respiration to be sufficient for metabolic demands. During recordings the mouth was shut. The ECG was monitored continuously using a right fore leg - left hind leg recording and served as a measure for pain or arousal of the animal during the experiments. The heart rate was very constant and slightly dependent on temperature and state of the paralysis. For the collection of frogs studied the heart rate at 16°C usually was between 25 and 35 per min. Any pain deliberately induced or presentation of intense wideband noise caused the ECG to increase in rate up to 10%. Therefore constancy of the heart rate was interpreted as an indication that neither pain nor arousal were present. Normally the preparation was kept intact, without any signs of deterioration, for at least two consecutive days.

2.2. Acoustic Stimulus Presentation

Acoustic stimuli were generated by a dual channel programmable stimulus generator, which is described in more detail elsewhere [14], build around a PDP 11/10. The generated stimuli were presented to the animals by two electrodynamic microphones (Sennheiser MD 211N) coupled to the tympanic membranes with a closed sound system. Care was taken to minimize mechanical crosstalk of stimulus apparatus to the ears. The sound pressure level (SPL) was measured in situ with a half-inch condensor microphone (Bruel and Kjaer 4143) connected to the coupler [32]. The frequency response of the sound system was flat within 5 dB for frequencies between 100 and 3000 Hz, a sufficient range for studying the auditory system in the grassfrog (e.g. [6]). The amplitude characteristics of left and right couplers were equal within 2 dB for the range of interest.

A large variety of stimulus ensembles has been applied, ranging from simple artificial stimuli to complex ensembles mimicking the mating call. A list of the stimulus ensembles containing a short description is given below. These stimuli have been described in detail and illustrated with single unit results elsewhere.

1) Tonepips. This stimulus ensemble consisted of short (16 or 48 ms) tonepips of pseudorandomly varied frequency covering the hearing range of the grassfrog and separated by silent periods of 128 ms or 1 s [2,14,33].
2) Gaussian wideband noise. Pseudorandomly generated Gaussian noise with a bandwidth of 1500 or 5000 Hz and a duration of about 6 min [14,32].
3) Periodic click trains. Stimulus ensemble consisting of trains of 10 equidistant clicks. The trains had onset intervals of 3 s and the click rate was pseudorandomly varied between 7.8 and 250/s [16].
4) Poisson distributed clicks. Long duration (12 min) ensemble of short (1 ms) clicks, separated by intervals drawn independently from a negative exponential distribution. Click rates were 4, 8 or 16/s [16].
5) Sinusoidally amplitude modulated sound bursts. The bursts had a duration of 500 ms and onset intervals of 3 s. The frequency of amplitude modulation was pseudorandomly varied between 7.8 and 250/s. Both tonal and wideband noise carriers have been used [17].
6) Noise amplitude modulated sound. A long duration (about 8 min) tone or wideband noise sound was amplitude modulated by a low-pass filtered (100 Hz) Gaussian noise envelope [17].
7) Variations on the mating call. This stimulus ensemble consisted of the grassfrog's mating call and manipulated versions thereof. The synthesized versions had an altered spectral or temporal structure. In addition different levels of a noise background were applied [Eggermont and Epping, in preparation].

The stimulus ensembles consisted of at least two (2-60) identical sequences presented immediately after each other. The presentation mostly was to the contralateral, with respect to recording side, ear and at natural sound pressure levels: 90 dB SPL.

2.3. Recording Procedure

Ultra-fine or tapered tungsten microelectrodes

coated with parylene-c, having a 10-15 µm exposed tip with a 1 kHz impedance of 1.5-2.5 MΩ (Micro Probe Inc) were used for extra-cellular recording. In a home-made micromanipulator two electrodes were installed slightly obliquely (~ 4°) with respect to each other and with tip separations ranging from 100 µm to 300 µm on the roof of the midbrain. The electrodes were advanced independently through the intact dura and lowered into the auditory midbrain using two motorized hydraulic microdrives (Trent-Wells 3-0661 and Frederick Haer & Co). Stepping precision was 1 µm. Electrode signals were amplified using Dagan 2400Z extracellular preamplifiers bandpassed between 100 Hz and 10 kHz. In this configuration simultaneous activity of small neural populations (up to 4 neurons located within a sphere of a diameter of about 50 µm) regularly was recorded on each electrode. Occasionally the two electrodes were both recording from the same neuron, indicating that the tips could be brought into close proximity.

In order to separate the superimposed few-unit activity recorded on one electrode into the component single-unit spiketrains a number of separation schemes have been devised. They all use features of the action-potential waveform, for a recent review see [8,59]. It is thereby assumed that the spike waveform is characteristic for a particular neuron in a given geometric position to the recording electrode. One of the most powerful procedures [59] is based on the Karhunen-Loève expansion, also called Principal Component Analysis. This scheme essentially is a generalized matched filter procedure which uses the entire spike waveform for feature extraction. This approach, which was made operational at first by Abeles and Goldstein [1], was adopted by us [12] and will be illustrated below with data from the auditory midbrain of the grassfrog.

In the auditory midbrain of the grassfrog a variety of spike waveforms have been observed, five representative types are shown in Fig. 1. Types I (15%) and II (29%) are of low amplitude (< 200 µV) whereas types III (32%), IV (5%) and V (19%) often are of larger voltage (> 300 µV). Correlations were found between spike waveform and various neural

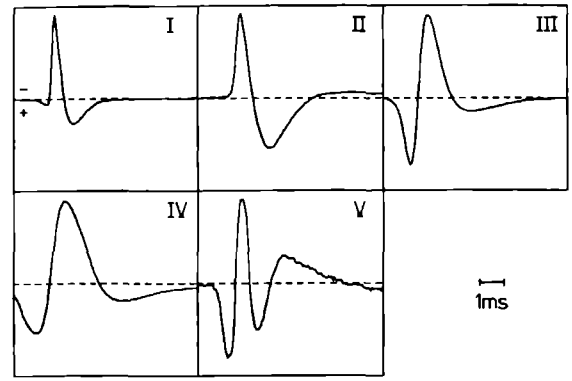

Fig. 1. Action potential waveform types from the auditory midbrain of the grassfrog. Negative polarity is upwards. Time base is 7.68 ms.

properties suggesting a function associated with spike waveform [10,14,32]. The waveforms were sampled with 128 points at an interval of 60 µs resulting in a total duration of 7.68 ms. After averaging individual waveforms to reduce the superimposed noise and normalizing to equal amounts of energy, the basisvectors were determined according to the Karhunen-Loève expansion procedure [22]. These basisvectors, which are the eigenvectors of the average autocorrelation matrix of waveforms, form as a consequence of their definition an orthonormal base. The eight most prominent basisvectors account already for almost all energy present in the collection of waveforms (Fig. 2). The first four basisvectors account on average for 95.6% of the energy which was considered sufficient for our pur-

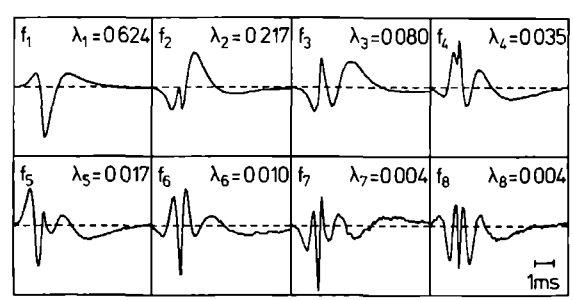

Fig. 2. Orthonormal basisvectors according to the Karhunen-Loève expansion. The indicated eigenvalues (λ_i) represent the fraction of the energy in the population of the spike waveforms that is represented by the particular basisvector.

pose. For on-line feature extraction a hardware spike analyzer was realized in digital form, in which the four most prominent basisvectors were stored as transversal filters. In our version detection of spikes was performed by level crossing separately from feature extraction which was done by projection of each detected spike waveform on the four selected basisvectors. The spike analyzer was unable to handle spikes which occurred within 3.84 ms of each other. For more details about the spike analyzer the reader is referred to [12]. Waveform features and spike-epochs were stored by a data-acquisition system build around a PDP 11/34 for subsequent off-line analysis on a PDP 11/44.

During the experiments the few-unit activity was represented real-time in various forms for each electrode separately to monitor the quality of recording and to get an impression about stimulus response and functional interneural relations. The levels for detecting spikes in background noise were set by hand upon inspection of the raw electrode signals on oscilloscopes, as well as the output of the spike analyzers, which were displayed on video screens. An illustration of the spike analyzer output for one electrode is given in Fig. 3a. In the upper row a dotdisplay of unseparated few-unit activity evoked by a tonepip (48 ms) stimulus with onset intervals of 1 s is represented. In the second and third row the six projection planes, formed out of all pair combinations of four basisvectors, are shown. Three clearly separated clusters can be distinguished in all planes, meaning that a triple-unit recording of good quality was obtained. About 5% of the dots fall outside the cluster boundaries and are not classified. Presumably most of these dots represent (partial) superpositions of spikes as can most clearly be observed in the projection plane spanned by basisvectors 3 and 4. Often separation of clusters could be improved by careful stepping with the microelectrodes and having some patience. To save time during the experiments the actual classification of spike waveforms was done off-line mostly.

The classification procedure is done interactively. It starts with the selection of that projection plane in which the separation is best. An ellipse is constructed around one of the clusters by indicating with a cursor the end points of the long axis and one end point of the short axis. Then the procedure repeats itself, optionally in another projection plane, for the other clusters (Fig. 3b). All spikes falling within a cluster boundary get a label and are interpreted as originating from the same neuron. After the classification procedure single-unit spiketrains are obtained (Fig. 3c) which can be used to study single-unit stimulus response relations as well as functional interneural relationships. As an additional quality check spike waveforms are reconstructed afterwards from their projections on (i.e. inproducts with) the four orthonormal basisvectors and are displayed superimposed per cluster (Fig. 3d). It can be concluded that the classification is reliable since the distribution of the individual waveforms around the mean is rather uniform, in contrast to the not classified waveforms. Note that our spike analyzer was clearly able to separate three units of which the action potentials had comparable amplitudes and were of the same type (type III, positivity upwards).

In case of very promising recordings the classification is done on-line in order to get more information already during the experiment. Then the separated single-unit recordings are not displayed in segregate dotdisplays (Fig. 3c) but superimposed again as in Fig. 3a, however, indentifiable now by using a colour code indicating neural origin of dots. This picture "the Neurochrome" [18] allows for a quick and convenient examination of multi unit activity patterns and possible stimulus influences there upon.

2.4. Data Analysis

The way single-unit stimulus-response relations to the various stimulus ensembles are obtained have been described elsewhere [13,14,15,16,17, 32,33]. Functional interrelationships between neurons were studied by pairwise crosscorrelation functions estimated by crosscoincidence histograms [28,42]. The simultaneous crosscoincidence histogram (SCH) $C_{12}(\tau)$, also called gross correlo-

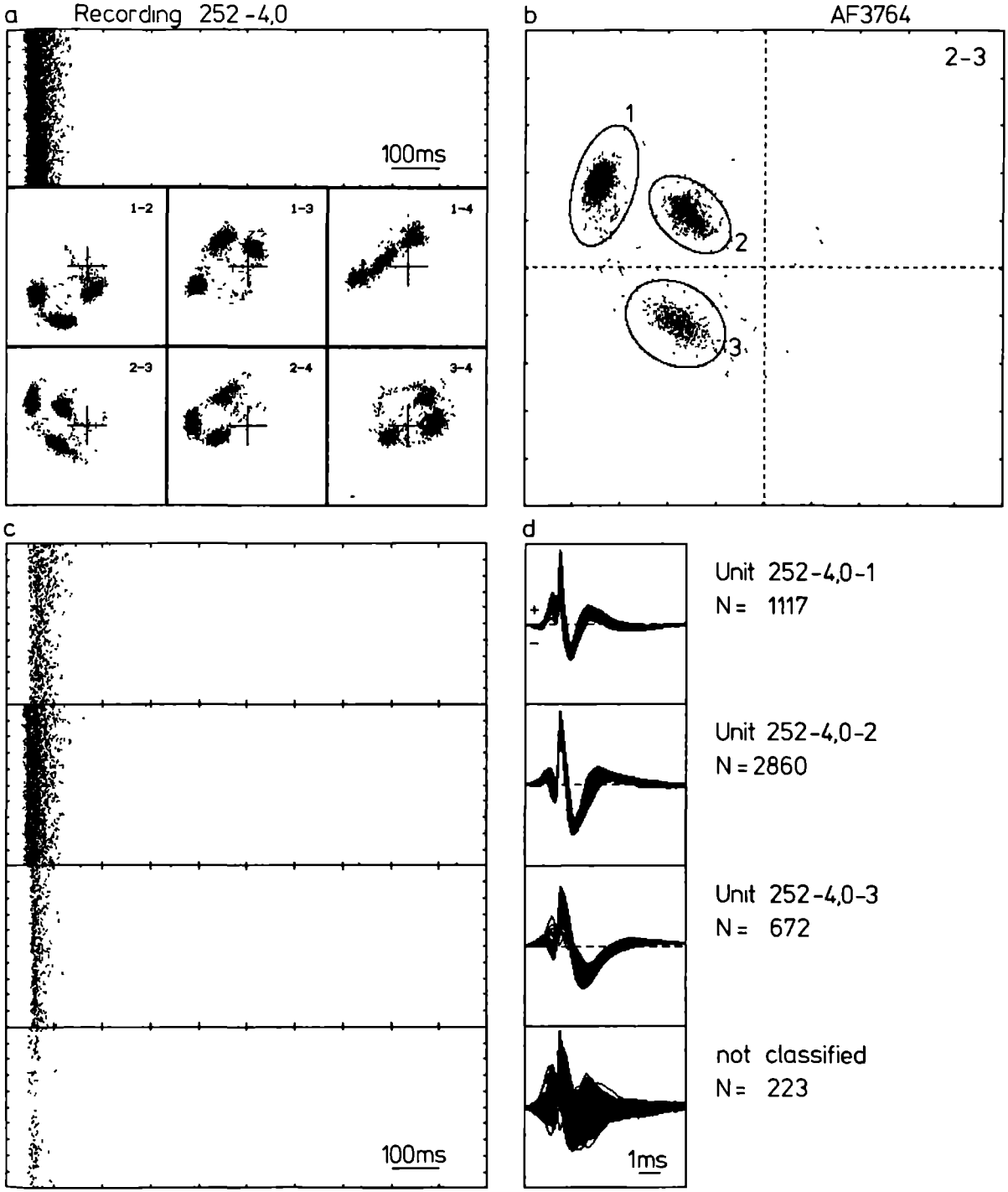

Fig. 3. Separation of few-unit activity. (a) Dotdisplay of unseparated few-unit activity (upper row) and projection on the 6 different basisvector planes. (b) Separation of waveforms by ellipsoidal boundaries. (c) Single-unit dotdisplays. (d) Reconstructed waveforms. Stimulus was a tonepip (48 ms) ensemble with onset intervals of 1 s, presented for 30 min.

gram [42], estimates the probability of two spikes occurring in close vicinity of each other:

$$C_{12}(\tau) := \lim_{\Delta\tau \to 0} \frac{1}{\Delta\tau} \text{prob}[\text{unit 1 spike on } t_o \text{ and unit 2 spike in } [t_o+\tau, t_o+\tau+\Delta\tau)]$$

Thereby it is assumed that the estimate is independent of t_o, implying stationarity of the joint distribution of the responses. Under stimulus conditions, however, the assumption will often not be fulfilled and a superposition of time varying effects will result. These effects may be unraveled using joint occurrence diagrams (JOD), also called joint peri stimulus time scatter diagrams [29,49], which depend explicitely on time.

The simultaneous crosscoincidence histogram (and also the JOD) generally exhibits the combined effects of neural and stimulus origin. In order to separate these two causes of possible coincidence non simultaneous crosscoincidence histograms (NCH), also called shuffled correlogram, shift predictor [42] or stimulus related correlogram [54] are determined. The NCH is computed in the same way as the SCH except that one of the spike trains is shifted circularly over one or more stimulus sequences of length P which need to be identical for this type of analysis:

$$C_{12}^{k}(\tau) = C_{12}(\tau+kP) \quad ; \quad k = 1,\ldots,K$$

Actually we computed the averaged NCH

$$C_{12}'(\tau) = \frac{1}{K-1} \sum_{k=1}^{K-1} C_{12}^{k}(\tau)$$

Note that for this type of analysis the spiketrains have to be periodically stationary, i.e. their firing probability density must remain identical to subsequent stimulus sequences. In our study lengths of stimulus sequences P varied from 32 to 1200 s, therefore neural influences on the NCH may be ruled out, leaving only stimulus effects. An example of this type of analysis is shown in Fig. 4a. The SCH and the NCH (shaded) are displayed superimposed. The stimulus was an ensemble of amplitude modulated (30 Hz) tonebursts (500 ms) with onset intervals of 3 s. It appears that the SCH and NCH are very much

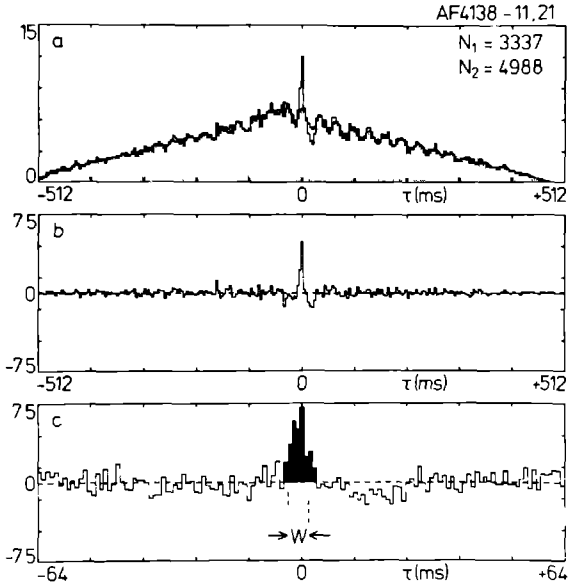

Fig. 4. Crosscorrelation analysis. (a) Simultaneous and non simultaneous (shaded) crosscoincidence histograms. (b), (c) Difference histogram shown on different timescales, the black area represents the association index A, W is the halfwidth of the peak. Binwidth was 4 ms in (a), (b) and 1 ms in (c).

alike except for a small region around the origin. The interpretation is that the gross structure seen in the SCH extending over 1 s and with an oscillation on top of it of 30 Hz is due to the stimulus. The small peak around the origin which stands out above the NCH indicates that there was also a neural effect on the SCH. In case there is no difference between the SCH and the NCH the interpretation is that neural effects are not obvious. However, this does not exclude the presence of neural influences, they may be much weaker than the stimulus effects or they may be of higher order not revealed by pairwise second-order crosscorrelation functions.

Under the assumption of additivity of stimulus and neural effects, which probably will not be true in most situations (see Discussion), the neural influence is estimated by the difference crosscoincidence histogram (DCH) $D_{12}(\tau)$, also called neurally related correlogram [54] (Fig. 4b):

$$D_{12}(\tau) = C_{12}(\tau) - C_{12}'(\tau)$$

The DCH is shown on a finer timescale in Fig. 4c, from which it can be concluded that the responsible neural mechanism presumably is neural common input because the peak has a rather symmetric form and straddles the origin.

Instead of raw crosscoincidence histograms $C_{12}(\tau)$ which are dependent on binwidth Δ, duration of recording T and spike numbers N_1,N_2 we used scaled crosscoincidence histograms $\hat{C}_{12}(\tau)$:

$$\hat{C}_{12}(\tau) = \frac{T}{N_1 N_2 \Delta} \cdot C_{12}(\tau)$$

In case of uncorrelated spiketrains the background level of the scaled crosscoincidence histogram is 1.

In order to quantify phenomena observed in the crosscoincidence histograms we determined half-widths (W) of peaks and a measure for strength called the association index (A). The association index is defined as the area under a certain peak in the scaled DCH (Fig. 4c):

$A = \int_{t_1}^{t_2} d\tau \, \hat{D}_{12}(\tau)$; t_1 and t_2 are the boundaries of the peak. The dimension of A is seconds. In the example shown in Fig. 4c W is 5 ms and A is 0.033 s. The association index is applicable in case of common input as well as direct excitation or inhibition. Other measures of strength such as contribution $A \cdot N_1/T$ and effectiveness $A \cdot N_2/T$ [37] are not symmetrical with respect to neuron and therefore only convenient in case of unidirectional neural effects.

2.5. Location of Recording Site

Electrode tracks were made approximately orthogonal to the surface of the midbrain in both hemispheres. Position in the rostrocaudal-mediolateral plane was determined by marking the entrance of a track on a photograph made of the surface of the midbrain. All entrances were made within a region extending from 300-1100 µm rostral to the boundary between midbrain and cerebellum and from 600-1100 µm lateral to the midline between the two hemispheres. Dorsal-ventral position was read from the stepping motor devices. All units were recorded on a depth between 800 µm and 1800 µm beneath the surface of the optic lobes. No lesions were made, but because the location of the recording sites as determined above was well within the classical boundaries of the torus semicircularis, as verified by Hermes et al. [33] in an analogous study with histological techniques, we are certain that almost all our auditory units were indeed located inside the torus.

3. Results

With our dual-electrode configuration a total of 113 double-unit recordings, 28 triple-unit, 6 quadruple-unit, 1 quintuple-unit and 1 7-unit recordings were obtained in 44 frogs. Out of these few-unit recordings a total of 264 unit pairs can be formed. The mutual distance of the units of a unit pair recorded on separate electrodes was estimated on basis of the separation of the electrode tips at the surface of the midbrain and the depths of recording. The mutual distance of units recorded on the same electrode was estimated on basis of the sight of the electrodes which depended on unit type but on average was about 50 µm. The number of unit pairs and their mutual separation is given in Table I.

Table I. Frequency distribution of mutual distance of units forming a pair.

one electrode	two electrodes		
0<d<100µm	100µm<d<200µm	200µm<d<300µm	d>300µm
140	67	27	30

3.1. Manifestations of Neural Coincidence

Crosscoincidence histograms of activity of unit pairs may show a deviation from a flat background for several reasons: stimulus influences, neural influences or a combination thereof. A hier-

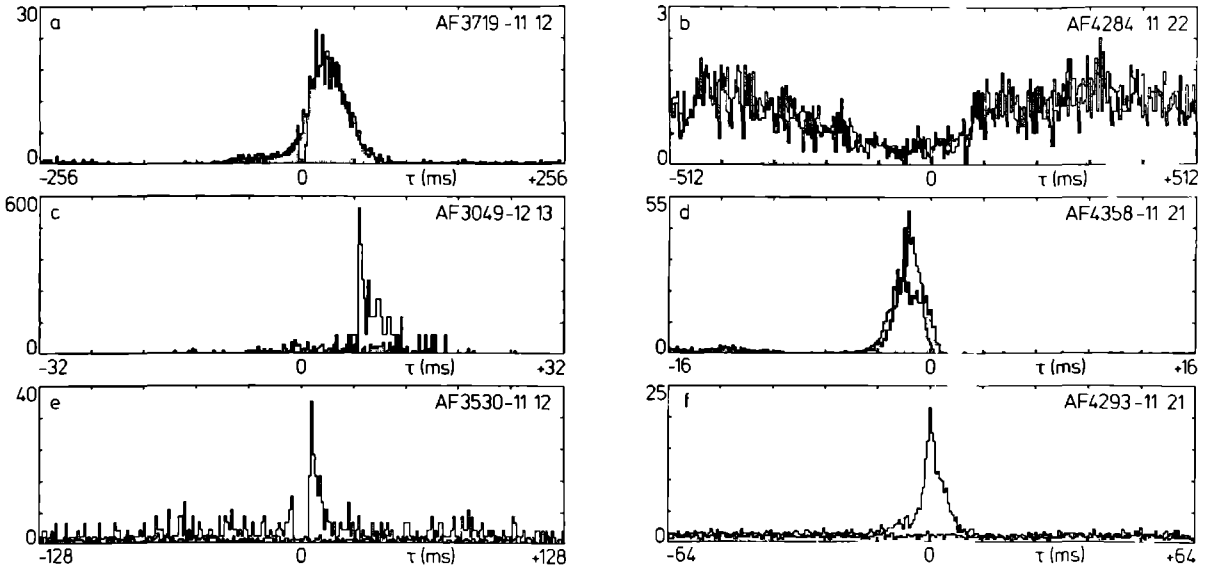

Fig. 5. Manifestations of neural crosscoincidence. Simultaneous and non-simultaneous (shaded) crosscoincidence histograms are displayed superimposed. (a) Neural synchrony, incremental correlogram N_1 = 570, N_2 = 1563. (b) Neural synchrony, decremental correlogram N_1 = 1366, N_2 = 733. (c) Unidirectional excitatory input, N_1 = 229, N_2 = 74. (d) Neural common input, N_1 = 6430, N_2 = 3130. (e) Unidirectional excitatory input, N_1 = 844, N_2 = 679. (f) Neural common input, N_1 = 3244, N_2 = 3456. Stimulus driven activity in (a)-(d), spontaneous activity in (e), (f). Note different timescales.

archical scheme [12] is proposed to describe the various manifestations of neural coincidence.

Neural synchrony is reflected by a peak or valley in the SCH, irrespective of stimulus conditions. A peak (incremental correlogram) points at near coincidence of the activity of the two units (Fig. 5a,c,d,e,f) while a valley (decremental correlogram) indicates coincidence of spikes of one unit and silent periods between spikes of the other unit (Fig. 5b).

Neural correlation is considered present if the SCH and the NCH are clearly different indicating, besides a possible stimulus effect, a neural influence on the crosscoincidence. The unit pairs in Fig. 5a,b have similar SCH's and NCH's and therefore do not exhibit neural correlation. The unit pair in Fig. 5c has a SCH clearly different from the hardly visible NCH and thus shows neural correlation. Its peak is highly asymmetrical and displaced + 6 ms from the origin. This is interpreted as a unidirectional (presumably disynaptical) excitatory influence of unit 1 on unit 2. The unit pair in Fig. 5d has a much more pronounced NCH reflecting a strong stimulus influence on the crosscoincidence. However, the SCH and NCH are clearly different pointing at an additional neural influence. The peak is rather symmetrical and encloses the origin slightly, which is indicative for neural common input. Two examples for neural correlation in spontaneous activity one for unidirectional excitation and one for common input are shown in Fig. 5e and f respectively. Note the flat NCH. The differences between SCH and NCH were, except for some secondary side effects, always positive. This implies that no unidirectional inhibitory influences or antagonistic neural common input could be demonstrated in our collection of unit pairs.

3.2. Stimulus Dependency of Neural Correlation

A difference of SCH and NCH indicates an effect of neural origin on the crosscoincidence. By comparing crosscoincidence histograms of neural ac-

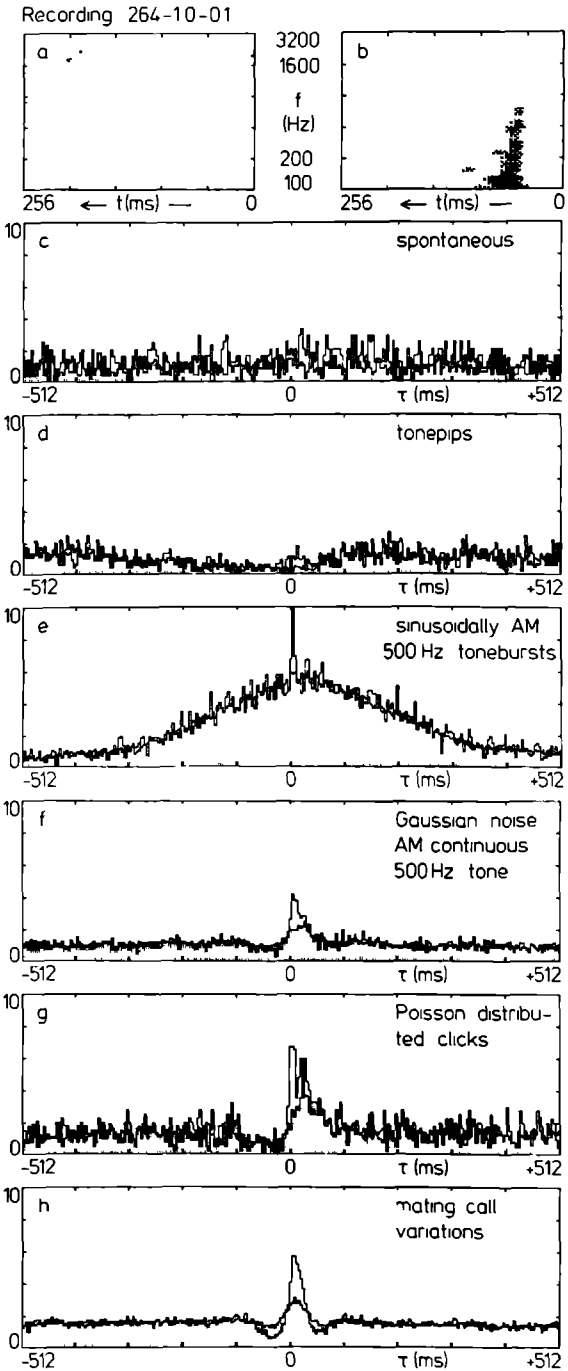

Fig. 6. Unit pair with a stimulus variant neural correlation. (a), (b) Spectro-temporal sensitivities of the two units as determined with tonepips. (c)-(h) Simultaneous and non-simultaneous (shaded) crosscoincidence histograms for a variety of stimuli. Binwidth is 4 ms. Number of spikes: (c) 1789, 243; (d) 1315, 439; (e) 1595, 730; (f) 2639, 754; (g) 1053, 895; (h) 8119, 1948.

tivity obtained for a large variety of stimulus ensembles a possible stimulus modulation of the neural effect may be studied. One has to be cautious in calling a neural effect stimulus dependent on basis of differences observed in the DCH's, because the assumption of additivity of stimulus and neural effects may not be fulfilled. Therefore we were conservative and did not rely on measures derived from the DCH such as the association index.

Our criteria for deciding a stimulus dependency were changes in form, especially width, of peaks and/or a change from a clear non-flat DCH under one stimulus condition to a flat DCH under another stimulus condition. An example is provided in Fig. 6. The two spontaneously active units shown were recorded on separate electrodes with an estimated tip separation of 130 µm. Their spectro-temporal sensitivities as determined with tonepips are shown in Fig. 6a,b. The spontaneous activity of unit 1 was suppressed by frequencies below 1000 Hz (Fig. 6a), while unit 2 was activated in this frequency range with a latency of about 35 ms (Fig. 6b). SCH's and NCH's of spontaneous and stimulus evoked activity are shown in Fig. 6c-h. A broad ($\pm$ 200 ms) small amplitude hump above the flat NCH can be observed for spontaneous activity (Fig. 6c). For tonepips the NCH (Fig. 6d) shows a decrement due to the antagonistic (suppression versus activation) stimulus influences, on top of it a rather symmetric peak around the origin having a width of about 30 ms and indicating neural common input can be observed. The NCH to sinusoidally AM tonebursts is broad and of incremental type (Fig. 6e) with a sharp (4 ms) peak of the SCH in excess. The crosscoincidence histograms to a low-pass noise AM tone (Fig. 6f) and to Poisson distributed clicks (Fig. 6g) are similar having an asymmetric peak of about 30 ms width. The crosscoincidence histograms to mating-call variations are rather symmetrical having a width of about 20 ms. In addition to the primary peak secondary valleys, due to the autocorrelation structure

of the individual spike trains, are present. So it can be concluded that this unit pair exhibits stimulus dependencies on both stimulus induced crosscoincidences as revealed by the NCH (e.g. compare Fig. 6d and e) as well as on neurally induced crosscoincidences because of changes in form and width of peaks.

3.3. Survey of Results

The frequency distribution of the various manifestations of neural coincidence and possible stimulus influences thereupon is summarized in Diagram 1. It appears that about 60% of all unit pairs exhibit synchronized behavior be it due to stimulus effects, neural effects or a combination thereof, with no differences between unit pairs recorded on one or two electrodes. The majority of the synchronization was of incremental type. Neural correlation indicating effects of neural origin was observed in about 15% of the unit pairs, again no difference was apparent between one and two electrode recordings, except that no neural correlation was observed for unit distances of more than 300 µm. Most of the neural correlations could be ascribed to neural common input. Unidirectional (always excitatory) neural influence was only observed in unit pairs recorded on the same electrode. About half of the neural correlations were found to be stimulus dependent.

The average displacement of the unidirectional excitatory peaks from the origin was 5 ms (range 4-8 ms, N = 6) indicating mono- and disynaptic connections. The average halfwidth W of these peaks was 9 ms (range 3-15 ms), and the average association index A 0.48 s (range 0.016-1.10 s). The mean halfwidth of the neural common inputs was 51 ms (range 1-250 ms, N = 31) and the mean association index was 0.50 s (range 0.018-6.7 s). No clear differences were apparent between common inputs recorded on one or two electrodes, although A was underestimated in case of some one electrode recorded pairs, because of the dead-time (3.84 ms) of our spikeanalyzer. The width of common input peaks could be as small as 1 ms indicating a strong coupling due to neural common input. Therefore the width of peaks may not be used to distinguish unidirectional from common input influences, although on average halfwidths of unidirectional peaks were much smaller than common input peaks.

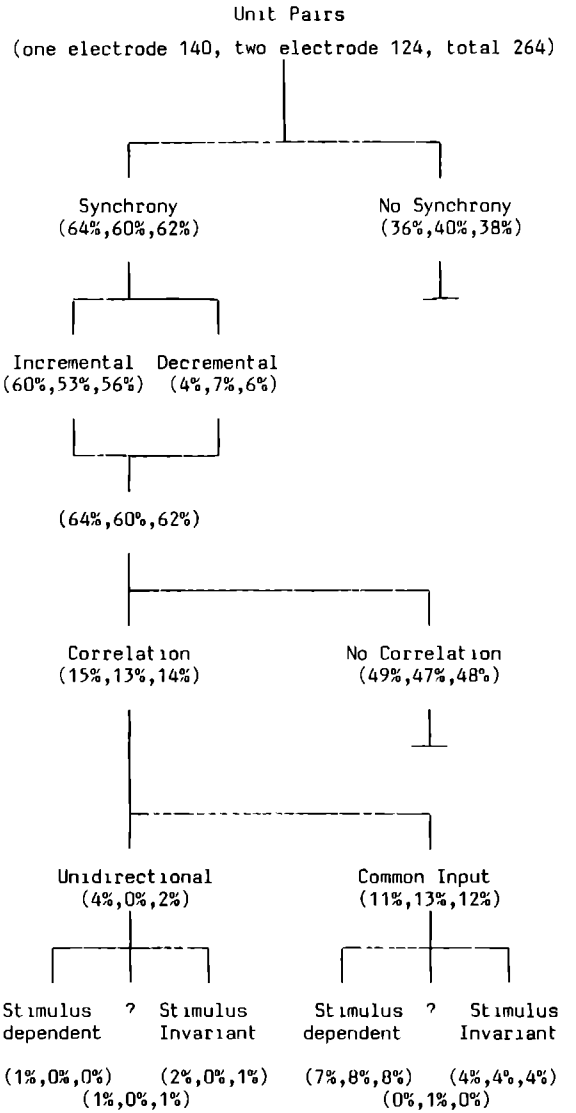

Diagram 1. Hierarchical scheme of the various manifestations of neural concidence. Presented are frequency distributions of unit pairs recorded on one electrode, two electrodes and the total collection of pairs respectively. A '?' indicates that stimulus dependency was not determined.

4. Discussion

4.1. Functional Organization

On basis of the observed distribution of the various manifestations of crosscoincidence several tentative implications for the functional organization of the auditory midbrain of the grassfrog may be proposed. The high incidence of synchrony (about 60%) versus neural correlation (about 15%) points at a dominant role of stimulus input as compared to neural mechanisms in shaping coherent firing patterns.

Often neural synchrony was not observed with tonepip stimulation as a consequence of non-overlapping tuning properties of the units, but became apparent if more complex stimuli such as AM sound were presented. We mainly used tonepip ensembles and unmodulated Gaussian wideband noise in initial stages of this investigation. Thus the 60% of neural synchrony probably is a lower bound of the actual percentage. The occurrence of synchrony, mostly due to pure stimulus effects, was not dependent on unit distance. This finding indicates that particular stimulus information is not conveyed to restricted regions of the auditory midbrain but instead is spread over a large part of it, which agrees well with the weak tonotopic and spatiotopic organization of the anuran auditory midbrain [14, 15,33,39,43,58]. This conclusion probably is not valid for the mammalian auditory midbrain, which exhibits a clear tonotopy and where neighbouring units often share comparable stimulus-response relations [53]. In mammalian cortical structures the picture is reversed, in the visual cortex of the cat for example only about 30% of the unit pairs shows stimulus induced synchronization as opposed to about 75% exhibiting neural correlation [38]. Therefore the cortex presumably acts much more autonomous, less dominated by external influences, than midbrain nuclei. The thalamus seems to take an intermediate position since in the cat medial geniculate body about 35% of the unit pairs is clearly neurally correlated [31]. Neural common input was observed only in units with a mutual separation < 300 µm and unidirectional effects were present only in unit pairs recorded on one electrode. This finding indicates that local circuits in the anuran auditory midbrain are contained in a region of about 50-100 µm. The distance dependent rate of occurrence of neural correlation and the portion of common inputs versus unidirectional influences was also observed in cortical structures. In the cortex probability of detecting neural correlation decreases with distance [7,40] and unidirectional effects occur mainly within a cortical column [38].

4.2. Stimulus Dependency of Neural Correlation

About half of the neurally correlated unit pairs exhibited strong stimulus dependencies, not caused by a possibly incorrect stimulus normalization procedure based on an additive model. Stimulus dependencies of neural correlation were also reported in the auditory cortex of the cat [7,21] and in the crayfish brain [61]. These stimulus dependencies might indicate that functional organization of neurons is not static, but instead dynamic; the particular functional connections depend on the particular stimulus applied. Stimulus dependency of functional interneural connections and the observed lack of stimulus invariance of single-unit spectrotemporal sensitivities, as mentioned in the Introduction, may therefore both be manifestations of the stimulus and, more generally, context dependency of the functional association of the underlying neural substrate. At least part of the information is not coded by single-units but by populations of neurons resulting in ensemble coding [41,50,51]. Ideally ensemble coding should be studied by simultaneous recording of larger (10-100) populations of units probably becoming feasible by recent advances in micro-electrode [36,46] and optical recording technology [30].

4.3. Possible Role of Ensemble Coding

A possible and probably the most basic function of ensemble coding over single-unit coding is the increased selectivity by reduction of background activity. A tentative example is provided by

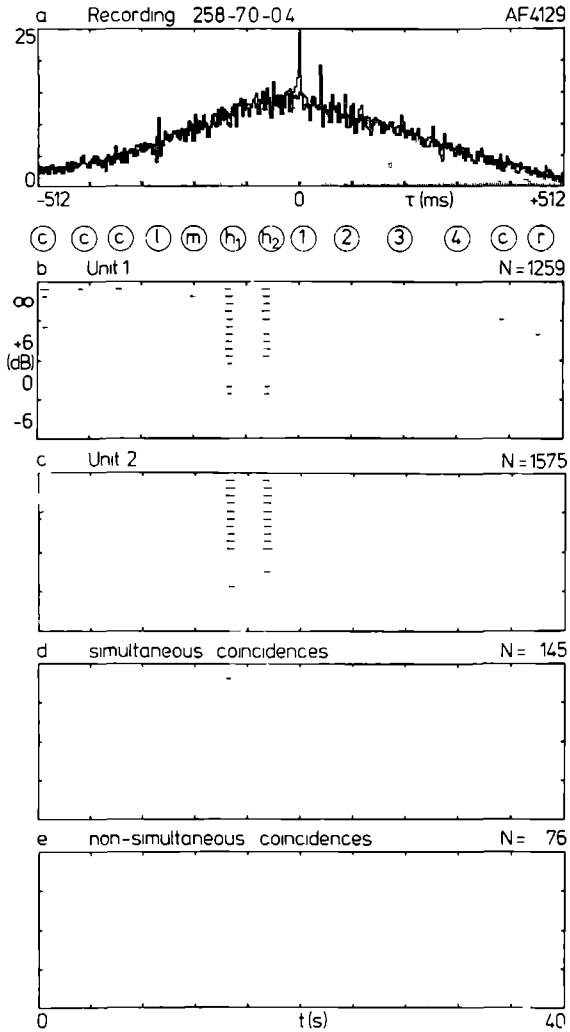

Fig. 7. Unit pair showing enhancement of selectivity in double-unit coding compared with single-unit coding. (a) Simultaneous and non-simultaneous (shaded) crosscoincidence histograms. (b), (c) Dotdisplay of single-unit activity. (d) Conditional dotdisplay of unit 1 spikes in close coincidence (± 2 ms) with unit 2 spikes. (e) Shift predicted version of the conditional spiketrain. The stimulus was the mating call variation ensemble, consisting of the original mating call (c) and synthesized versions of it. Both spectral (l: carrier is 201 Hz, m: 557 Hz, h_1: 1067 Hz, h_2: 1542 Hz) and temporal (different intervals between the individual phonemes, 1: original interval length, 2: double interval length, 3: three times the interval length, 4: four times the interval length) variations were presented in addition to a time-reversed mating call (r). Moreover a noise background was added reducing the signal to noise ratio, in 4 steps of 6 dB. The total stimulus ensemble consisted of 5 identical sequences. The responses to identical calls, indicated above the dotdisplays, were arrayed vertically. For convenience responses to calls in equal amounts of noise were grouped together, no noise background (SNR = ∞) shown in the first 5 rows, maximal noise background (SNR = -6 dB) represented in the last 5 rows. Note that even the activity burst due to a small disturbance during the recording, as observed in the sixth row of both single-unit dotdisplays is not apparent in the conditional dotdisplays.

the unit pair shown in Fig. 7. Stimulated with the mating call variation ensemble both units responded nearly similarly, the most effective response was evoked by high frequency carriers, as is apparent from the dotdisplays (Fig. 7b,c) of neural activity. Crosscoincidence histograms (Fig. 7a) revealed a broad synchronization due to shared stimulus response properties and a sharp (~ 4 ms) neurally induced peak on top of it indicating neural common input. Subsequently we simulated a coincidence circuit detecting which unit-1 spikes were in close coincidence (± 2 ms) with unit-2 spikes. The dotdisplay of the unit-1 spikes fulfilling the coincidence condition is pictured in Fig. 7d. From this dotdisplay it appears that the conditional unit-1 spikes were almost all located in the activity band due to the high frequency carriers as opposed to the single-unit activity which is also present for other mating call variations. For comparison also the "shift-predicted" version is shown in Fig. 7e, which was obtained by an identical procedure, except that one spiketrain was shifted over one stimulus sequence. The shift predicted conditional dotdisplay exhibits the same features as the original one but with a 50% reduction in number of conditional spikes. This once more underlines the paramount importance of recording simultaneous activity of neural populations instead of consecutive separate single-unit recordings.

Acknowledgements

This investigation forms part of the research program "Brain and Behaviour" at the Department of Medical Physics and Biophysics of the University of Nijmegen and was supported by the Netherlands Organization for the Advancement of Pure Research

(ZWO). The authors wish to thank Jan Bruijns and Wim van Deelen for software development, Koos Braks for the animal preparations and technical assistance, Hans Krijt and his group for electronic support. Henk van den Boogaard provided valuable comments on the manuscript, which was put into the wordprocessor patiently by Marianne Nieuwenhuizen.

References

1 Abeles, M. and Goldstein, M.H., Jr. (1977): Multispike train analysis. Proc. IEEE 65, 762-773.

2 Aertsen, A.M.H.J. and Johannesma, P.I.M. (1981): A comparison of the spectro-temporal sensitivity of auditory neurons to tonal and natural stimuli. Biol. Cybern. 42, 145-156.

3 Bibikov, N.G. (1974): The impulse activity of torus semicircularis neurons of the frog *Rana temporaria*. Zh. Evol. Biokhim. Fiziol. 10, 40-47.

4 Bibikov, N. and Gorodetscaya, O. (1981): Coding of amplitude-modulated tones in the midbrain auditory region of the frog. In: Neuronal mechanisms of hearing, pp. 347-352. Editors: J. Syka and L. Aitkin. Plenum Press, London, New York.

5 Bibikov, N.G. and Soroka, S.K. (1979): Neuronal structure in the auditory midbrain center of the frog *Rana ridibunda*. Zh. Evol. Biokhim. Fiziol. 15, 608-616.

6 Brzoska, J., Walkowiak, W. and Schneider, H. (1977): Acoustic communication in the grass frog (*R. temporaria*): calls, auditory thresholds and behavioral responses. J. Comp. Physiol. A 118, 173-186.

7 Dickson, J.W. and Gerstein, G.L. (1974): Interaction between neurons in auditory cortex of the cat. J. Neurophysiol. 37, 1239-1261.

8 Dinning, G.J. and Sanderson, A.C. (1981): Real-time classification of multi-unit neural signals using reduced feature sets. IEEE BME-28, 804-811.

9 Eggermont, J.J., Aertsen, A.M.H.J., Hermes, D.J. and Johannesma, P.I.M. (1981a): Spectro temporal characterization of auditory neurons: redundant or necessary? Hearing Res. 5, 109-121.

10 Eggermont, J.J., Hermes, D.J., Aertsen, A.M.H.J. and Johannesma, P.I.M. (1981b): Response properties and spike waveforms of single units in the torus semicircularis of the grassfrog (*Rana temporaria*) as related to recording site. In: Neuronal mechanisms of hearing, pp. 341-346. Editors: J. Syka and L. Aitkin. Plenum Press, London, New York.

11 Eggermont, J.J., Aertsen, A.M.H.J. and Johannesma, P.I.M. (1983a): Prediction of the responses of auditory neurons in the midbrain of the grassfrog based on the spectro-temporal receptive field. Hearing Res. 10, 191-202.

12 Eggermont, J.J., Epping, W.J.M. and Aertsen, A.M.H.J. (1983b): Stimulus dependent neural correlations in the auditory midbrain of the grassfrog (*Rana temporaria* L.). Biol. Cybern. 47, 103-117.

13 Eggermont, J.J., Johannesma, P.I.M. and Aertsen, A.M.H.J. (1983c): Reverse-correlation methods in auditory research. Quarterly Reviews of Biophysics 16, 341-414.

14 Epping, W.J.M. and Eggermont, J.J. (1985a): Single-unit characteristics in the auditory midbrain of the immobilized grassfrog. Hearing Res. (in press).

15 Epping, W.J.M. and Eggermont, J.J. (1985b): Relation of binaural interaction and spectro-temporal characteristics in the auditory midbrain of the grassfrog. Hearing Res. (in press).

16 Epping, W.J.M. and Eggermont, J.J. (1986a): Sensitivity of neurons in the auditory midbrain of the grassfrog to temporal characteristics of sound. I. Stimulation with acoustic clicks. (submitted).

17 Epping, W.J.M. and Eggermont, J.J. (1986b): Sensitivity of neurons in the auditory midbrain of the grassfrog to temporal characteristics of sound. II. Stimulation with amplitude modulated sound. (submitted).

18 Epping, W., Boogaard, H. van den, Aertsen, A., Eggermont, J. and Johannesma, P. (1984): The Neurochrome. An identity preserving representation of activity patterns from neural populations. Biol. Cybern. 50, 235-240.

19 Feng, A.S. (1981): Directional response characteristics of single neurons in the torus semicircularis of the leopard frog (*Rana pipiens*). J. Comp. Physiol. A 144, 419-428.

20 Feng, A.S. (1983): Morphology of neurons in the torus semicircularis of the northern leopard frog, *Rana pipiens pipiens*. J. Morphol. 175, 253-269.

21 Frostig, R.D., Gottlieb, Y., Vaadia, E. and Abeles, M. (1983): The effects of stimuli on the activity and functional connectivity of local neuronal groups in the cat auditory cortex. Brain Res. 272, 211-221.

22 Fukunaga, K. (1972): Introduction to statistical pattern recognition. Academic Press, New York.

23 Fuzessery, Z.M. and Feng, A.S. (1982): Frequency selectivity in the anuran auditory midbrain: single unit responses to single and multiple tone stimulation. J. Comp. Physiol. A 146, 471-484.

24 Fuzessery, Z.M. and Feng, A.S. (1983): Frequency selectivity in the anuran medulla: excitatory and inhibitory tuning properties of single neurons in the dorsal medullary and superior olivary nuclei. J. Comp. Physiol. A 150: 107-119.

25 Gelder, J.J. van, Evers, P.M.G. and Maagnus, G.J.M. (1978): Calling and associated behaviour of the common frog, *Rana temporaria*, during breeding activity. J. Anim. Ecol. 47, 667-676.

26 Gerhardt, H.C. (1974): The significance of some spectral features in mating call recognition in the green treefrog (*Hyla cinerea*). J. Exp. Biol. 61, 229-241.

27 Gerhardt, H.C. (1978): Mating call recognition in the green treefrog (*Hyla cinerea*): the significance of some fine-temporal properties. J. Exp. Biol. 74, 59-73.

28 Gerstein, G.L. (1970): Functional association of neurons: detection and interpretation. Neurosci. second study program, 648-661.

29 Gerstein, G.L. and Perkel, D.H. (1972): Mutual temporal relationships among neuronal spike trains. Statistical techniques for display and analysis. Biophys. J. 12, 453-473.

30 Grinvald, A. (1984): Real-time optical imaging of neuronal activity. TINS 7, 143-150.
31 Heierli, P., Ribaupierre, F. de, Toros, A. and Ribaupierre, Y. de (1981): Functional organization of the medial geniculate body studied by simultaneous recordings of single unit pairs. In: Neuronal mechanisms of hearing, pp. 183-186. Editors: J. Syka and L. Aitkin. Plenum Press, London, New York.
32 Hermes, D.J., Aertsen, A.M.H.J., Johannesma, P.I.M. and Eggermont, J.J. (1981): Spectro-temporal characteristics of single units in the auditory midbrain of the lightly anaesthetised grass frog (*Rana temporaria* L.) investigated with noise stimuli. Hearing Res. 5, 147-178.
33 Hermes, D.J., Eggermont, J.J., Aertsen, A.M.H.J. and Johannesma, P.I.M. (1982): Spectro-temporal characteristics of single units in the auditory midbrain of the lightly anaesthetised grassfrog (*Rana temporaria* L.) investigated with tonal stimuli. Hearing Res. 6, 103-126.
34 Hillery, C.M. (1984): Detection of amplitude-modulated tones by frogs: Implications for temporal processing mechanisms. Hearing Res. 14, 129-143.
35 Johannesma, P.I.M. and Eggermont, J.J. (1983): Receptive fields of auditory neurons in the frog's midbrain as functional elements for acoustic communication. In: Advances in vertebrate neuroethology, pp. 901-910. Editors: J.-P. Ewert, R.R. Capranica and D.J. Ingle. Plenum Press, New York, London.
36 Kruger, J. and Bach, M. (1981): Simultaneous recording with 30 microelectrodes in monkey visual cortex. Exp. Brain Res. 41, 191-194.
37 Levick, W.R., Cleland, B.G. and Dubin, M.W. (1972): Lateral geniculate neurons of cat: retinal inputs and physiology. Invest. Ophthalm. 11, 302-311.
38 Michalski, A., Gerstein, G.L., Czarkowska, J. and Tarnecki, R. (1983): Interactions between cat striate cortex neurons. Exp. Brain Res. 51, 97-107.
39 Mohneke, R. (1983): Tonotopic organisation of the auditory midbrain nuclei of the midwife toad (*Alytes obstetricans*). Hearing Res. 9, 91-102.
40 Murphy, J.T., Kwan, H.C. and Wong, Y.C. (1985): Cross correlation studies in primate cortex: synaptic interaction and shared input. Can. J. Neurol. Sci. 12, 11-23.
41 Palm, G. (1982): Neural assemblies. An alternative approach to artificial intelligence. In: Studies in brain function, Vol. 7, pp. 1-244.
42 Perkel, D.H., Gerstein, G.L. and Moore, G.P. (1967): Neuronal spike trains and stochastic point processes. II. Simultaneous spike trains. Biophys. J. 7, 419-440.
43 Pettigrew, A.G., Anson, M. and Chung, S.-H. (1981): Hearing in the frog: a neurophysiological study of the auditory response in the midbrain. Proc. R. Soc. Lond. B. 212, 433-457.
44 Potter, H.D. (1965): Mesencephalic auditory region of the bullfrog. J. Neurophysiol. 28, 1132-1154.
45 Priot-Droy, M.T. (1977): La typologie neuronique du tegmentum des anoures. J. Hirnforsch. 18, 321-333.
46 Reitboeck, H.J. (1983): A 19-channel matrix drive with individually controllable fiber microelectrodes for neurophysiological applications. IEEE SMC-13, 676-683.
47 Rheinlaender, J., Walkowiak, W. and Gerhardt, H.C. (1981): Directional hearing in the green treefrog: a variable mechanism? Naturwissenschaften 67, S.430.
48 Rose, G.J. and Capranica, R.R. (1985): Sensitivity to amplitude modulated sounds in the anuran auditory nervous system. J. Neurophysiol. 53, 446-465.
49 Schneider, J., Eckhorn, R. and Reitboeck, H. (1983): Evaluation of neuronal coupling dynamics. Biol. Cybern. 46, 129-134.
50 Sejnowski, T.J. (1976): On global properties of neuronal interaction. Biol. Cybern. 22, 85-95.
51 Shaw, G.L., Harth, E. and Scheibel, A.B. (1982): Cooperativity in brain function: assemblies of approximately 30 neurons. Exp. Neurol. 77, 324-358.
52 Stevens, J.K. and Gerstein, G.L. (1976): Interactions between cat lateral geniculate neurons. J. Neurophysiol. 39, 239-256.
53 Syka, J., Radionova, E.A. and Popelár, J. (1981): Discharge characteristics of neuronal pairs in the rabbit inferior colliculus. Exp. Brain Res. 44, 11-18.
54 Toyama, K., Kimura, M. and Tanaka, K. (1981): Organization of cat visual cortex as investigated by cross-correlation technique. J. Neurophysiol. 46, 202-214.
55 Walkowiak, W. (1980): The coding of auditory signals in the torus semicircularis of the firebellied toad and the grass frog: responses to simple stimuli and to conspecific calls. J. Comp. Physiol. A 138, 131-148.
56 Walkowiak, W. (1984): Neuronal correlates of the recognition of pulsed sound signals in the grass frog. J. Comp. Physiol. A 155, 57-66.
57 Walkowiak, W. and Brzoska, J. (1982): Significance of spectral and temporal call parameters in the auditory communication of male grassfrogs. Behav. Ecol. Sociobiol. 11, 247-252.
58 Walkowiak, W., Capranica, R.R. and Schneider, H. (1981): A comparative study of auditory sensitivity in the genus *Bufo* (Amphibia). Behav. Processes 6, 223-237.
59 Wheeler, B.C. and Heetderks, W.J. (1982): A comparison of techniques for classification of multiple neural signals. IEEE BME-29, 752-759.
60 Wilczynski, W. and Capranica, R.R. (1984): The auditory system of anuran amphibians. Progress in Neurobiol. 22, 1-38.
61 Wood, H.I. and Glantz, R.M. (1980): Distributed processing by visual interneurons of crayfish brain. II. Network organization and stimulus modulation of synaptic efficacy. J. Neurophysiol. 43, 741-753.

THE NEUROCHROME

An Identity Preserving Representation of Activity Patterns from Neural Populations

Willem Epping, Henk van den Boogaard, Ad Aertsen, Jos Eggermont and Peter Johannesma

Department of Medical Physics and Biophysics, University of Nijmegen, Geert Grooteplein Noord 21, NL-6525 EZ Nijmegen, The Netherlands

Recording of simultaneous but separated activity of neural populations overwhelms the experimenter with a large amount of information. A clearly structured display technique the *"Neurochrome"* is introduced, usable on-line and real-time. It shows neural activity patterns while preserving neural identity by employing a color code. The Neurochrome assists the experimenter in generating and verifying hypotheses about neural correlations and stimulus-event relations already during the experiment. In auditory research single neurons are characterized by their spectro-temporal sensitivity to auditory stimuli. A straightforward generalization of this concept, applicable to neural populations, is proposed leading to a global indication of a populations' activity to stimuli: the *Multi-Unit Spectro-Temporal Sensitivity*. This approach is inversely related to the Neurochrome, the latter however containing more information. The combination of both approaches seems quite powerful in the investigation of neural assemblies. The procedures are illustrated with examples of extracellular multi-unit recordings from the auditory midbrain of the grassfrog (*Rana temporaria* L.).

1. Introduction

Nowadays in a number of laboratories extracellular recordings of simultaneous activity from small neural populations are being made routinely with a single microelectrode [7] or with multi-electrode configurations (e.g. [10]). These experiments aim to measure correlations between firing activity of neurons in order to reveal possible underlying neural connectivity schemes. Usually correlations are estimated by means of cross-coincidence histograms [12] or joint occurrence scattergrams [13]. These procedures discard information originally present in the experimental data because of averaging or being sensitive to only very specific firing patterns. Recently a method was described [5,6] which enables the detection of complex activity patterns in single neuron spike trains; this method, however, appears rather time consuming.

In this paper a display-technique is presented the "Neurochrome", containing all original information by preserving both identity of and temporal relation between neural events. Neural identity is characterized by color. Use is made of the human color-processing capability (color contrast, pattern recognition) to note associations of colored events in the plane of representation, which points to coherent activity in small neural populations. This may be indicative for the existence of neural assemblies [11,15] or synfire chains [1]. The procedure can be used on-line and real-time, thus enabling multi-unit experiments of high efficiency with respect to the search for populations exhibiting correlated activity as well as to presentation of adequate sensory stimuli.

Studying sensory systems often one or more stimulus parameters are varied, be it systematically or (pseudo-)randomly. By rearranging the original Neurochrome according to these parameters, e.g. tonal frequency in auditory research, a second representation emerges showing possible stimulus-dependencies of neural firing patterns. The second representation of the Neurochrome, with frequency as variable, is closely related to the concept of Spectro-Temporal Sensitivity: STS [3,8] defined for

single neurons. This is extended to multi-neuron networks, showing their combined sensitivity area in spectro-temporal space by superimposing individual STS's. The outcome is the Mult-Unit Spectro Temporal Sensitivity MUSTS. Whereas the Neurochrome is a forward experimenter oriented approach the MUSTS is a backward one, reflecting the brain's view of the outside world.

2. Methods

2.1. Preparation and Recording

Recordings were obtained from the auditory midbrain (torus semicircularis) in the immobilized (Buscopan) and locally anesthetized grassfrog (Rana temporaria L.) using single metal microelectrodes (tungsten or stainless steel, Bak Electronics) with an exposed tip of about 10 µm and a 1 kHz impedance in the 1-3 MΩ range. The multi-unit spike-trains were separated into the component single-unit spike-trains on basis of spike waveform by using an on-line matched filter approach (e.g. [1]) and interactive setting of ellipsoidal cluster boundaries. For details of physiological preparation, stimulus presentation, data registration and separation procedures the reader is referred to Eggermont et al. [7].

2.2. Chromatic Representation

The Neurochrome is displayed on a Ramtek RM 9300 colorgraphics system, coupled to a general purpose PDP 11/45 computer. The resolution is 640 pixels in horizontal direction and 512 pixels in vertical direction. Each pixel has 6 bits color information leading to 64 simultaneously displayable colors, selectable from a palet of 4096 colors. The color key was chosen to be of equal luminance and given this restriction the perceptual distances between the colors should be as large as possible. Therefore we selected the three principal colors: red, green, blue and their complements: magenta (purple), yellow and cyan (blue/green) located in between the former three in perceptual space, all colors being maximally saturated. For on-line assistance during experiments a Ramtek RM 6211 colorgraphics terminal attached to a PDP 11/34 in use for data acquisition is available.

3. Representation of Multi-Unit Activity

3.1. The Neurochrome

The experimental datarecord, containing neural activity from a small population usually is divided into segments with duration T seconds. The segment duration can be set equal to e.g. duration of period in case of a periodic stimulus, or the interval between successive tones. The first representation of the Neurochrome, useful under stimulus conditions as well as non-stimulus conditions, is a 2-dimensional image, color indicating neural origin. In this type of Neurochrome the k^{th} line displays the k^{th} data segment: a so called "lexicographic" dotdisplay, analogous to the lines on a page of text. In this way possible overall alterations of population characteristics during the experiment can be revealed.

In the second representation of the Neurochrome the lines are rearranged according to a varying stimulus parameter, expressing stimulus influences on e.g. latency, structure of neural firing patterns. In the case of an auditory stimulus consisting of tonepips of varying frequencies applied at regular intervals each line gives the population's response to a tonepip of a parti cular frequency, time after tonepip onset running from left to right.

3.2. Multi-Unit Spectro-Temporal Sensitivity

The Spectro-Temporal Sensitivity (STS) as defined for single neurons [3,8] is an average functional on the pre-event stimulus ensemble, giving the combined spectro-temporal structure of stimuli preceding the occurrence of action potentials. A straightforward generalization of this concept, applicable to neural populations is the superposition of the individual STS's, showing the sensitivity of

the entire population in spectro-temporal domain; the same color identification as in case of the Neurochrome is employed. No use is made of number of spikes nor of detailed structure in firing patterns: crosscorrelations among neural activity of the contributing neurons and autocorrelations within separate spike-trains are not considered. The name Multi-Unit Spectro-Temporal Sensitivity (MUSTS) is proposed.

4. Results

The procedures presented in this paper are illustrated with three multi-unit recordings from the auditory midbrain of the grassfrog. For reasons of paucity only experiments under identical stimulus conditions, apart from a different localization of sound source, are shown. The stimulus ensemble lasts 508 s and consists of tonepips with a duration of 48 ms, intervals of 1 s between onset of tonepips and intensity of 90 dB SPL. The frequency of the tonepips was varied in pseudorandom order and was drawn from a uniform distribution (on log-scale) between 125 and 2000 Hz. The first column of Fig. 1 shows the original Neurochromes, the second column the Neurochromes rearranged according to tonal frequency and the third column the MUSTS.

In the first row of Fig. 1 results are expressed of recording 216-1, which contains three units coded in red, green and blue respectively. No trends in their firing activity throughout the experiment were observed (Fig. 1a). Unit 1 (red) has the shortest latency: 10 ms and is spontaneously active; unit 2 (green) has a latency of 32 ms; unit 3 (blue) with a latency of 26 ms shows a prolonged activation period of over 300 ms after a tonepip; units 2 and 3 are hardly spontaneously active. Unit 1 is broadly tuned over the entire frequency range (Fig. 1b); unit 2 is excited mainly in the 250-2000 Hz range like unit 3, the latter being particularly sensitive to frequencies above 900 Hz indicating a strong input from the basilar papillae. Note that latency of units 1 and 3 is frequency dependent. The spectro-temporal sensitivities are displayed in Fig. 1c: because of the chromatic display procedure only the more pronounced sensitivity areas can be discerned resulting in somewhat restricted areas as compared to Fig. 1b. The broadly tuned unit 1 is most effectively stimulated by tonepips in the mid-frequency range 350-1200 Hz as could already be concluded from Fig. 1b for unit 1 has the shortest latency in that frequency range. Moreover unit 1 expresses limited temporal spread as compared to the longer latency units 2 and 3, the latter having more diffused spectro-temporal sensitivities especially for frequencies above 1000 Hz.

For a color photograph of Fig. 1,
the reader is referred to
Biol. Cybern. (1984) 50: 235-240.

Fig. 1a-i. Representation of event-event and stimulus-event relations of multi-unit recordings. Units are identified according to the color key placed at the right of the figures. In the first column original Neurochromes are displayed, giving the exact timing relationships between spikes, apart from a segmentation in lines. The horizontal axis lasts 1 s, being the interval between onset of tonepips, and represents time after a tonepip running from left to right. The vertical axis gives the index of lines. Rearranged Neurochromes appear in the second column, lines are reordered according to frequency of tonepips; note the logarithmic frequency scale. In the third column Multi-Unit Spectro-Temporal Sensitivities are shown. The horizontal axis now represents time before a neural event running from right to left. The vertical axis is the same as in the second column. Results of multi-unit recording 216-1 containing three units are shown in the first row. Unit 1 has 528 spikes, unit 2 565 spikes and unit 3 933 spikes. Second row: recording 224-4 with four units; unit 1 519 spikes, unit 2 237 spikes, unit 3 88 spikes and unit 4 73 spikes. Third row: recording 227-3 with three units, unit 1 1119 spikes, unit 2 2244 spikes and unit 3 278 spikes. In case of recordings 216-1 and 227-3 the stimulus was applied to both ears, whereas recording 224-4 was made under contra-lateral stimulus presentation.

Recording 224-4 containing four units is represented in the second row of Fig. 1. From Fig. 1d a strong locking to the stimulus appears for all units with latencies in the 20-30 ms range, albeit that unit 1 (red) obscures spikes of the other units in the initial activity band because of its strong responsiveness. The units are spontaneously active in varying degrees. Furthermore a clear multi-unit activity pattern can be discerned notably in spontaneous activity: green-blue, green blue-blue and green-blue-purple, pointing to coherent activity of units 2, 3, and 4. The rearranged Neurochrome (Fig. 1e) reveals a large similarity of properties of units 2, 3, and 4 being excited in the 1200-2000 Hz range, in which the green-blue purple pattern can also be distinguished now. Moreover the activity of units 2, 3 and 4 is suppressed after the initial activity band for frequencies above 500 Hz, including a frequency band where no initial excitation occurred. Correlation analysis corroborates the relationship between units 2, 3 and 4, and establishes that the activity pattern is not entirely due to stimulus influences. As an example crosscoincidence histograms between units 2 and 3 are shown in Fig. 2. A preference for unit 3 firing about 6 ms after unit 2 can be discerned. The difference between both histograms points to existence of a neural pathway, be it direct or common, between units 2 and 3 (for details see [7, 12]. Unit 1 is complementary to the other units in the sense that its frequency sensitivity lies in the 125-1200 Hz range. Correlation analysis does not indicate a relation of unit 1 with the other units apart from common stimulus influences. Spectro-temporal sensitivities of the units are shown in Fig. 1f, substantiating former observations.

In the third row of Fig. 1 recording 227-3 containing three units is represented. From Fig. 1g it appears that the units have latencies greater than 50 ms and that spontaneous activity of units 1 and 2 is substantial. Occasionally purple dots can be observed due to coincidence of spikes of units 1 (red) and 3 (blue) (see discussion). Unit 1 is broadly tuned (Fig. 1h) with a preference to frequencies below 600 Hz. The same holds for unit 2, note that its activity is prolonged in the 300-600 Hz range but suppressed in the 600-2000 Hz range and after an initial activation band also in the 125-300 Hz frequency range. Unit 3 is only sensitive to frequencies above 500 Hz. Correlation analysis points to weak excitatory influence of units 2 and 3 on unit 1. Spectro-temporal properties are clearly expressed in Fig 1i; whereas unit 2 leads with respect to unit 1 in the 125-300 Hz range, their roles are changed for frequencies above 300 Hz.

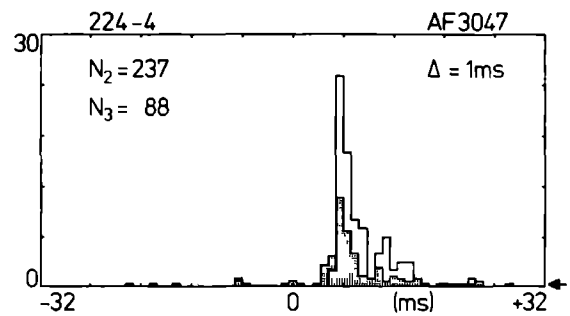

Fig. 2. Simultaneous and nonsimultaneous crosscoincidence histograms of unit 2 (green) and unit 3 (blue) of multi-unit recording 224-4. The nonsimultaneous (shaded) histogram is obtained by shifting one spike-train over one or more stimulus periods with respect to the other spiketrain. The vertical axis represents number of coincidences per bin, binwidth Δ is 1 ms. The arrow indicates the expected number of coincidences in case of uncorrelated spike-trains.

5. Discussion

In previous studies of the auditory midbrain of the grassfrog it was demonstrated that this center can hardly be understood on basis of the single-unit approach. A substantial fraction of neurons exhibits STS's under various stimulus conditions, which cannot be brought in line with one another [4,9]. Likewise crosscoincidence histograms of simultaneously recorded activity from pairs of neurons differ under altered stimulus conditions [7]. It is hypothetized that simultaneous recording of activity of a neural population, subsequent se-

paration into single-unit spike-trains, correlating the spike-trains with one another as well as with stimulus can clarify underlying neural connectivity schemes and will contribute to an understanding of the brain. The minimum size of the population, that has to be recorded from, will depend on specific questions posed and on the part of the brain under investigation; this is still a matter of debate (e.g. [15]).

Both representations of the Neurochrome are constructed real-time during the experiment, offering the opportunity of influencing the experimental procedure interactively and thus to investigate possible significance of hypotheses while the neurons are still on-line. This can hardly be expected from statistical and timeconsuming procedures as correlation methods and pattern detecting techniques. These procedures, however, together with the Neurochrome as possible starting point, may offer more quantitative and detailed results allowing conclusions to be stricter. The Neurochrome as used by us permits the analysis of a population of six neurons at most. This number can be extended by the addition of extra colors, however, at the expense of reduced discrimination of events from different neural origin. The applicability of the Neurochrome is limited by spike-density: when in the 2-dimensional image dots overlap additive colors, which may hard to be distinguished from the original colors, are generated and perceived. This problem can be circumvented by displaying the Neurochrome in parts.

To investigate spectro-temporal properties of neural populations the MUSTS was proposed as a first attempt, showing global sensitivity areas. Taking seriously the possibility that the brain codes and transforms at least a part of incoming and outgoing information by highly structured firing patterns of cooperating cell assemblies (this type of coding is called ensemble correlation [14]), the information content of the original datarecords should be much richer than expressed in the MUSTS. One way to exploit this information more exhaustively is through detection of significant neural activity patterns, e.g. on basis of the Neurochrome, and using these as "superevents" in the construction of a higher level pre-event stimulus ensemble in order to come to a more coherent spectro-temporal measure. By applying these ideas, in combination with a rich stimulus repertoire, to multi-unit experiments it may be concluded whether firing patterns of populations are more robust to stimulus and/or environmental alterations than single-neuron activity.

Acknowledgements

This investigation forms part of the researchprogram "Brain and Behaviour" at the Department of Medical Physics and Biophysics, University of Nijmegen and was supported by the Netherlands Organization for Advancement of Pure Research (Z.W.O.). The authors wish to thank Koos Braks, *Hans Broeren, and Jan Peter de Valk for their* expertise in chromatic display procedures and Jan Bruijns and Wim van Deelen for software development. Marianne Nieuwenhuizen prepared the manuscript.

References

1 Abeles, M. and Goldstein, M.H. (1977): Multiple spike train analysis. Proc. IEEE 65, 762-773.
2 Abeles, M. (1982): Local cortical circuits, an electrophysiology study. Studies of brain function. Springer, Berlin, Heidelberg, New York.
3 Aertsen, A.M.H.J., Johannesma, P.I.M., Hermes, D.J. (1980): Spectro-temporal receptive fields of auditory neurons in the grassfrog. II. Analysis of the stimulus-event relation for tonal stimuli. Biol. Cybern. 38, 235-248.
4 Aertsen, A.M.H.J., Johannesma, P.I.M. (1981): A comparison of the spectro-temporal sensitivity of auditory neurons to tonal and natural stimuli. Biol. Cybern. 42, 145-156.
5 Dayhoff, J.E., Gerstein, G.L. (1983): Favored patterns in spike trains. I. Detection. J. Neurophysiol. 49, 1334-1348.
6 Dayhoff, J.F., Gerstein, G.L. (1983): Favored patterns in spike trains. II. Application. J. Neurophysiol. 49, 1349-1361.
7 Eggermont, J.J., Epping, W.J.M. and Aertsen, A.M.H.J. (1983): Stimulus dependent neural correlations in the auditory midbrain of the grassfrog (*Rana temporaria* L.). Biol. Cybern. 47, 103-117.
8 Hermes, D.J., Eggermont, J.J., Aertsen, A.M.H.J. and Johannesma, P.I.M. (1982): Spectro-temporal characteristics of single units in the auditory midbrain of the lightly anaesthetised grassfrog (*Rana temporaria* L.) investigated with tonal stimuli. Hearing Res. 6, 103-126.
9 Johannesma, P.I.M. and Eggermont, J.J. (1983): Receptive fields of auditory neurons in the frog's midbrain as functional elements for

acoustic communication. In: Advances in vertebrate neuroethology. pp. 901-910. Editors: J.-P. Ewert, R.R. Capranica and D.J. Ingle. Plenum Press, New York.

10 Kruger, J. and Bach, M. (1981): Simultaneous recording with 30 microelectrodes in monkey visual cortex. Exp. Brain Res. 41, 191-194.

11 Palm, G. (1982): Neural assemblies, an alternative approach to artificial intelligence. Studies of brain function. Springer, Berlin, Heidelberg, New York.

12 Perkel, D.H., Gerstein, G.L. and Moore, G.P. (1967): Neuronal spike trains and stochastic point processes. II. Simultaneous spike trains. Biophys. J. 7, 419-440.

13 Perkel, D.H., Gerstein, G.L., Smith, M.S. and Tatton, W.G. (1975): Nerve impulse patterns: a quantitative display technique for three neurons. Brain Res. 100, 271-296.

14 Sejnowski, T.J. (1976): On the stochastic dynamics of neuronal interaction. Biol. Cybern. 22, 203-211.

15 Shaw, G.L., Harth, E. and Scheibel, A.B. (1982): Cooperativity in brain function: assemblies of approximately 30 neurons. Exp. Neurol. 77, 324-358.

Samenvatting

Kikkers en padden zijn geevolueerd tot, auditief gezien, sociale dieren. In het paarseizoen produceren met name de mannetjes een beperkt repertoire van soort-specifieke roepen, die ieder een eigen functie hebben. De meest karakteristieke, voor de voortplanting essentiele, roep is de mannelijke paarroep. Deze roep wordt enerzijds door de vrouwtjes herkend en als akoestisch baken beschouwd tijdens hun tocht naar de paarplaatsen. Anderzijds fungeert het als vliegwiel voor de mannetjes die als reactie langdurig, soms in bepaalde regelmatige patronen, in koor gaan kwaken. In het geval van de inheemse bruine kikker (*Rana temporaria* L.), het proefdier gebruikt voor dit proefschrift, is vooral de laatst genoemde functie van belang. De paarroep van de bruine kikker heeft een tamelijk breedbandige spectrale inhoud gelegen rond 500 Hz en een uitgesproken temporele structuur door de pulsachtige aard van zijn omhullende (hoofdstuk 1). De spectro-temporele karakteristiek van een geluid, zoals zichtbaar gemaakt in bijvoorbeeld een sonogram, kan beschouwd worden als een vingerafdruk die het geluid en daarmee vaak zijn bron identificeert.

Het auditieve systeem van kikkers en padden is meegeevolueerd met het geluid voortbrengende systeem zó dat beide aan elkaar aangepast zijn. Door deze ontwikkeling zijn deze dieren uitstekend in staat soort-specifieke geluiden te herkennen (identificeren) en te plaatsen (localiseren) . Het basisplan van het auditieve systeem is gelijkvormig met dat van de andere gewervelde dieren, al zijn reeds op perifeer nivo soort-specifieke specialisaties te onderkennen gericht op een optimale aanpassing aan de omgeving. Het centraal auditieve systeem bestaat uit ten minste vijf kernen gelegen in achterhersenen, middenhersenen, tussenhersenen en voorhersenen (hoofdstuk 1). Deze kernen zijn verbonden door een uitgebreid netwerk van opstijgende en afdalende vezelbanen, die zowel seriele, parallelle alsmede gedistribueerde informatieverwerking toelaten. Binnen elke auditieve kern bevinden zich zo'n 1000-10.000 zenuwcellen, die elk duizenden contacten met andere zenuwcellen maken. In deze in hoge mate verbonden structuur worden binnenkomende geluiden gecodeerd en verwerkt om uiteindelijk geintegreerd met informatie van de andere zintuig systemen te leiden tot een adequate reactie op prikkels vanuit de buitenwereld.

In dit proefschrift zijn de resultaten beschreven van onderzoek naar de auditieve informatieverwerking in de torus semicircularis, de grote auditieve kern gelegen in de middenhersenen. De torus semicircularis neemt in het basisplan van het auditieve systeem dezelfde plaats in als de colliculus inferior van hogere dieren. Deze kern wordt gedacht een belangrijke rol te spelen bij zowel identificatie ('wat') als localisatie ('waar') van geluid. Aandacht werd geschonken aan de verwerking van spectrale (frequentie-inhoud), temporele (tijdstructuur) en in mindere mate spatiele (ruimtelijke) aspecten van geluid. Daartoe werden met een dubbele micro-electrode opstelling registraties gemaakt van de electrische activiteit van kleine groepen (kleiner dan acht) zenuwcellen, waarin de individuele bijdragen van de afzonderlijke cellen onderscheiden konden worden. Deze zogenaamde multi-neuron afleidingen laten enerzijds de analyse van stimulus-respons relaties van afzonderlijke zenuwcellen toe (hoofdstukken 2 tot en met 5), anderzijds geven ze functionele verbanden tussen zenuwcellen aan (hoofdstuk 6). In hoofdstuk 7 wordt een eerste poging gedaan deze beide complementaire analyses te integreren in multi-neuron stimulus-respons relaties, die een populatie-eigenschap beschrijven. De resultaten in dit proefschrift zijn gebaseerd op materiaal van 497 zenuwcellen verkregen bij 50 (verlamde) kikkers. Van deze 497 neuronen werden er 181 als enkelvoudige

afleiding verkregen, de andere 316 cellen werden in groepjes, ter grootte van twee tot zeven, geregistreerd. De neurale responsies werden uitgelokt door een grote verscheidenheid aan auditieve stimuli. Deze varieerden van simpele kunstmatige geluiden, zoals korte toonstootjes en breedband ruis, via kliktreinen en amplitude gemoduleerde geluiden naar complexe stimuli, die de paarroep nabootsen. De geluidsintensiteit was veelal bovendrempelig op een nivo dat voor deze kikkers als natuurlijk beschouwd kan worden.

Het verband tussen een aangeboden stimulus en de opgewekte neurale reactie, de zogeheten stimulus-respons relatie, van afzonderlijke zenuwcellen wordt traditioneel op twee complementaire wijzen bestudeerd. De meest toegepaste is de voorwaarts-correlatie methode, die waarnemer-georienteerd genoemd kan worden. Deze methode gaat uit van kortdurende, goed gedefinieerde en controleerbare stimuli. De neurale responsies worden vaak als functie van de tijd na aangaan van de stimulus in peri-stimulus tijd histogrammen of 'dotdisplays' weergegeven; of men middelt over de tijd en zet de gemiddelde neurale activiteit uit als functie van een bepaalde stimulus parameter, bijvoorbeeld spectrale frequentie, resulterend in afstem-krommen. De andere methode is de terugwaarts-correlatie methode, die als brein-georienteerd beschouwd kan worden. Deze methode legt de neurale activiteit in de oorsprong en kijkt terug in de tijd welke geluiden aan deze activiteit voorafgingen, en derhalve er een verband mee hebben. De laatste methode is nauw verwant aan de niet-lineaire systeemtheorie en abstracter dan de eerste methode, hetgeen de toepassing beperkt heeft tot die laboratoria waarvan de onderzoekers enigszins gecharmeerd zijn van mathematische elegantie. De stimuli gebruikt bij de terugwaarts-correlatie methode zijn vaak langdurend en met een statistisch ongecorreleerde structuur, zoals Gaussisch breedband ruis of Poisson verdeelde kliktreinen. De stimulus-respons relatie wordt dan in een orthogonale functionaalreeks ontwikkeld en gevisualiseerd door de bijbehorende Wiener-Volterra of Poisson kernen. In dit proefschrift zijn beide procedures gebruikt en met elkaar geconfronteerd.

De stimulus-respons relaties van afzonderlijke zenuwcellen in de auditieve middenhersenen van de bruine kikker bleken vaak complex van aard te zijn. Ongeveer de helft van de zenuwcellen heeft spectrale gevoeligheden, die een combinatie van verschillende frequentie banden te zien geven, zij het in excitatoire (respons verhogende) dan wel in inhibitoire (respons verlagende) zin (hoofdstuk 2), hetgeen duidt op een hoge mate van spectrale integratie. De gevoeligheden van neuronen voor temporele geluidstructuur laat evenzeer een grote diversiteit van respons typen zien (hoofdstukken 4 en 5). De meest selectieve responsies voor amplitude modulatie frequentie worden geobserveerd in de gemiddelde vuurfrequentie en niet in het synchronisatiegedrag van neuronen. Op basis van terugwaarts-correlatie procedures werden synaptische, actiepotentiaal genererende en neurale interactie mechanismen bepaald, die vermoedelijk verantwoordelijk zijn voor de waargenomen temporele selectiviteit. In hoofdstuk 3 werden spatiele gevoeligheden, in de zin van wisselwerking van de informatie komend van de twee oren (binaurale interactie) bestudeerd. Informatie van het ene oor kon de informatie komend van het andere oor zowel versterken als onderdrukken, resulterend in verschillende richtingskarakteristieken voor geluid. Een belangrijk resultaat van deze studies naar spectrale, temporele en spatiele gevoeligheden voor geluid was dat deze drie aspecten niet gescheiden van elkaar te bestuderen zijn. Temporele gevoeligheden en binaurale interactie typeringen bleken sterk afhankelijk van de spectrale inhoud van de stimulus. Daarom zouden stimulus-respons relaties idealerwijs als gekoppelde spatio-spectro-temporale gevoeligheden bestudeerd moeten worden. Een neven-resultaat, verkregen dankzij de multi-neuron aanpak, was dat stimulus-respons relaties van naburige neuronen vaak zeer verschillend bleken, hetgeen duidt op ten hoogste een zwakke topografische afbeelding van stimulus kenmerken op de auditieve middenhersenen van de bruine kikker.

Functionele verbanden in neurale populaties werden vastgesteld op basis van paar-correlaties tussen zenuwcellen. Zowel afhankelijkheden ten gevolge van overlappende stimulus eigenschappen, gemeenschappelijke neurale verbindingen alsmede di-

recte invloeden werden waargenomen (hoofdstuk 6). In het algemeen zijn deze functionele verbanden afhankelijk van de aangeboden stimulus. Dit doet vermoeden dat de functionele structuur van het zenuwstelsel geen star geheel is, maar een flexibel dynamisch karakter heeft, georganiseerd ten dele door autonome processen en ten dele door externe invloeden zoals stimulus en context. In overeenstemming met de afzonderlijk neuron resultaten werd vastgesteld dat binnenkomende stimulus informatie zich over grote delen van de auditieve middenhersenen verspreidt. Daarentegen lijken gemeenschappelijke neurale verbindingen zich niet verder uit te breiden dan 300 µm. Directe neurale verbindingen werden alleen binnen 100 µm geobserveerd, daarmede de afmeting van locale circuits aangevend.

CURRICULUM VITAE

Ik werd geboren op 26 september 1957 te Silvolde. De middelbare school opleiding heb ik genoten aan het Isala College te Silvolde en het St. Ludgercollege te Doetinchem en afgesloten met het gymnasium-β diploma in 1975. In datzelfde jaar werd met de studie Natuurkunde begonnen aan de Universiteit van Nijmegen. Het kandidaatsexamen Natuurkunde met tweede hoofdvak Wiskunde en bijvak Sterrenkunde werd afgelegd in april 1978. Het afstudeeronderzoek heb ik onder leiding van Prof.Dr. J.J. Eggermont verricht op het Laboratorium voor Medische Fysica en Biofysica. Dit onderzoek had betrekking op de separatie van gesuperponeerde multi-neuron activiteit ter verkrijging van simultaan geregistreerde activiteitspatronen van afzonderlijke zenuwcellen. In maart 1981 werd de studie cum laude afgesloten met het doctoraal examen Experimentele Natuurkunde.

Van april 1981 tot april 1985 ben ik als Z.W.O. promovendus verbonden geweest aan het Laboratorium voor Medische Fysica en Biofysica aan de Universiteit van Nijmegen. Onder leiding van Prof.Dr. J.J. Eggermont werd de neurale informatieverwerking in de auditieve middenhersenen van de bruine kikker bestudeerd. Voor dit onderzoek werd in 1985 de Shell studiereis toegekend.

Stellingen

1. In het algemeen zijn spatiele, spectrale en temporele eigenschappen van centraal auditieve zenuwcellen onderling afhankelijk, hetgeen pleit voor een gecombineerde spatio-spectro-temporele beschrijving van stimulus-respons relaties van deze zenuwcellen.

2. De functionele betekenis van de hoge mate van intrinsieke en extrinsieke verbondenheid van neurale structuren is alleen te begrijpen op basis van scheidbare multi-unit afleidingen.

3. Hersenen hebben zich fylogenetisch en ontogenetisch ontwikkeld in wisselwerking met de buitenwereld. Neurofysiologische experimenten dienen daarom bij voorkeur plaats te vinden onder voor het proefdier natuurlijke omstandigheden zowel wat betreft de sensorische omgeving als de mogelijkheid tot vertonen van gedrag.

4. Gezien het steeds complexer en duurder worden van experimentele opstellingen voor een geïntegreerde studie van hersenen en gedrag verdient een Europees herseninstituut naar model van het CERN aanbeveling.

5. Multidisciplinair onderzoek, zoals de studie van hersenen en gedrag, wordt bemoeilijkt doordat subsidies vanuit de 1e en 2e geldstroom disciplinegewijs worden toegekend.

6. De samenwerking van hersenonderzoekers en informatici in een multidisciplinair onderzoeksverband Neuroinformatica zal enerzijds leiden tot een groter begrip van het functioneren van hersenen en anderzijds een belangrijke bijdrage leveren aan de ontwikkeling van zichzelf organiserende systemen (6e generatie computers).

7. Het gebrek aan concepten om de immense stroom van gegevens, opgeleverd door geavanceerde neurofysiologische opstellingen waarin individuele aktiviteitspatronen van grote aantallen hersencellen gelijktijdig worden geregistreerd, adequaat te analyseren, wijst op de noodzaak van vergrote aandacht voor theorievorming omtrent het functioneren van hersenen.

8. Het houden en verzorgen van proefdieren door onderzoekers zelf, verhoogt de zorgvuldigheid waarmee deze tijdens experimenten behandeld worden.

9. Ambitieus management en gedegen onderzoek zijn slecht te combineren.

10. Het gevoerde bezuinigingsbeleid op wetenschappelijk onderwijs en onderzoek leidt tot het vertrek van een relatief groot deel van de meest getalenteerden en veroorzaakt daardoor een algehele nivoverlaging op universiteiten.

11. Doorstroombeleid zou niet alleen voor promovendi, maar - in aangepaste vorm - ook voor de senior staf inclusief hoogleraren moeten gelden.

12. Een betere integratie van wetenschap en samenleving wordt verkregen door universiteitsnieuwbouw in stadscentra in plaats van in buitenwijken te plaatsen.

13. De grote invloed van omgevingsfactoren op de ontwikkeling van individuen, gevoegd bij de desolate bouwstijl en steriele sfeer van veel β-faculteiten, doet het ergste vermoeden voor een evenwichtige ontwikkeling van β-studenten.

14. De universiteit dient te beschikken over bewaakte fietsenstallingen.

15. Voor het in stand houden van sociale contacten in de werksfeer dient de koffieverstrekking in lunchpauzes niet geautomatiseerd te worden.

Nijmegen, 20 september 1985

Willem Epping